Update of Snapshot of Tevatron Flying Wire and Synchrotron Light Detector Transverse Emittance Measurements at 980GeV VERSION 1.0

Krzysztof Genser
September 19th 2003

Computing Division, Fermilab

Abstract

This note presents plots related to Tevatron Transverse Emittance measurements done using Flying Wire and Synchrotron Light detectors for stores in the 2650-3000 range. It is an update of an earlier note [1] on the same topic for another set of stores.

Data Selection

The stores for the plots were selected from June-September 2003 running period after insertion of the attenuators in the antiproton Flying Wire detector system (stores 2650 to 3000).

The Tevatron Case chosen for analysis was "Remove Halo" (with the beam energy of 980GeV) as this is one of the cases where both FW and SL systems are activated. The requirements imposed on the data were:

1. The FW freshness number (ACcelerator NETwork (ACNET) variable T:FWFRSH) in case "Remove Halo" had to be incremented by at least one with respect to the case "Initiate Collisions".

2. The Transverse Emittance as measured by the FW E11 (combined with SBD in the Horizontal cases) had to be between 0 and 40 ($\pi \cdot mm \cdot mrad$) in the vertical cases and between 0 and 25 ($\pi \cdot mm \cdot mrad$) in the horizontal cases (to avoid both nonphysical or difficult to measure cases).

3. The antiprotons intensity had to be greater than 15E9 (to avoid difficult to measure cases)

In addition to the above cuts the following stores were removed from the sample: 2792, 2795, 2813, 2826, 2828, 2908, 2910, 2912, 2916 due to inconsistencies in the Synchrotron Light System and 2868, 2817 due to inconsistencies in the Flying Wire Systems. Store 2971 was a test store and was also rejected.

References

[1] K. Genser, *A Snapshot of Tevatron Flying Wire and Synchrotron Light Detector Transverse Emittance Measurements at 980GeV* dated June 3rd 2003, Beams Division Document 656-v1

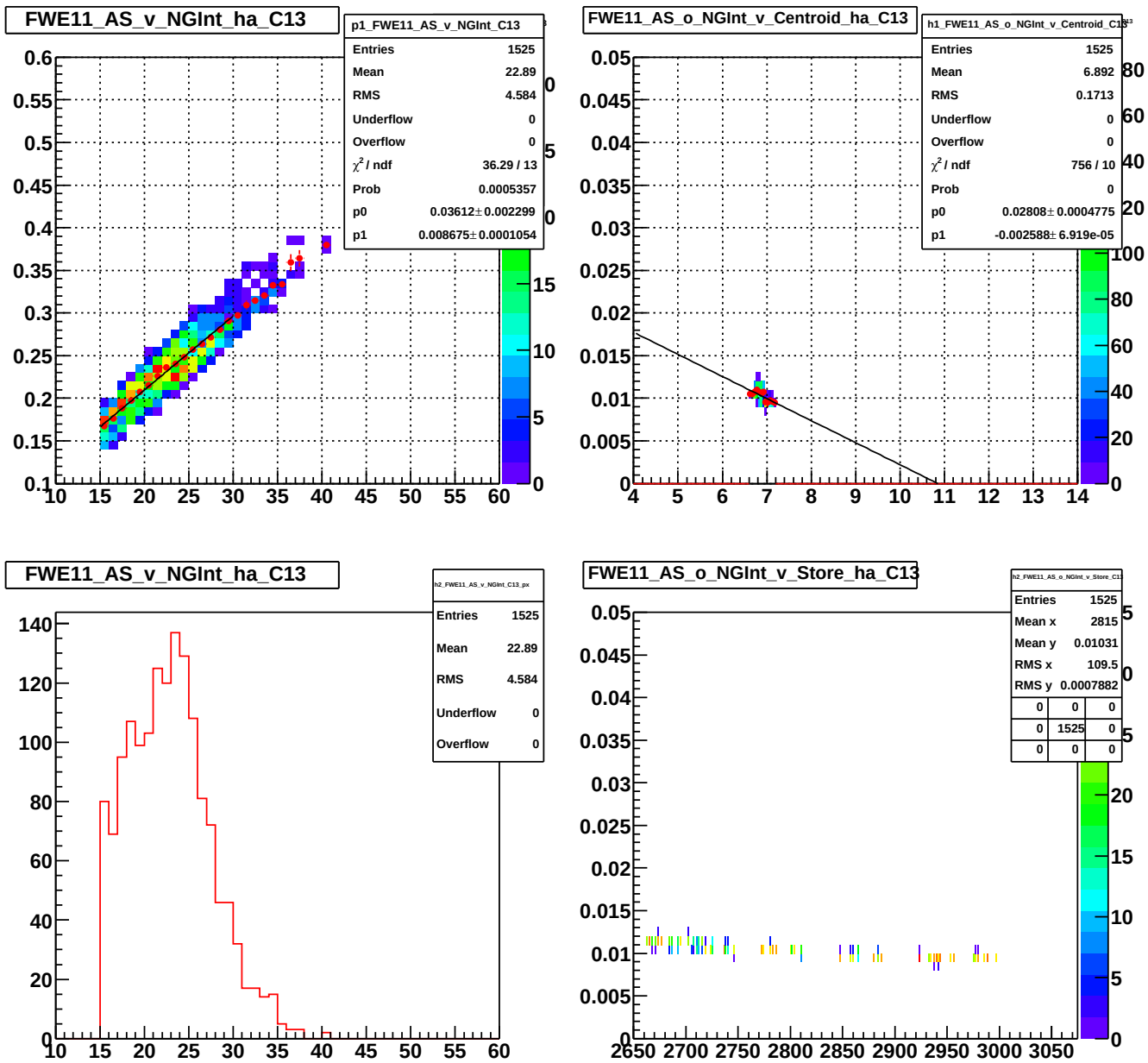

Figure 1: Antiproton beam, horizontal detectors: Performance of the Flying Wire Detector at the E11 location during Tevatron Remove Halo case: Amplitude (in arbitrary units) times sigma of the bunch width distribution (in *mm*) of the front end FW detector data versus bunch intensity (ACNET variables T:FBI[A,P]NG) (in E9) with an overlaid horizontal profile of that distribution with a straight line fit; Amplitude times sigma of the bunch width distribution of the front end FW detector data over bunch intensity versus bunch E11 centroid (in *mm*) (based on the T:FW[E,H,V][A,P]CE ACNET variable) with an overlaid horizontal profile of that distribution with a straight line fit; bunch intensity; amplitude times sigma of the bunch width distribution (in *mm*) of the raw FW detector distribution over bunch intensity versus store number.

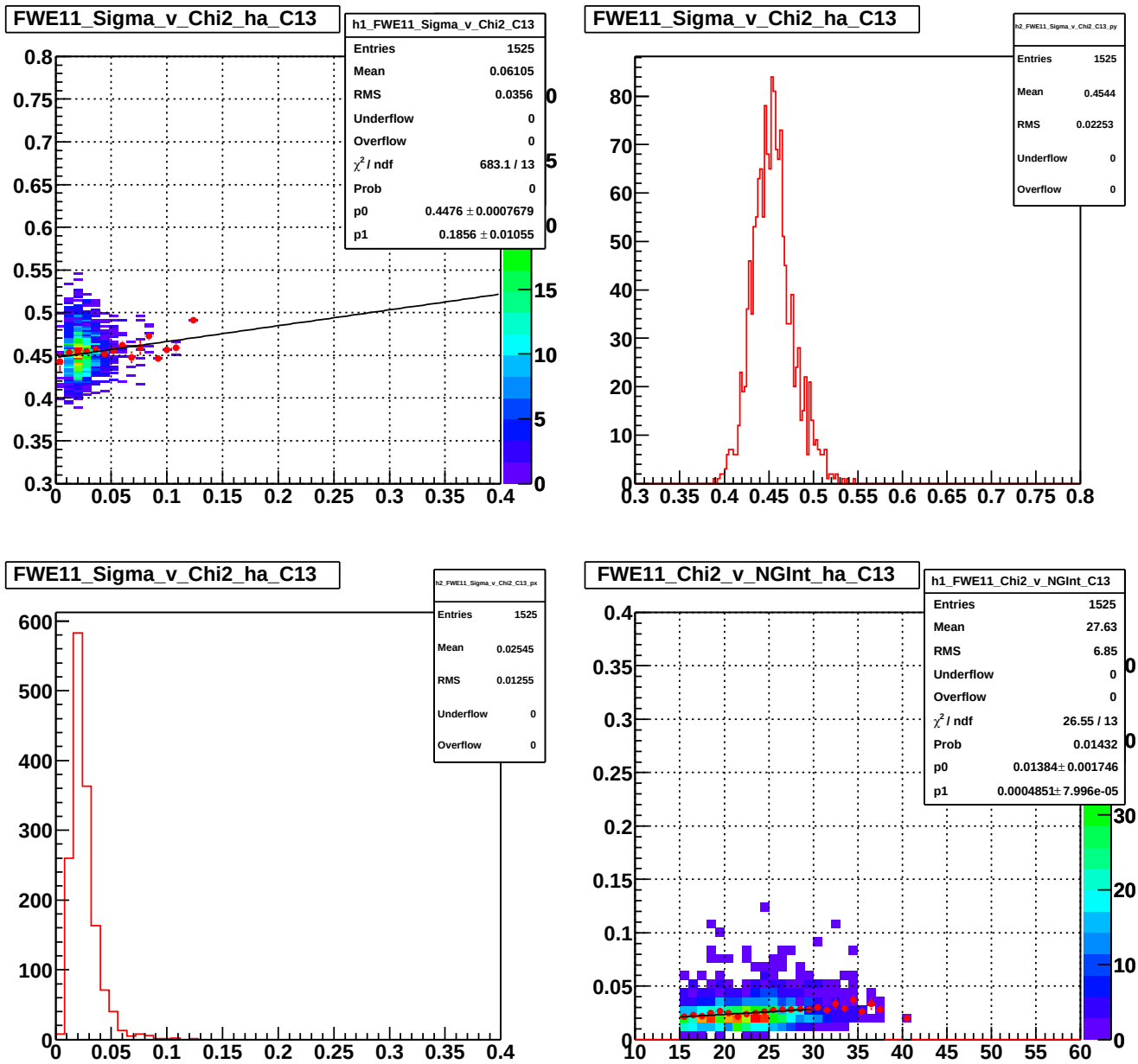

Figure 2: Antiproton beam, horizontal detectors: Performance of the Flying Wire Detector at the E11 location during Tevatron Remove Halo case: Sigma of the bunch width distribution (in *mm*) as measured by the FW detector versus front end measure of the goodness of fit together with an overlaid horizontal profile and a straight line fit; sigma itself, goodness of fit itself; goodness of fit versus bunch intensity together with an overlaid horizontal profile and a straight line fit;

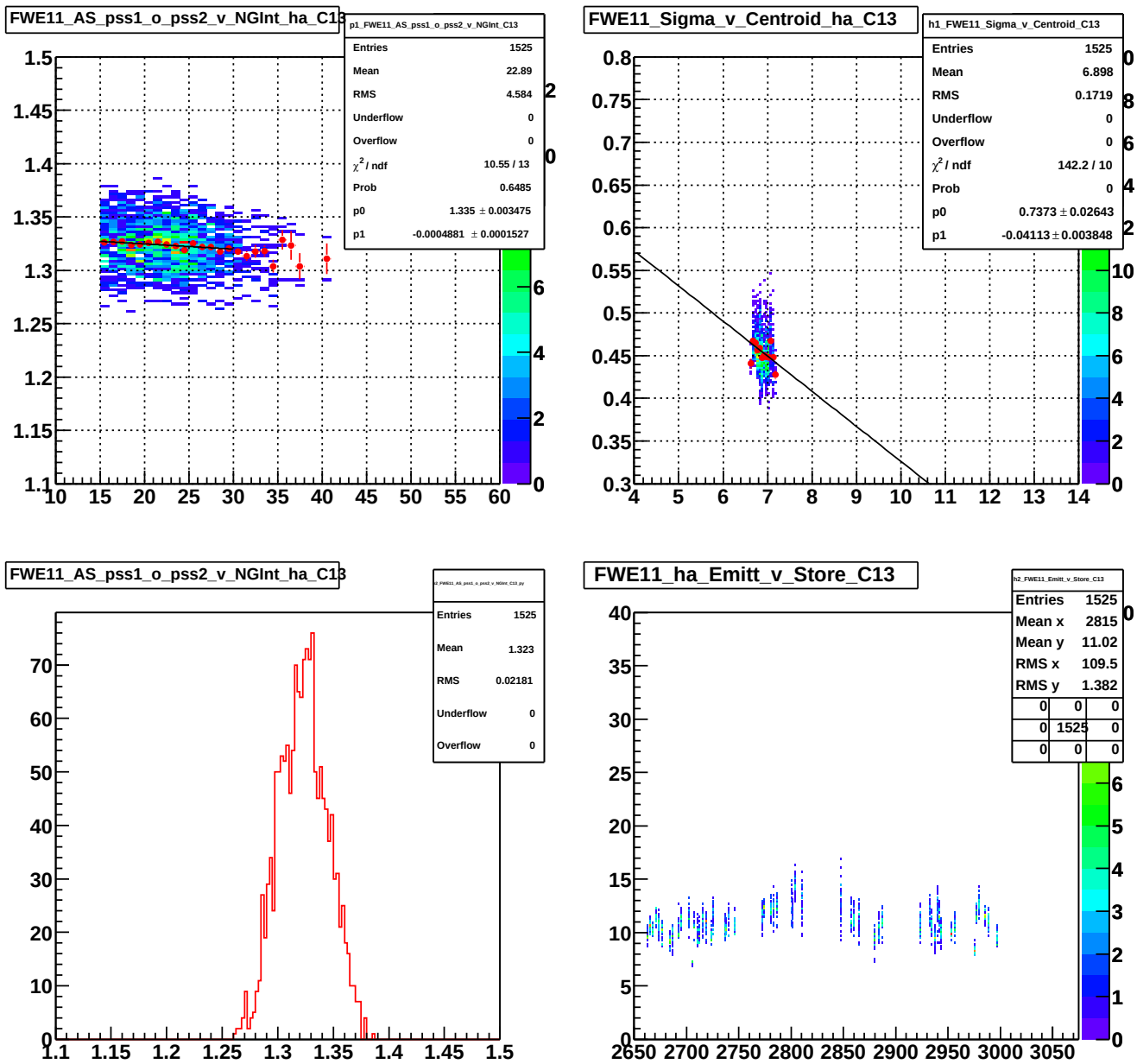

Figure 3: Antiproton beam, horizontal detectors: Performance of the Flying Wire Detector at the E11 location during Tevatron Remove Halo case: Amplitude (in arbitrary units) times sigma of the bunch width distribution (in *mm*) of the pass 1 over pass 2 of the front end FW detector data versus bunch intensity (ACNET variables T:FBI[A,P]NG) (in E9) together with an overlaid horizontal profile of that distribution with a straight line fit; sigma of the bunch width distribution versus bunch centroid (in *mm*) (based on the T:FW[E,H,V][A,P]CE ACNET variable) with an overlaid horizontal profile of that distribution with a straight line fit; amplitude (in arbitrary units) times sigma of the bunch width distribution (in *mm*) of the pass 1 over pass 2 of the front end FW detector data itself, bunch emittance (in $\pi \cdot mm \cdot mrad$) versus store number.

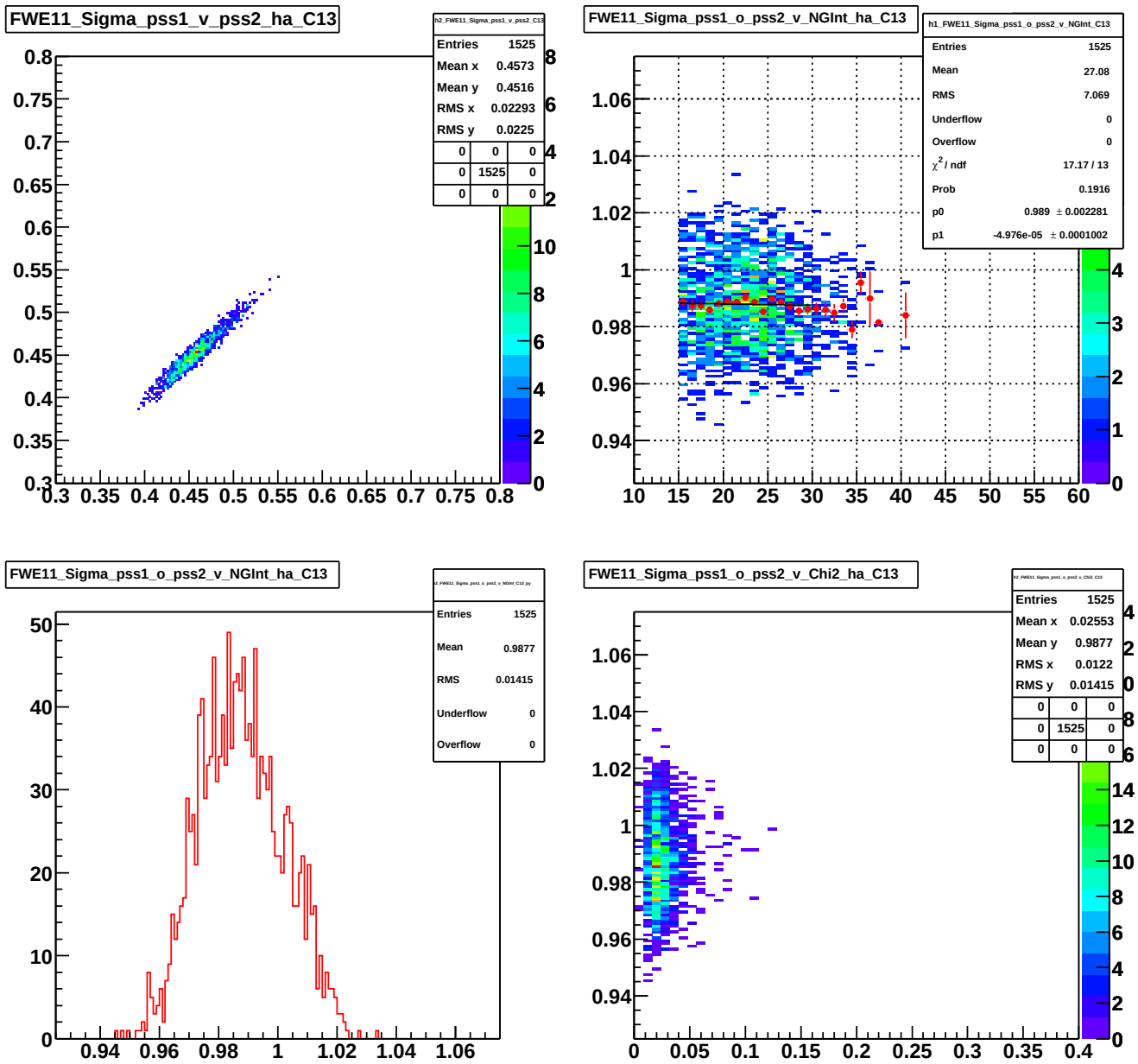

Figure 4: Antiproton beam, horizontal detectors: Performance of the Flying Wire Detector at the E11 location during Tevatron Remove Halo case: Sigma of the bunch width distribution (in *mm*) of the pass 1 versus pass 2 of the FW detector; sigma of the bunch width distribution (in *mm*) of the pass 1 over pass 2 of the FW detector versus bunch intensity (ACNET variables T:FBI[A,P]NG) (in E9) together with an overlaid horizontal profile and a straight line fit; sigma of the bunch width distribution (in *mm*) of the pass 1 over pass 2 of the FW detector itself, sigma of the bunch width distribution (in *mm*) of the pass 1 over pass 2 of the FW detector versus front end measure of the goodness of fit.

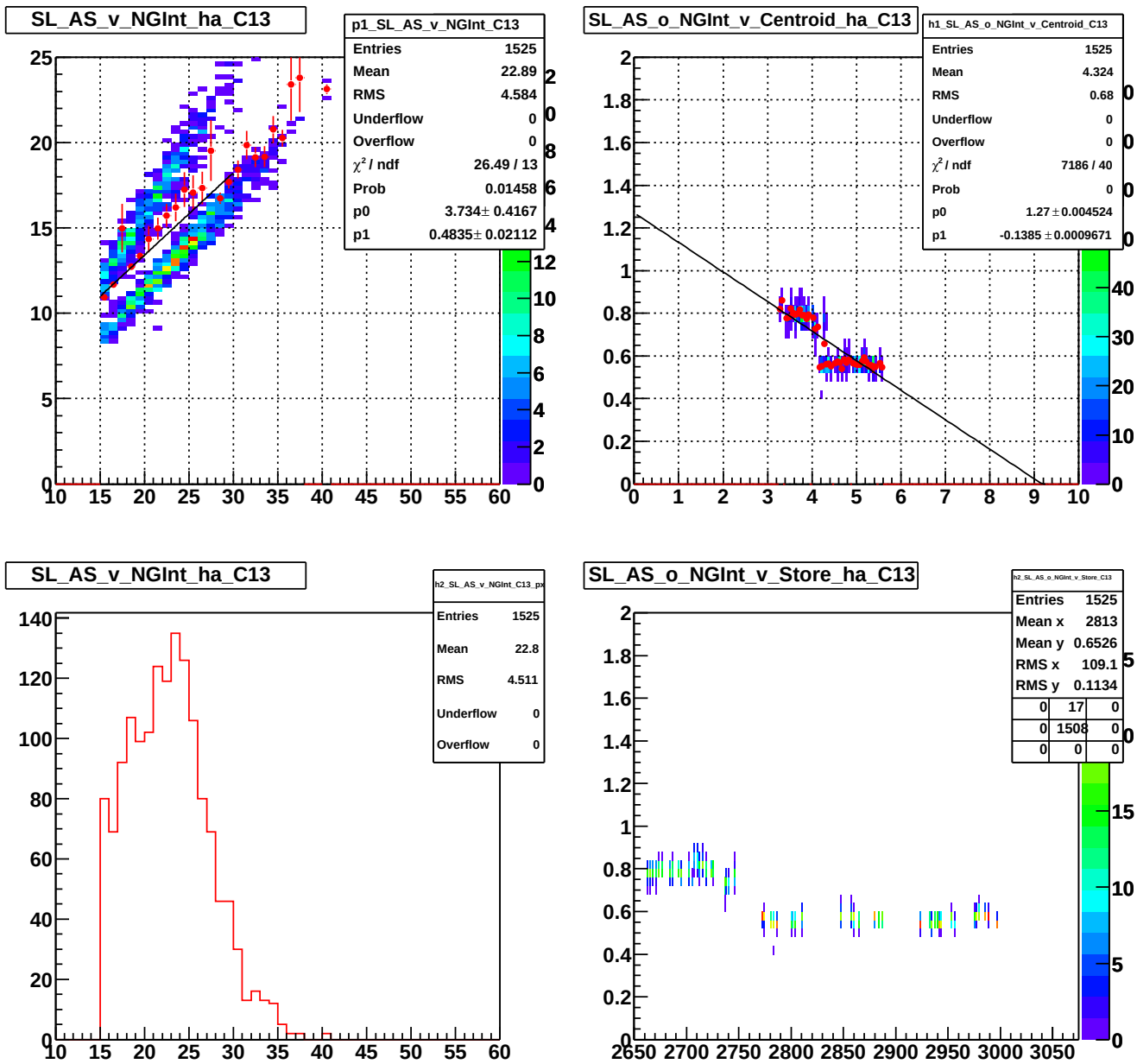

Figure 5: Antiproton beam, horizontal detectors: Performance of the Synchrotron Light Detector at the C11 location during Tevatron Remove Halo case: Amplitude (in arbitrary units) times sigma of the bunch width distribution (in *mm*) of the raw SL detector distribution versus bunch intensity (ACNET variables T:FBI[A,P]NG) (in E9) with an overlaid horizontal profile of that distribution with a straight line fit; amplitude times sigma of the bunch width distribution (in *mm*) of the raw SL detector distribution over bunch intensity versus bunch E11 centroid (in *mm*) (based on the T:FW[E,H,V][A,P]CE ACNET variable) with an overlaid horizontal profile of that distribution with a straight line fit; bunch intensity; amplitude times sigma of the bunch width distribution (in *mm*) of the raw SL detector distribution over bunch intensity versus store number.

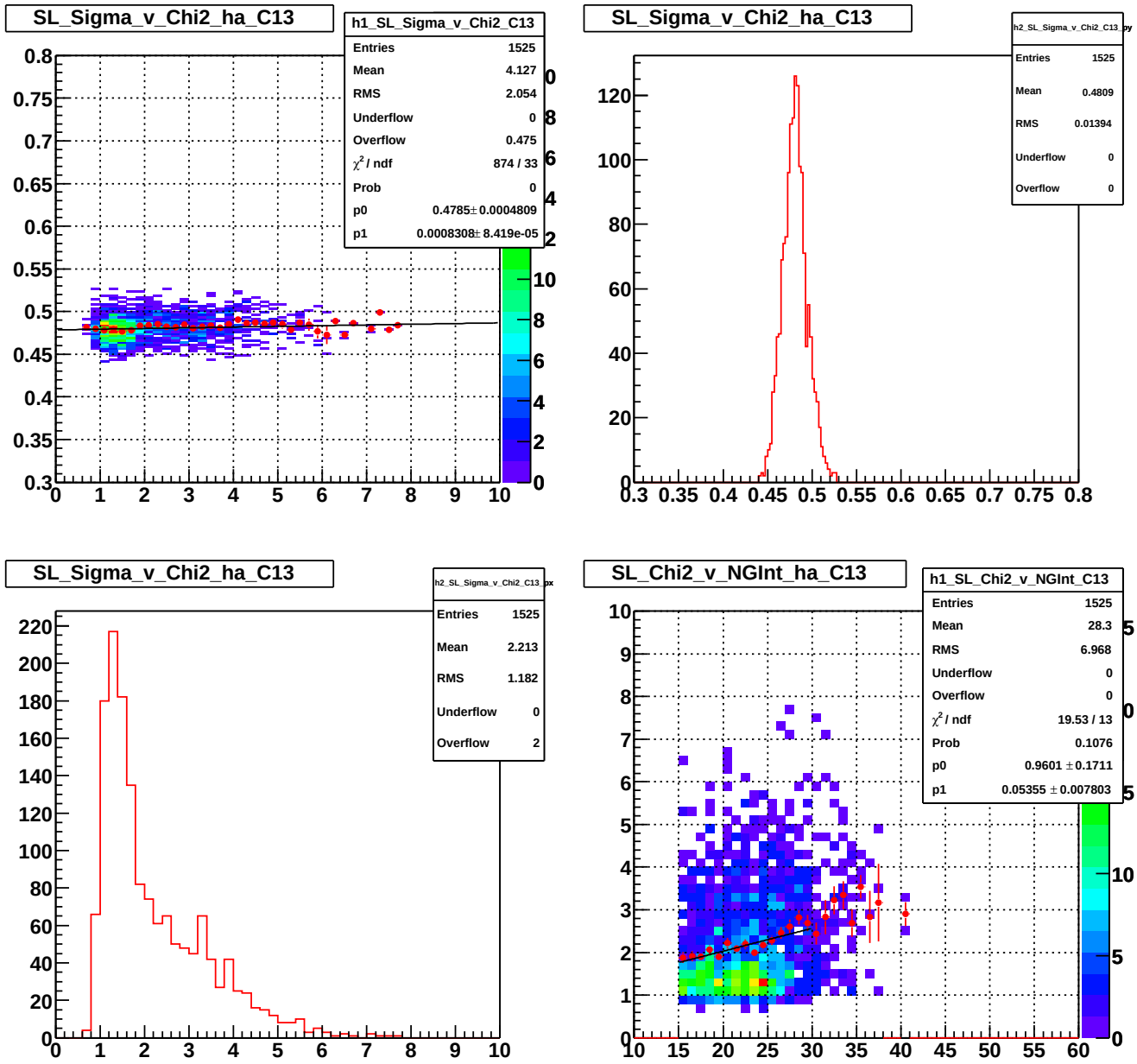

Figure 6: Antiproton beam, horizontal detectors: Performance of the Synchrotron Light Detector at the C11 location during Tevatron Remove Halo case: Sigma of the bunch width distribution (in *mm*) as measured by the SL detector versus front end measure of the goodness of fit together with an overlaid horizontal profile and a straight line fit; sigma of the bunch width distribution (in *mm*) itself; goodness of fit itself; goodness of fit versus bunch intensity together with an overlaid horizontal profile and a straight line fit.

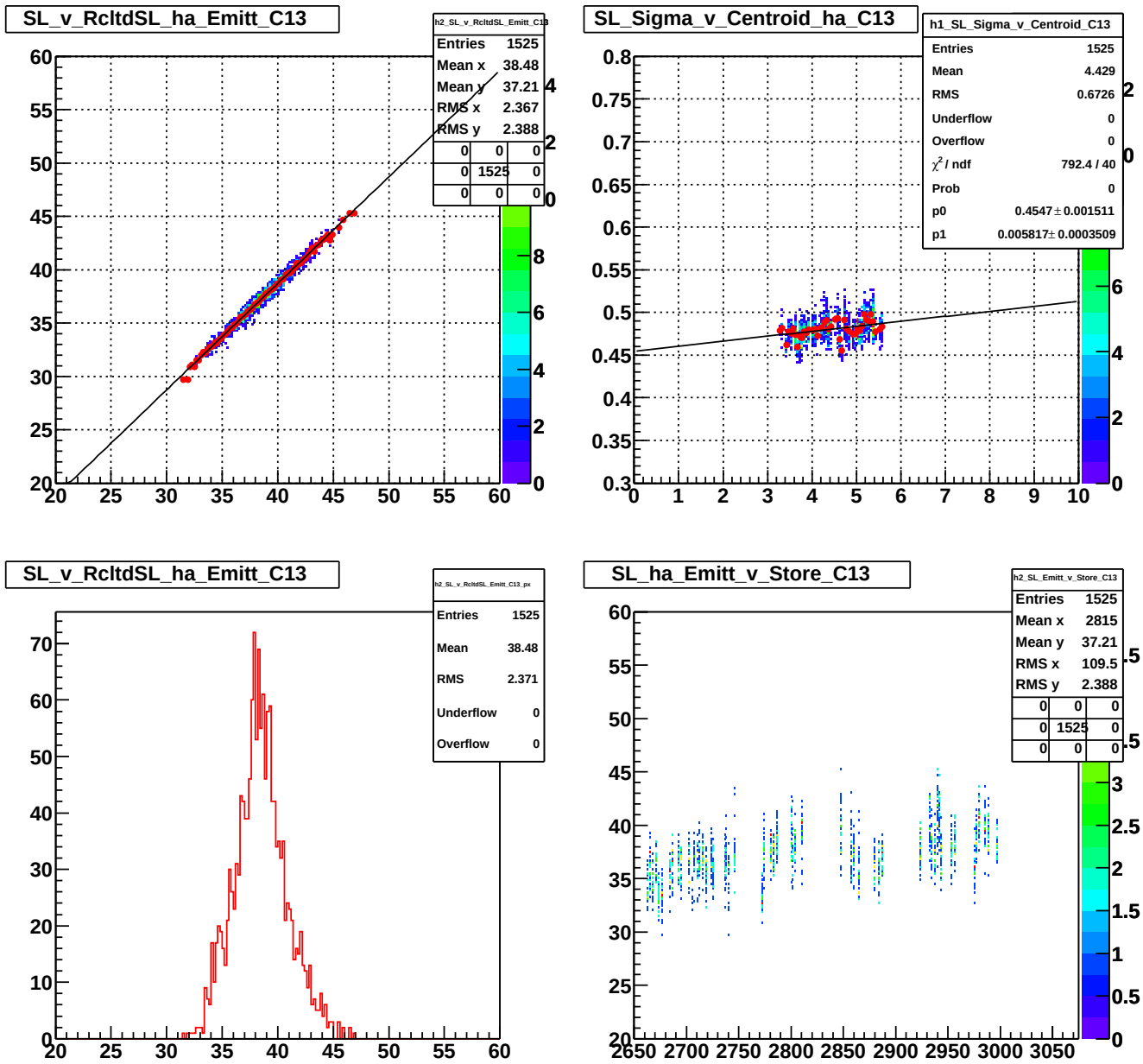

Figure 7: Antiproton beam, horizontal detectors: Performance of the Synchrotron Light Detector at the C11 location during Tevatron Remove Halo case: Bunch emittance (in $\pi \cdot mm \cdot mrad$) as measured by the front end SL detector versus bunch emittance as recalculated using front end sigma of the bunch width distribution (in *mm*) (combined with SBD timing information in the horizontal cases) together with an overlaid horizontal profile of that distribution with a straight line fit; sigma of the bunch width distribution versus bunch E11 centroid (in *mm*) (based on the T:FW[E,H,V][A,P]CE ACNET variable) with an overlaid horizontal profile of that distribution with a straight line fit; bunch emittance; bunch emittance versus store number.

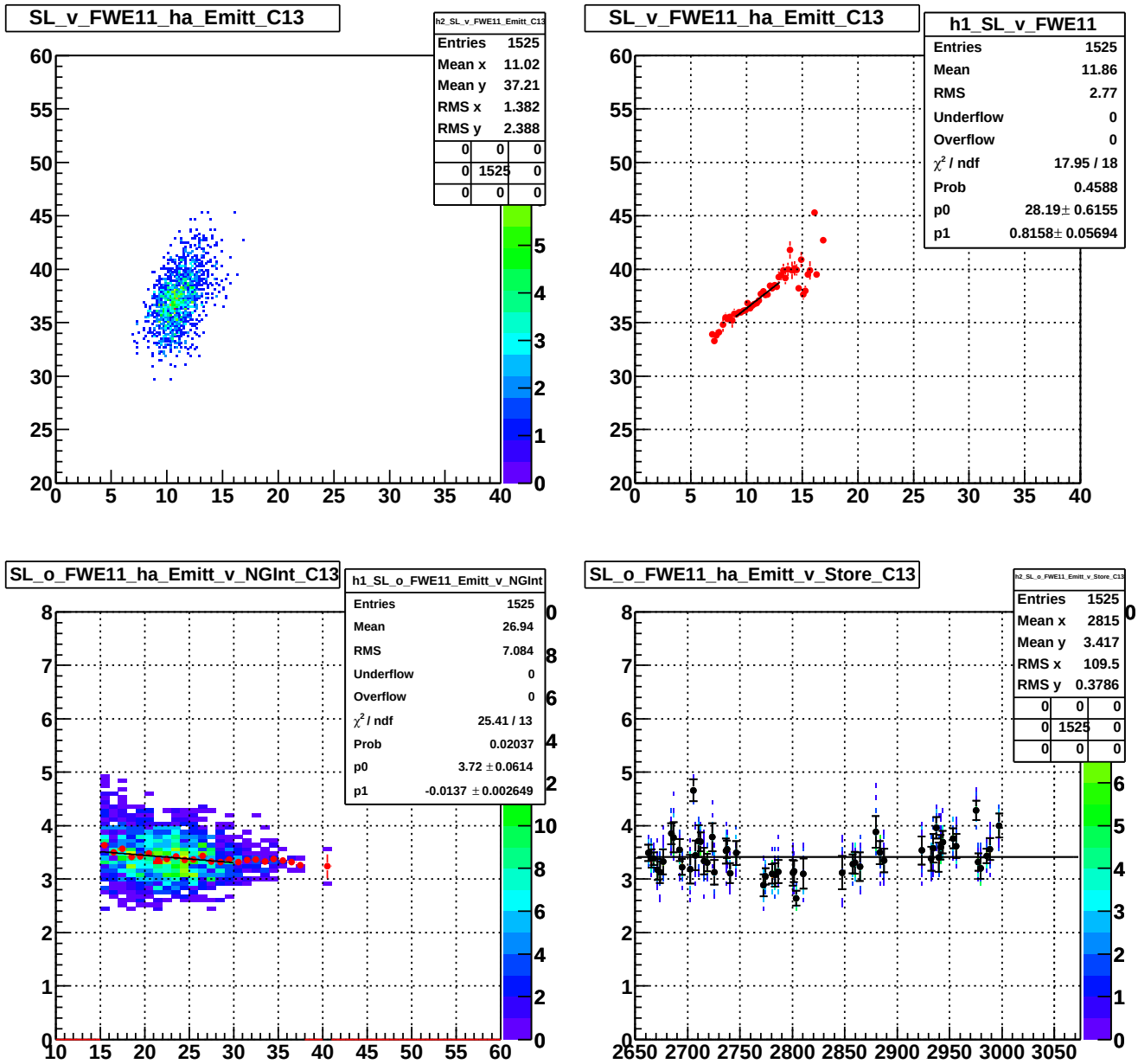

Figure 8: Antiproton beam, horizontal detectors: Comparisons of Emittance measurements as done by Synchrotron Light Detector at C11 and Flying Wire Detector at E11 during Tevatron Remove Halo case: Bunch emittance (in $\pi \cdot mm \cdot mrad$) as measured by Synchrotron Light Detector versus bunch emittance as measured by the Flying Wire Detector at E11; horizontal profile of the previous distribution with a straight line fit; bunch emittance as measured by Synchrotron Light Detector over bunch emittance as measured by the Flying Wire Detector at E11 versus bunch intensity (ACNET variables T:FBI[A,P]NG) (in E9) together with an overlaid horizontal profile and a straight line fit; bunch emittance as measured by Synchrotron Light Detector over bunch emittance as measured by the Flying Wire Detector at E11 versus store number with overlaid averaged ratios for each store and a horizontal line fit.

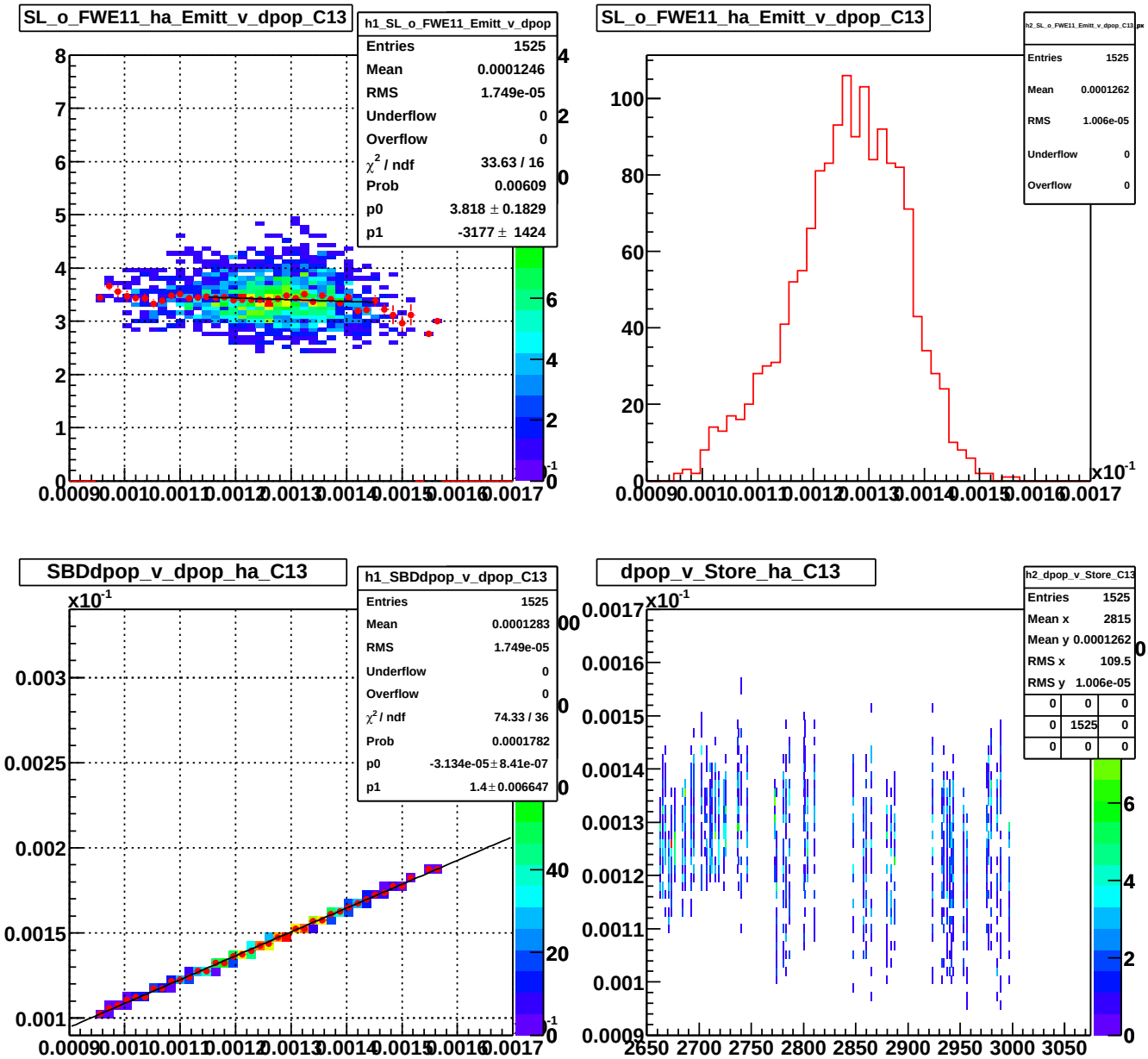

Figure 9: Antiproton beam, horizontal detectors: Comparisons of Emittance measurements as done by Synchrotron Light Detector at C11 and Flying Wire Detector at E11 during Tevatron Remove Halo case: Bunch emittance as measured by Synchrotron Light Detector over bunch emittance as measured by the Flying Wire Detector at E11 versus recalculated $\delta p/p$ (based on δt the T:SBD[A,P]SS ACNET variable) with an overlaid horizontal profile of the previous distribution with a straight line fit; $\delta p/p$ itself; frontend value of $\delta p/p$ versus recalculated $\delta p/p$; $\delta p/p$ versus store number.

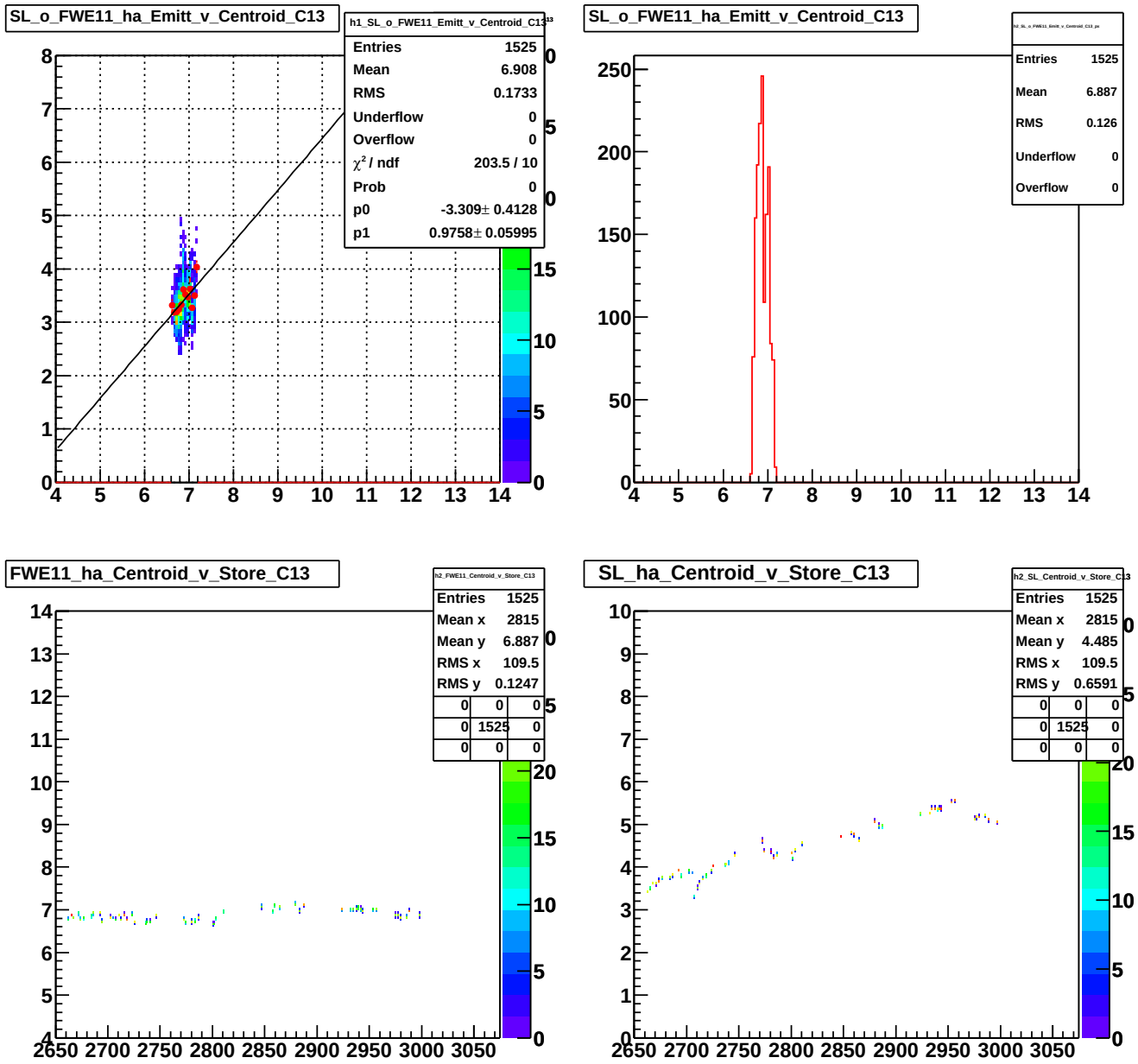

Figure 10: Antiproton beam, horizontal detectors: Comparisons of Emittance measurements as done by Synchrotron Light Detector at C11 and Flying Wire Detector at E11 during Tevatron Remove Halo case: Bunch emittance as measured by Synchrotron Light Detector over bunch emittance as measured by the Flying Wire Detector at E11 versus bunch E11 centroid (in *mm*) (based on the T:FW[E,H,V][A,P]CE ACNET variable) with an overlaid horizontal profile of the previous distribution with a straight line fit; bunch E11 centroid itself; bunch E11 centroid versus store number. bunch C11 centroid versus store number.

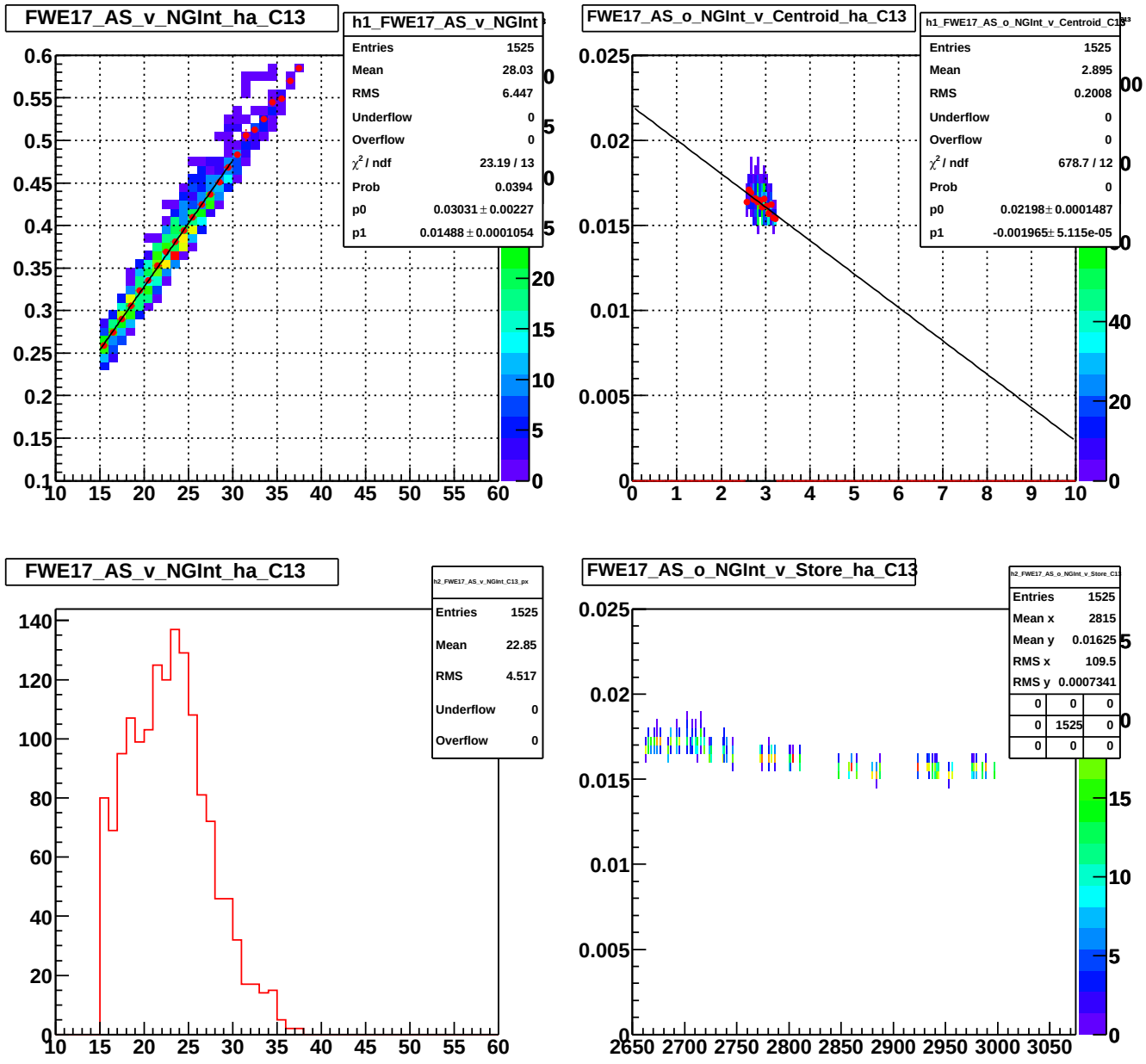

Figure 11: Antiproton beam, horizontal detectors: Performance of the Flying Wire Detector at the E17 location during Tevatron Remove Halo case: Amplitude (in arbitrary units) times sigma of the bunch width distribution (in *mm*) of the front end FW detector data versus bunch intensity (ACNET variables T:FBI[A,P]NG) (in E9) with an overlaid horizontal profile of that distribution with a straight line fit; Amplitude times sigma of the bunch width distribution of the front end FW detector data over bunch intensity versus bunch E17 centroid (in *mm*) (based on the T:FW[E,H,V][A,P]CE ACNET variable) with an overlaid horizontal profile of that distribution with a straight line fit; bunch intensity; amplitude times sigma of the bunch width distribution (in *mm*) of the raw FW detector distribution over bunch intensity versus store number.

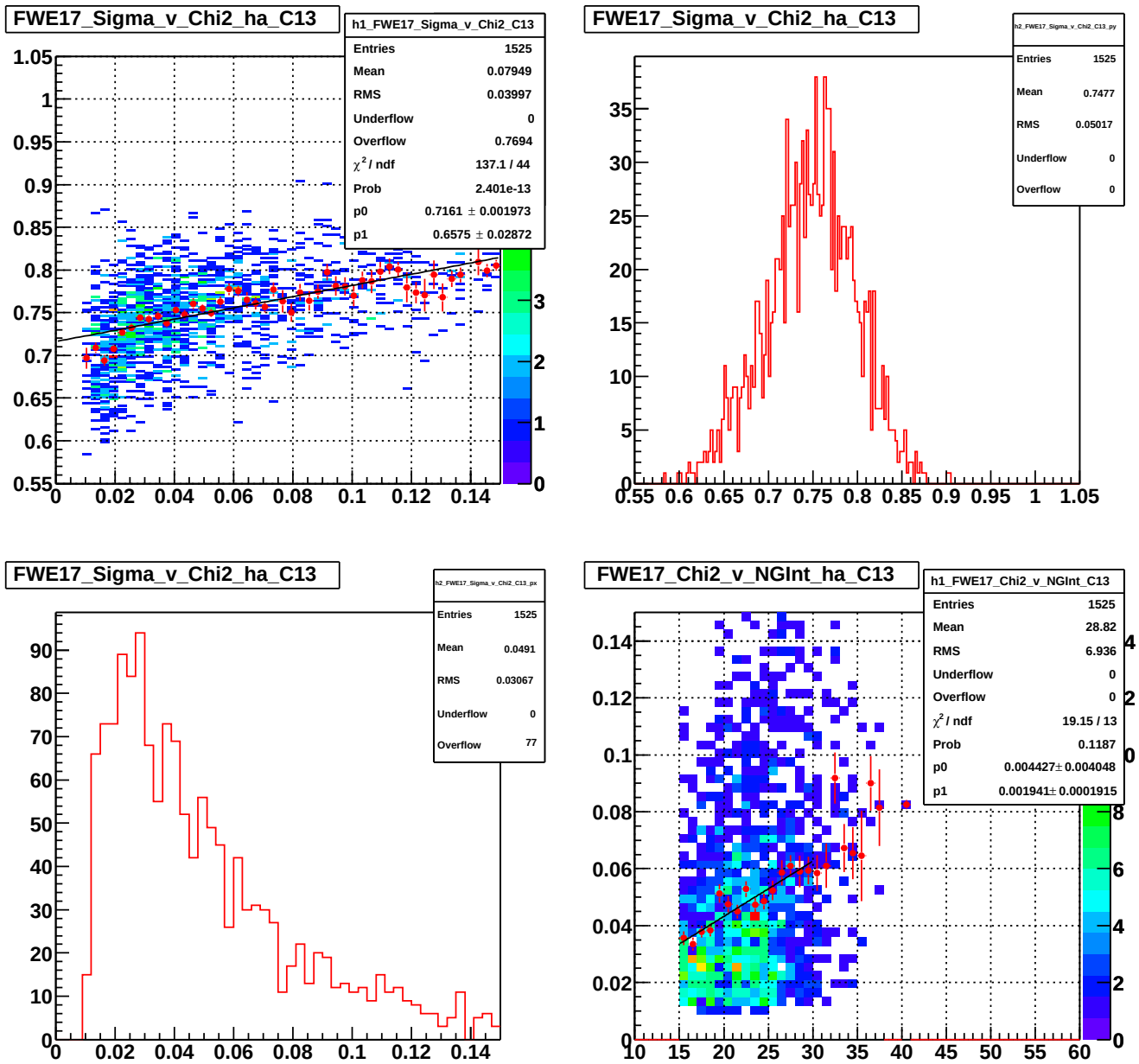

Figure 12: Antiproton beam, horizontal detectors: Performance of the Flying Wire Detector at the E17 location during Tevatron Remove Halo case: Sigma of the bunch width distribution (in *mm*) as measured by the FW detector versus front end measure of the goodness of fit together with an overlaid horizontal profile and a straight line fit; sigma itself, goodness of fit itself; goodness of fit versus bunch intensity together with an overlaid horizontal profile and a straight line fit.

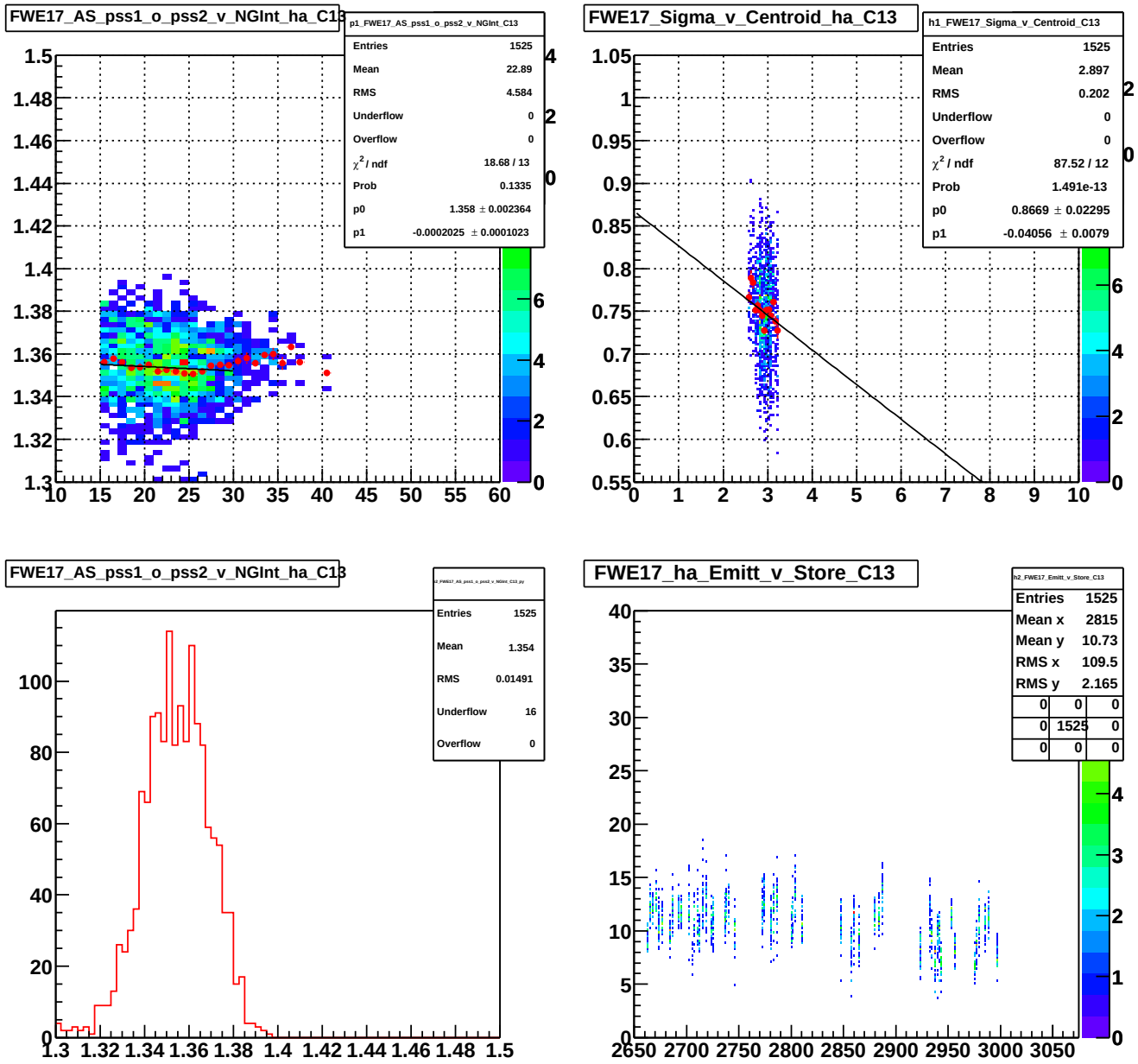

Figure 13: Antiproton beam, horizontal detectors: Performance of the Flying Wire Detector at the E17 location during Tevatron Remove Halo case: Amplitude (in arbitrary units) times sigma of the bunch width distribution (in *mm*) of the pass 1 over pass 2 of the front end FW detector data versus bunch intensity (ACNET variables T:FBI[A,P]NG) (in E9) together with an overlaid horizontal profile of that distribution with a straight line fit; sigma of the bunch width distribution versus bunch centroid (in *mm*) (based on the T:FW[E,H,V][A,P]CE ACNET variable) with an overlaid horizontal profile of that distribution with a straight line fit; amplitude (in arbitrary units) times sigma of the bunch width distribution (in *mm*) of the pass 1 over pass 2 of the front end FW detector data itself, bunch emittance (in $\pi \cdot mm \cdot mrad$) versus store number.

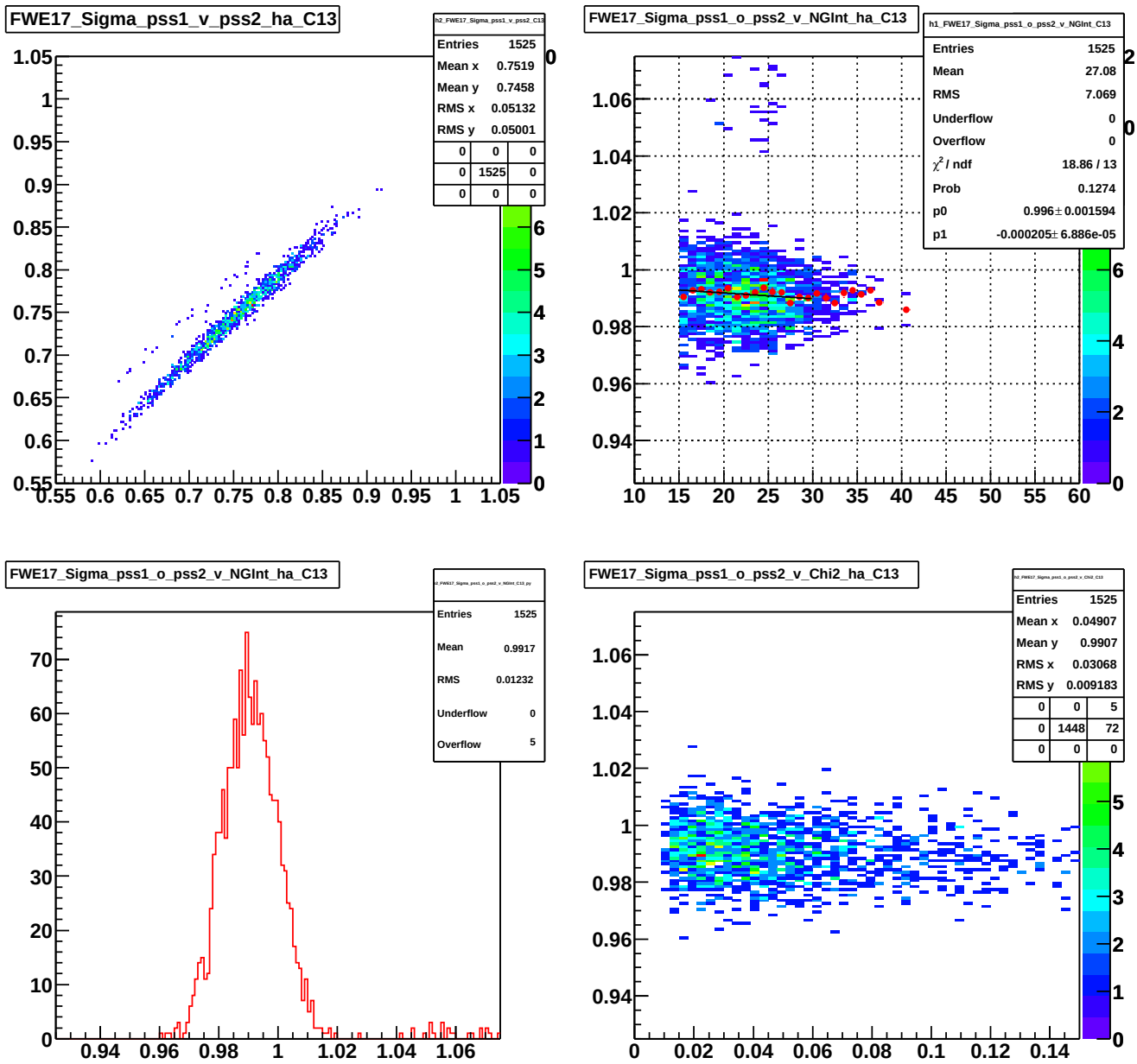

Figure 14: Antiproton beam, horizontal detectors: Performance of the Flying Wire Detector at the E17 location during Tevatron Remove Halo case: Sigma of the bunch width distribution (in *mm*) of the pass 1 versus pass 2 of the FW detector; sigma of the bunch width distribution (in *mm*) of the pass 1 over pass 2 of the FW detector versus bunch intensity (ACNET variables T:FBI[A,P]NG) (in E9) together with an overlaid horizontal profile and a straight line fit; sigma of the bunch width distribution (in *mm*) of the pass 1 over pass 2 of the FW detector itself, sigma of the bunch width distribution (in *mm*) of the pass 1 over pass 2 of the FW detector versus front end measure of the goodness of fit.

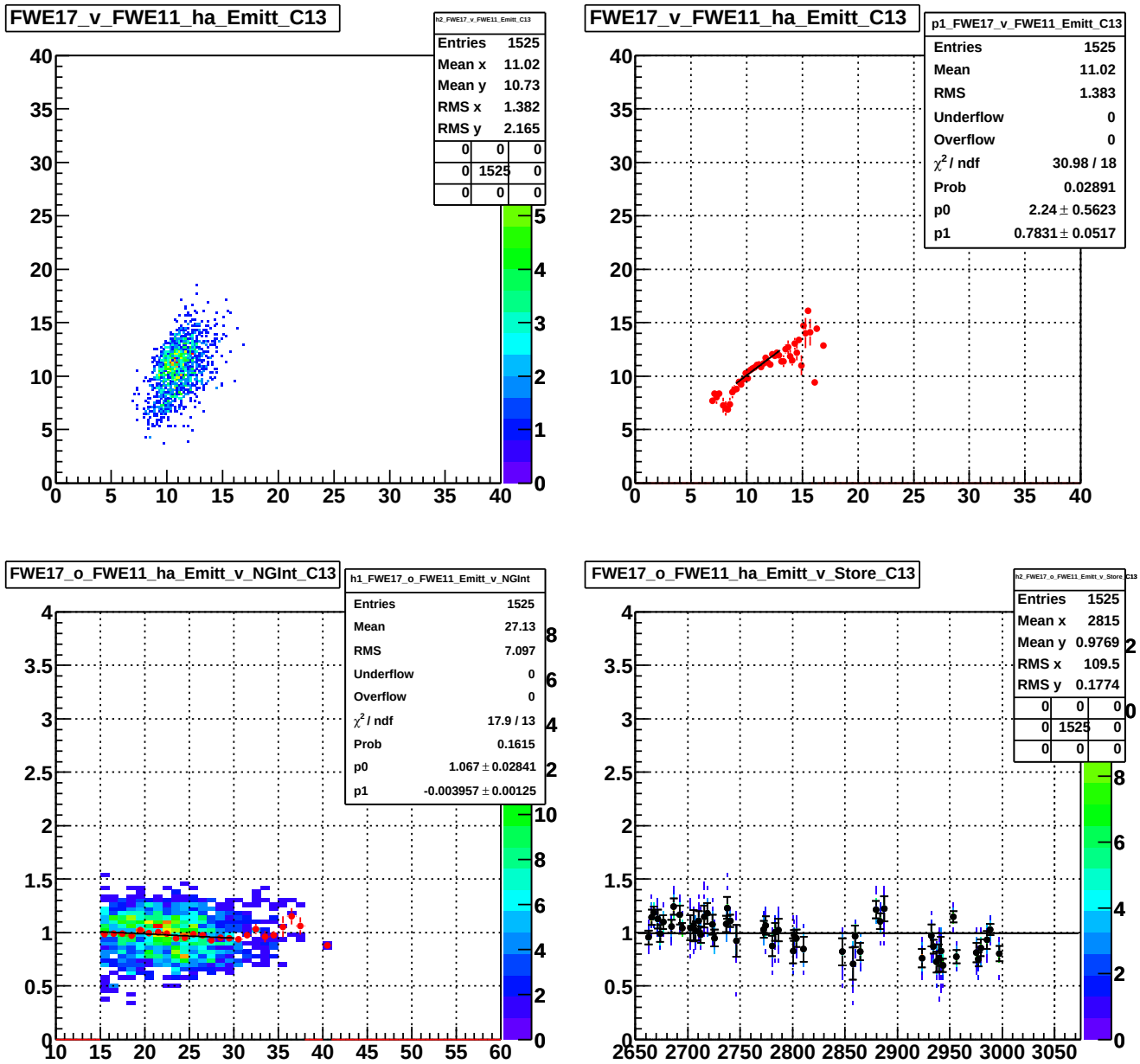

Figure 15: Antiproton beam, horizontal detectors: Comparisons of Emittance measurements as done by Flying Wire Detector at E17 and Flying Wire Detector at E11 during Tevatron Remove Halo case: Bunch emittance (in $\pi \cdot mm \cdot mrad$) as measured by Flying Wire Detector at E17 versus bunch emittance as measured by the Flying Wire Detector at E11; horizontal profile of the previous distribution with a straight line fit; bunch emittance as measured by Flying Wire Detector at E17over bunch emittance as measured by the Flying Wire Detector at E11 versus bunch intensity (ACNET variables T:FBI[A,P]NG) (in E9) together with an overlaid horizontal profile and a straight line fit; bunch emittance as measured by Flying Wire Detector at E17 over bunch emittance as measured by the Flying Wire Detector at E11 versus store number with overlaid averaged ratios for each store and a horizontal line fit.

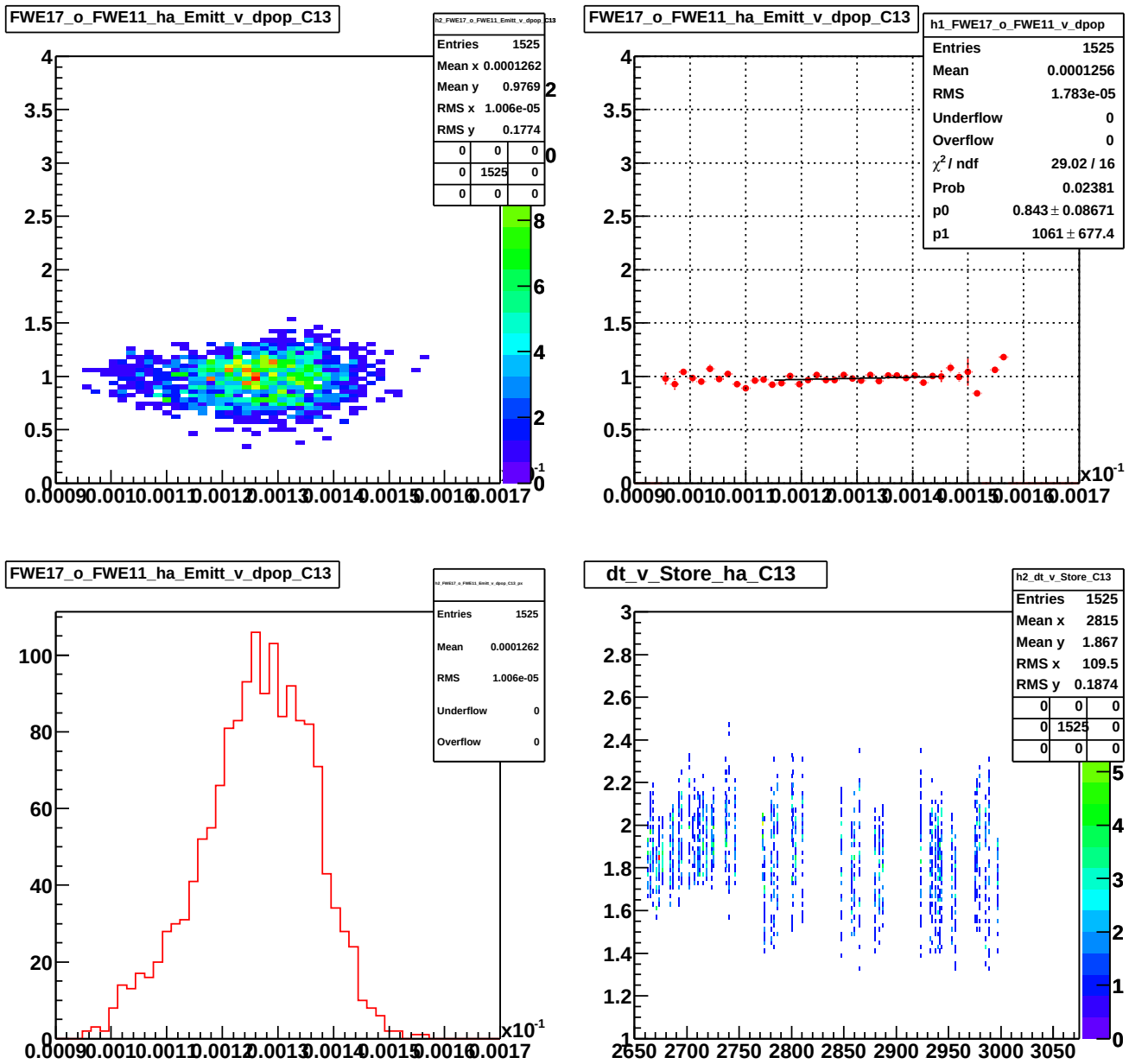

Figure 16: Antiproton beam, horizontal detectors: Comparisons of Emittance measurements as done by Flying Wire Detector at E17 and Flying Wire Detector at E11 during Tevatron Remove Halo case: Bunch emittance as measured by Flying Wire Detector at E17 over bunch emittance as measured by the Flying Wire Detector at E11 versus recalculated $\delta p/p$ (based on δt the T:SBD[A,P]SS ACNET variable); horizontal profile of the previous distribution with a straight line fit; $\delta p/p$ itself; δt versus store number.

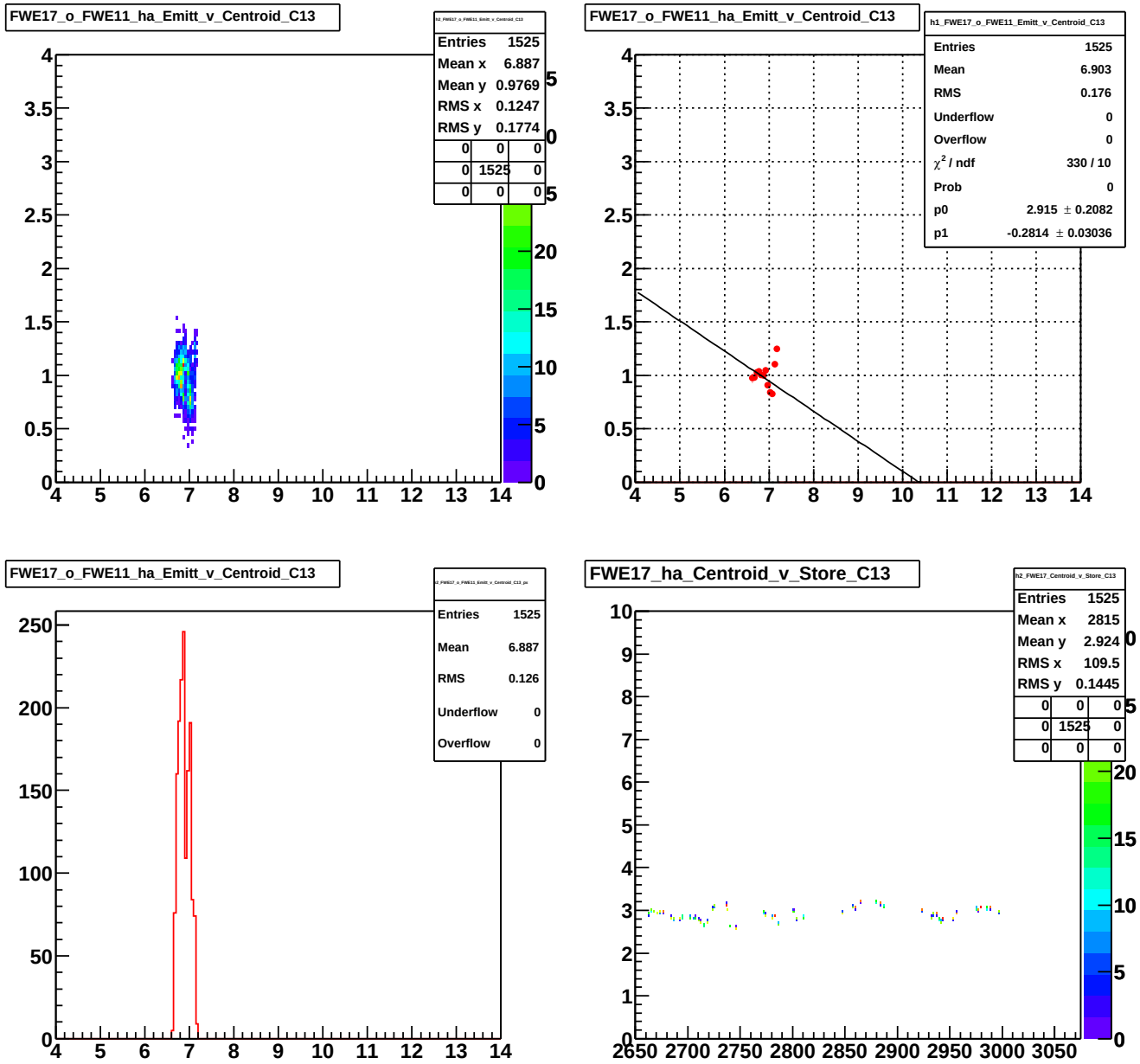

Figure 17: Antiproton beam, horizontal detectors: Comparisons of Emittance measurements as done by Flying Wire Detector at E17 and Flying Wire Detector at E11 during Tevatron Remove Halo case: Bunch emittance as measured by Flying Wire Detector at E17 over bunch emittance as measured by the Flying Wire Detector at E11 versus bunch E11 centroid (in *mm*) (based on the T:FW[E,H,V][A,P]CE ACNET variable); horizontal profile of the previous distribution with a straight line fit; bunch E17 centroid; bunch E17 centroid versus store number.

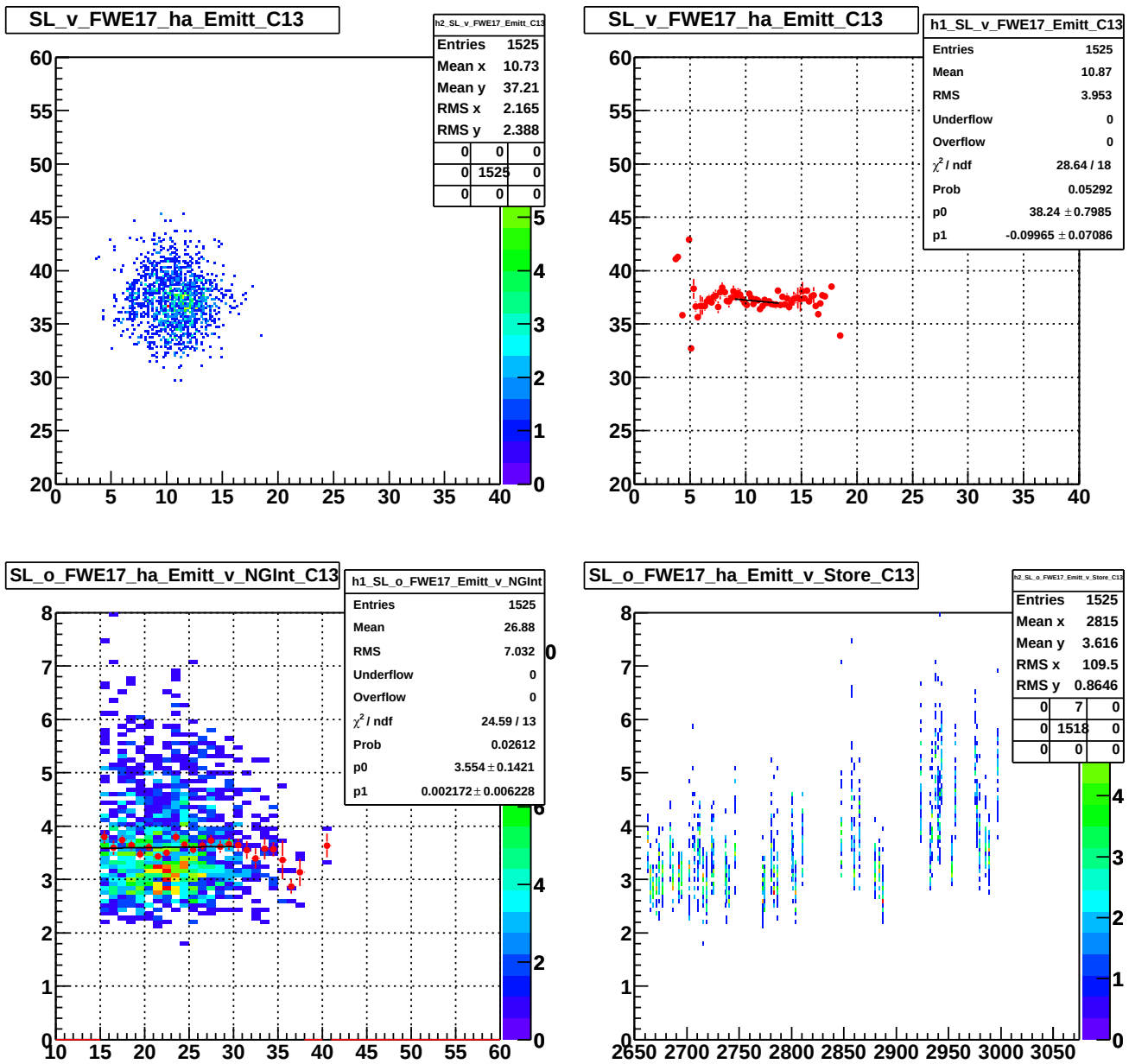

Figure 18: Antiproton beam, horizontal detectors: Comparisons of Emittance measurements as done by Synchrotron Light Detector at C11 and Flying Wire Detector at E17 during Tevatron Remove Halo case: Bunch emittance (in $\pi \cdot mm \cdot mrad$) as measured by Synchrotron Light Detector versus bunch emittance as measured by the Flying Wire Detector at E17; horizontal profile of the previous distribution with a straight line fit; bunch emittance as measured by Synchrotron Light Detector over bunch emittance as measured by the Flying Wire Detector at E17 versus bunch intensity (ACNET variables T:FBI[A,P]NG) (in E9) together with an overlaid horizontal profile and a straight line fit; bunch emittance as measured by Synchrotron Light Detector over bunch emittance as measured by the Flying Wire Detector at E17 versus store number.

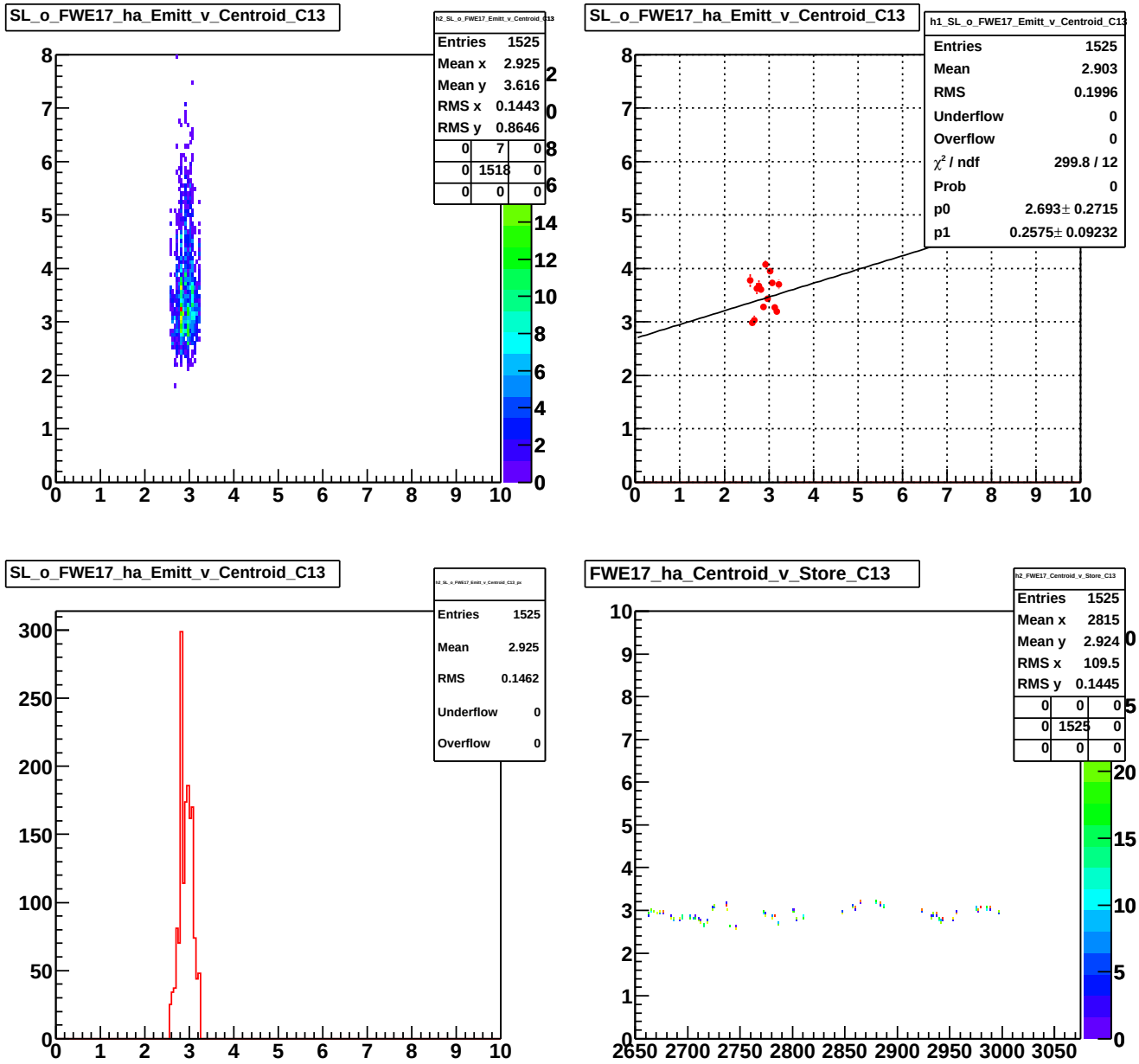

Figure 19: Antiproton beam, horizontal detectors: Comparisons of Emittance measurements as done by Synchrotron Light Detector at C11 and Flying Wire Detector at E17 during Tevatron Remove Halo case: Bunch emittance as measured by Synchrotron Light Detector over bunch emittance as measured by the Flying Wire Detector at E17 versus bunch E17 centroid (in *mm*) (based on the T:FW[E,H,V][A,P]CE ACNET variable); horizontal profile of the previous distribution with a straight line fit; bunch E17 centroid itself; bunch E17 centroid versus store number.

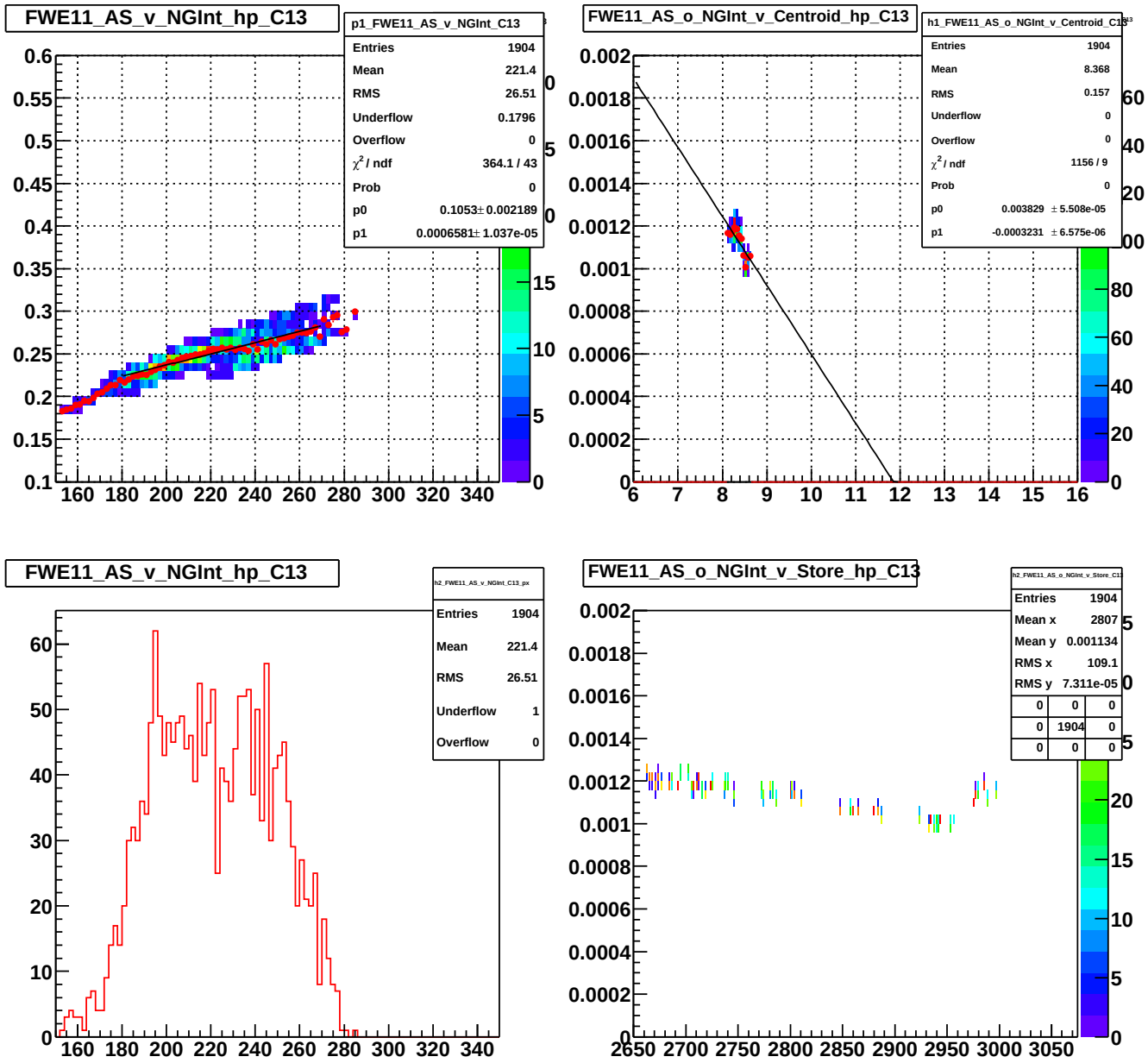

Figure 20: Proton beam, horizontal detectors: Performance of the Flying Wire Detector at the E11 location during Tevatron Remove Halo case: Amplitude (in arbitrary units) times sigma of the bunch width distribution (in *mm*) of the front end FW detector data versus bunch intensity (ACNET variables T:FBI[A,P]NG) (in E9) with an overlaid horizontal profile of that distribution with a straight line fit; Amplitude times sigma of the bunch width distribution of the front end FW detector data over bunch intensity versus bunch E11 centroid (in *mm*) (based on the T:FW[E,H,V][A,P]CE ACNET variable) with an overlaid horizontal profile of that distribution with a straight line fit; bunch intensity; amplitude times sigma of the bunch width distribution (in *mm*) of the raw FW detector distribution over bunch intensity versus store number.

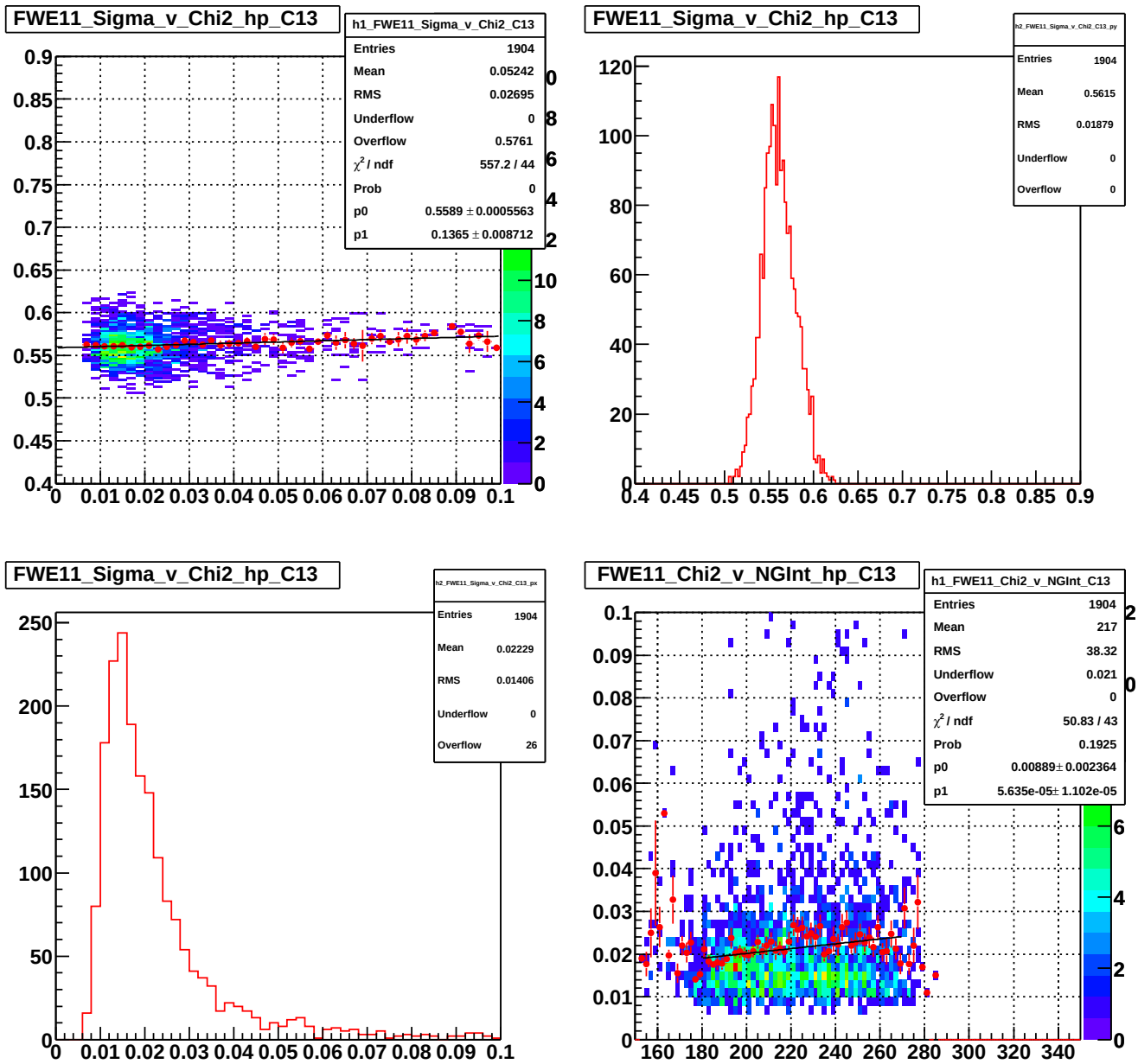

Figure 21: Proton beam, horizontal detectors: Performance of the Flying Wire Detector at the E11 location during Tevatron Remove Halo case: Sigma of the bunch width distribution (in *mm*) as measured by the FW detector versus front end measure of the goodness of fit together with an overlaid horizontal profile and a straight line fit; sigma itself, goodness of fit itself; goodness of fit versus bunch intensity together with an overlaid horizontal profile and a straight line fit;

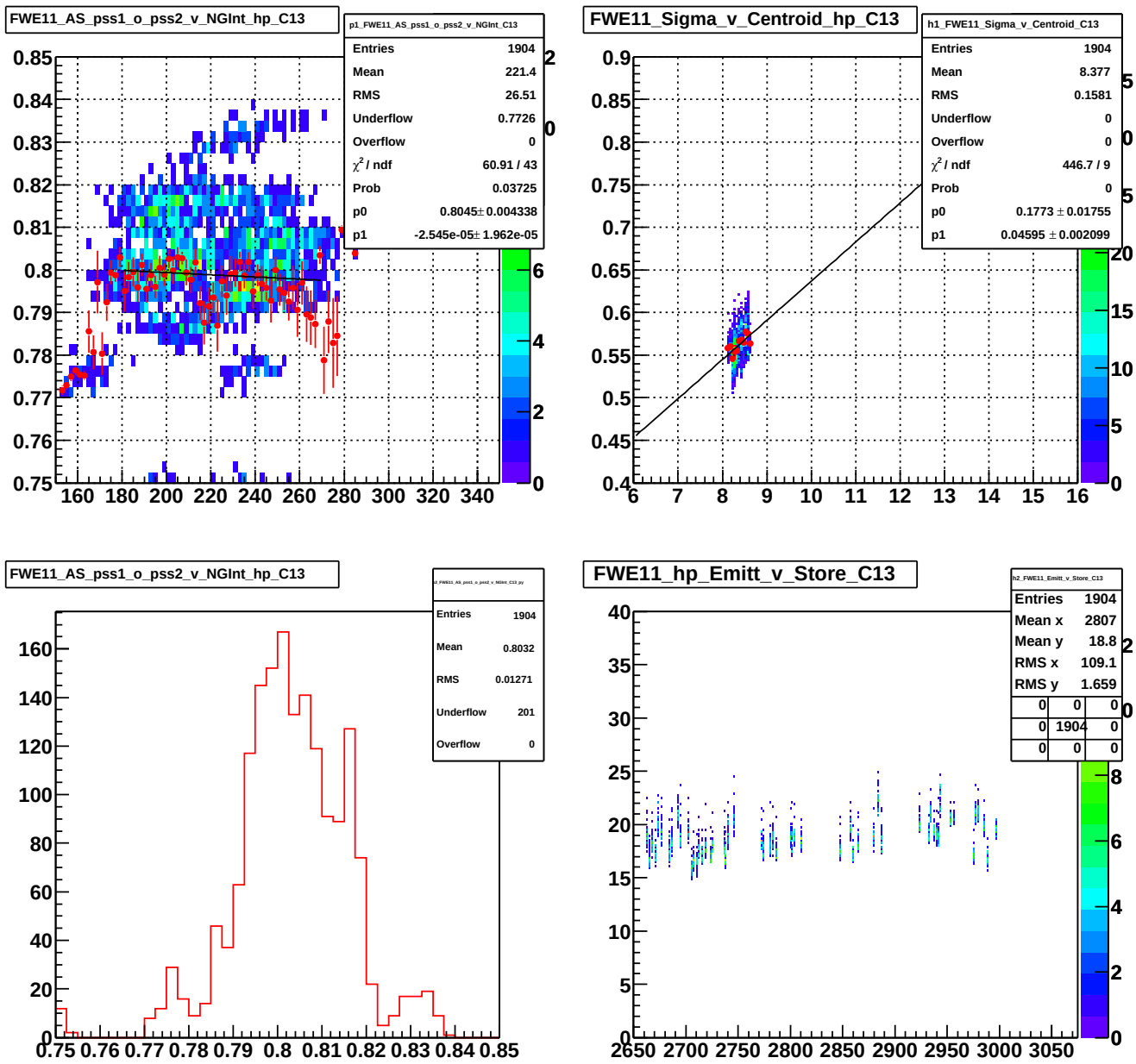

Figure 22: Proton beam, horizontal detectors: Performance of the Flying Wire Detector at the E11 location during Tevatron Remove Halo case: Amplitude (in arbitrary units) times sigma of the bunch width distribution (in *mm*) of the pass 1 over pass 2 of the front end FW detector data versus bunch intensity (ACNET variables T:FBI[A,P]NG) (in E9) together with an overlaid horizontal profile of that distribution with a straight line fit; sigma of the bunch width distribution versus bunch centroid (in *mm*) (based on the T:FW[E,H,V][A,P]CE ACNET variable) with an overlaid horizontal profile of that distribution with a straight line fit; amplitude (in arbitrary units) times sigma of the bunch width distribution (in *mm*) of the pass 1 over pass 2 of the front end FW detector data itself, bunch emittance (in $\pi \cdot mm \cdot mrad$) versus store number.

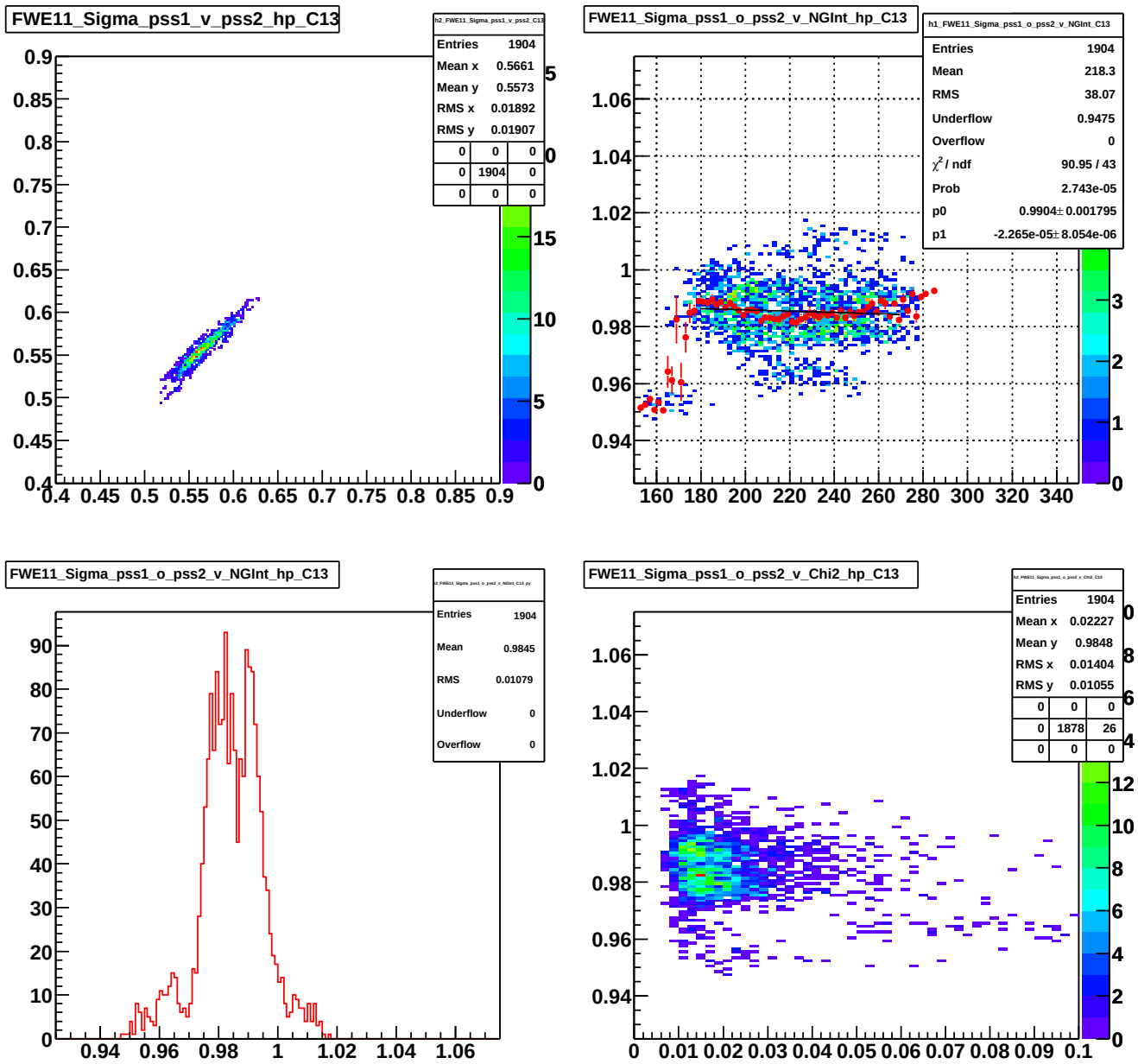

Figure 23: Proton beam, horizontal detectors: Performance of the Flying Wire Detector at the E11 location during Tevatron Remove Halo case: Sigma of the bunch width distribution (in *mm*) of the pass 1 versus pass 2 of the FW detector; sigma of the bunch width distribution (in *mm*) of the pass 1 over pass 2 of the FW detector versus bunch intensity (ACNET variables T:FBI[A,P]NG) (in E9) together with an overlaid horizontal profile and a straight line fit; sigma of the bunch width distribution (in *mm*) of the pass 1 over pass 2 of the FW detector itself, sigma of the bunch width distribution (in *mm*) of the pass 1 over pass 2 of the FW detector versus front end measure of the goodness of fit.

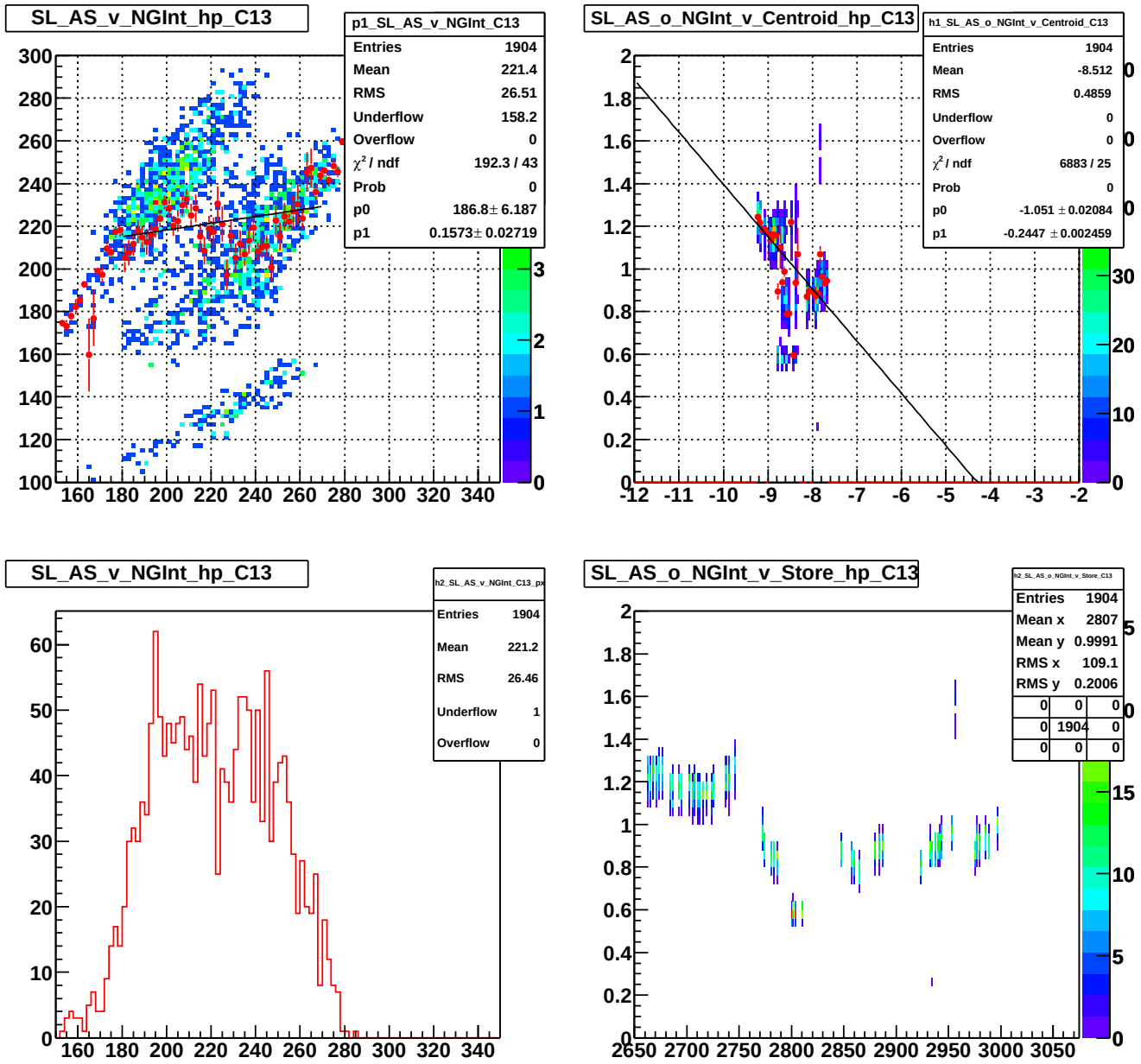

Figure 24: Proton beam, horizontal detectors: Performance of the Synchrotron Light Detector at the C11 location during Tevatron Remove Halo case: Amplitude (in arbitrary units) times sigma of the bunch width distribution (in *mm*) of the raw SL detector distribution versus bunch intensity (ACNET variables T:FBI[A,P]NG) (in E9) with an overlaid horizontal profile of that distribution with a straight line fit; amplitude times sigma of the bunch width distribution (in *mm*) of the raw SL detector distribution over bunch intensity versus bunch E11 centroid (in *mm*) (based on the T:FW[E,H,V][A,P]CE ACNET variable) with an overlaid horizontal profile of that distribution with a straight line fit; bunch intensity; amplitude times sigma of the bunch width distribution (in *mm*) of the raw SL detector distribution over bunch intensity versus store number.

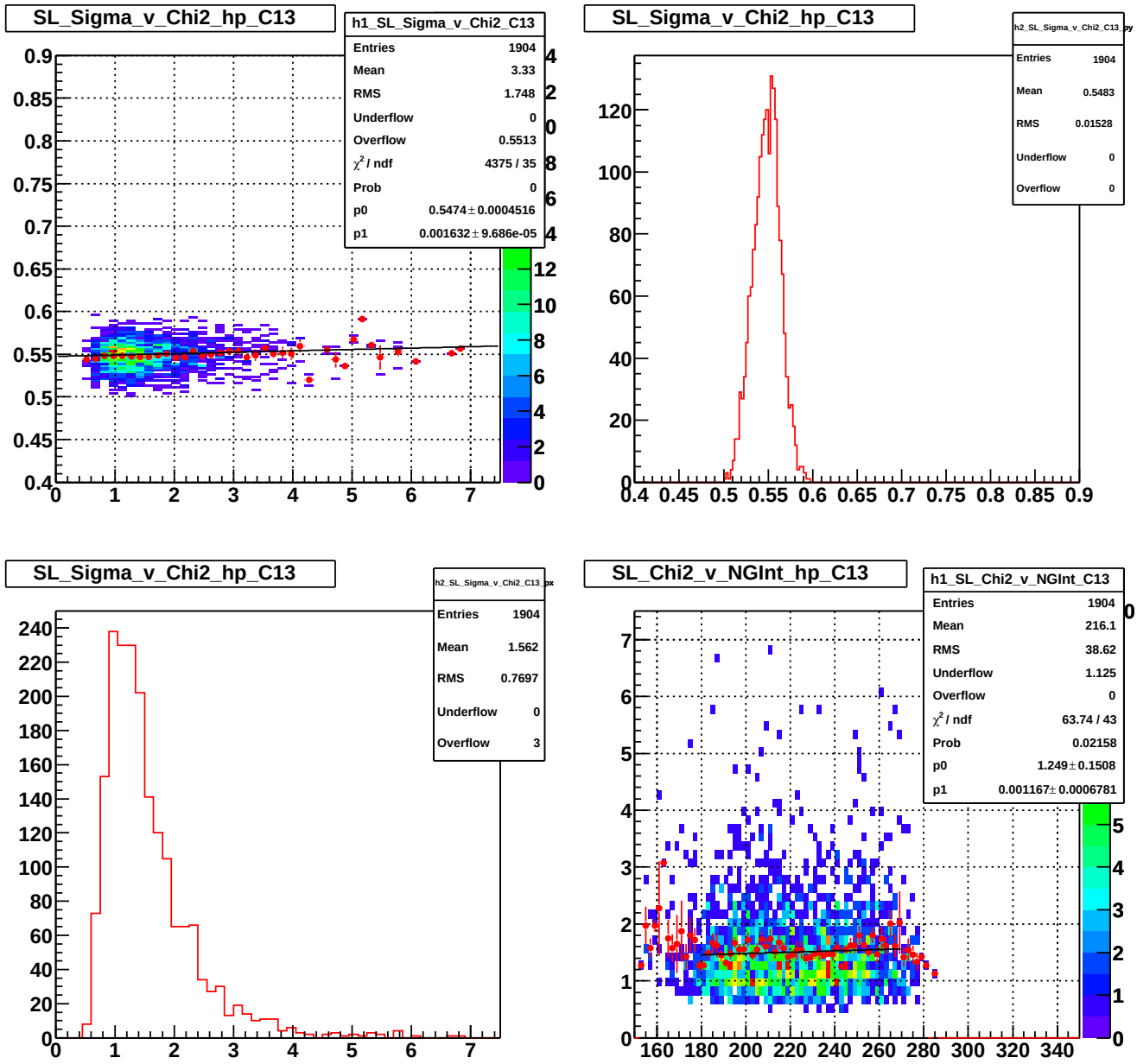

Figure 25: Proton beam, horizontal detectors: Performance of the Synchrotron Light Detector at the C11 location during Tevatron Remove Halo case: Sigma of the bunch width distribution (in *mm*) as measured by the SL detector versus front end measure of the goodness of fit together with an overlaid horizontal profile and a straight line fit; sigma of the bunch width distribution (in *mm*) itself; goodness of fit itself; goodness of fit versus bunch intensity together with an overlaid horizontal profile and a straight line fit.

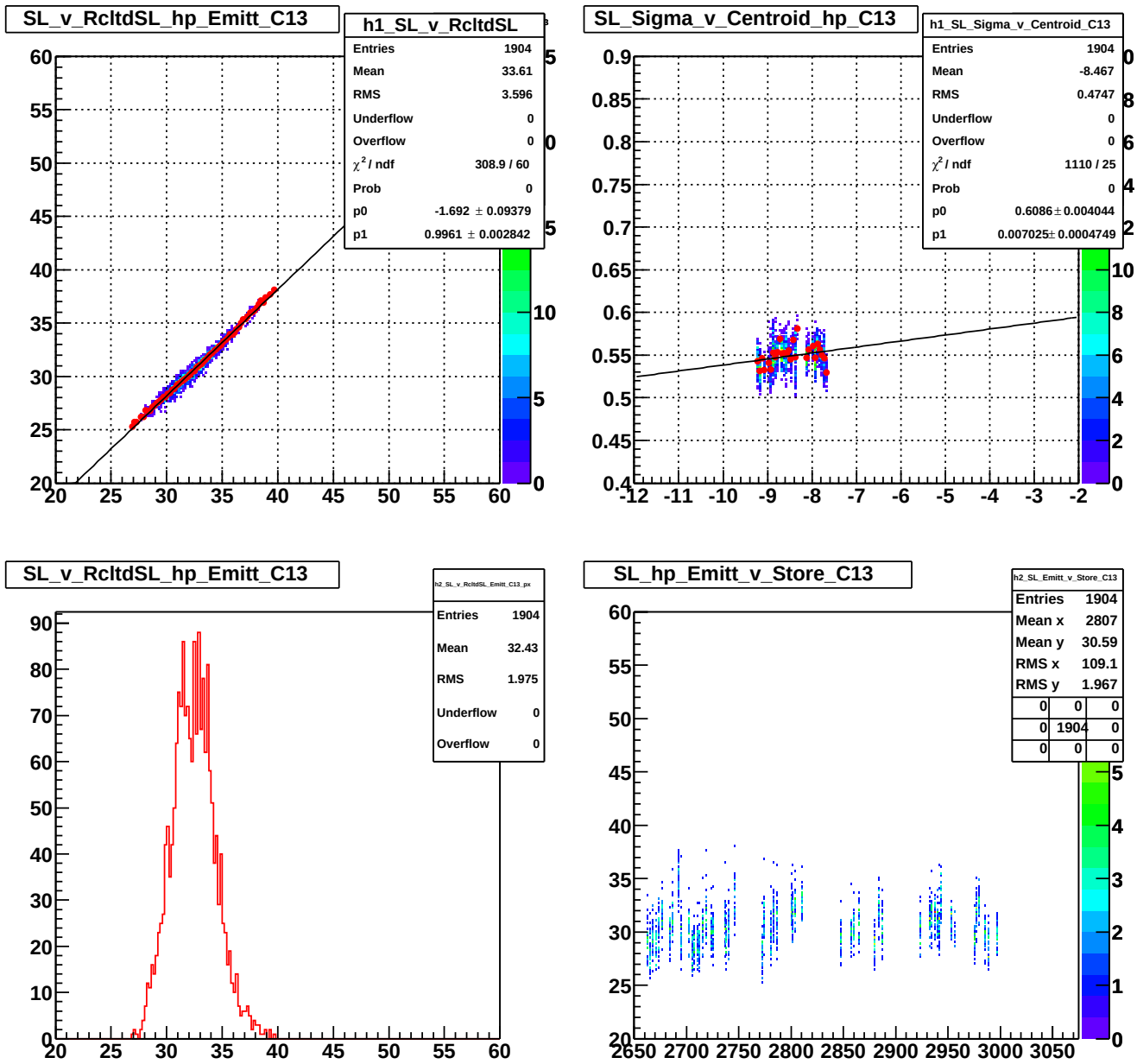

Figure 26: Proton beam, horizontal detectors: Performance of the Synchrotron Light Detector at the C11 location during Tevatron Remove Halo case: Bunch emittance (in $\pi \cdot mm \cdot mrad$) as measured by the front end SL detector versus bunch emittance as recalculated using front end sigma of the bunch width distribution (in *mm*) (combined with SBD timing information in the horizontal cases) together with an overlaid horizontal profile of that distribution with a straight line fit; sigma of the bunch width distribution versus bunch E11 centroid (in *mm*) (based on the T:FW[E,H,V][A,P]CE ACNET variable) with an overlaid horizontal profile of that distribution with a straight line fit; bunch emittance; bunch emittance versus store number.

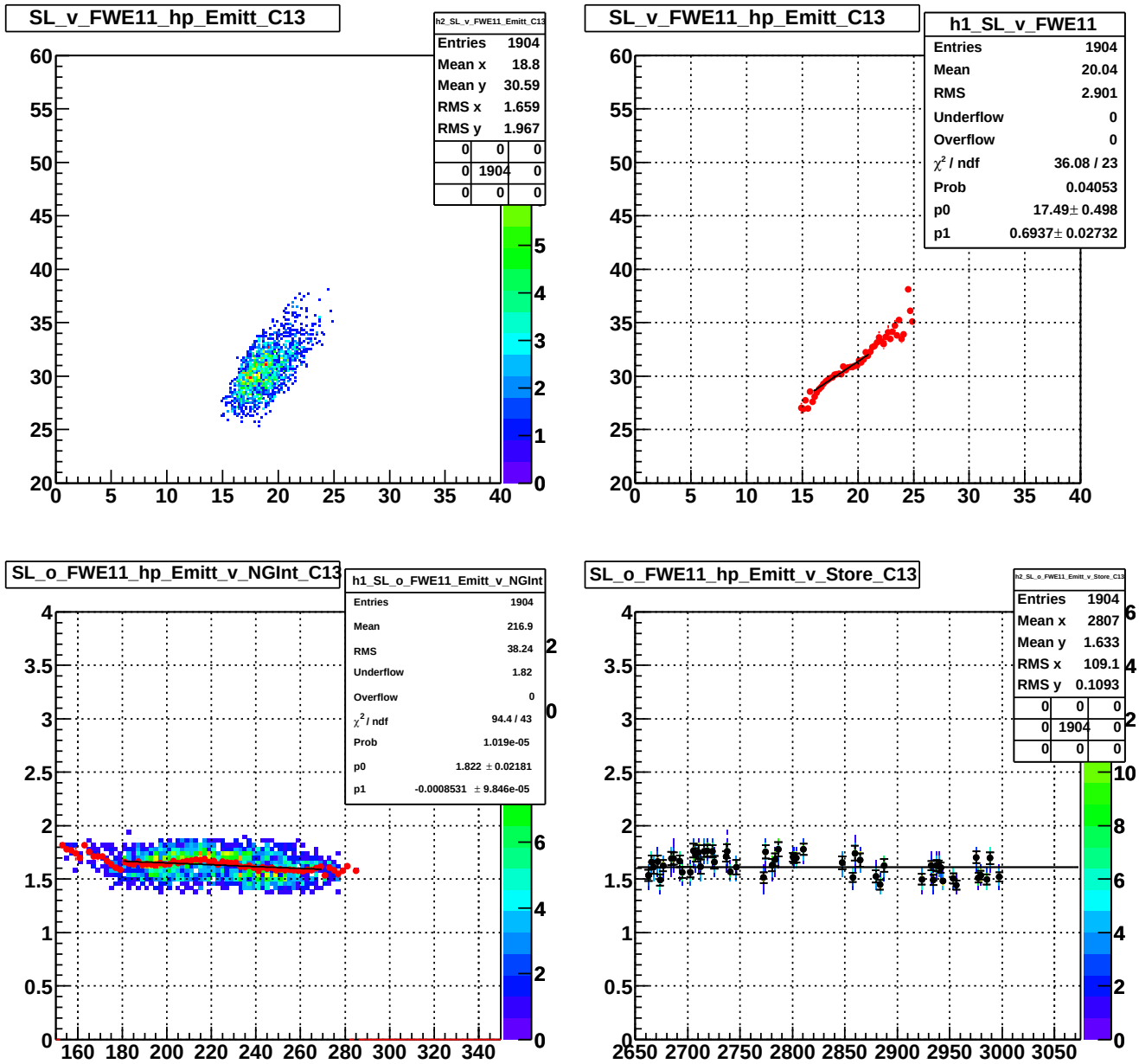

Figure 27: Proton beam, horizontal detectors: Comparisons of Emittance measurements as done by Synchrotron Light Detector at C11 and Flying Wire Detector at E11 during Tevatron Remove Halo case: Bunch emittance (in $\pi \cdot mm \cdot mrad$) as measured by Synchrotron Light Detector versus bunch emittance as measured by the Flying Wire Detector at E11; horizontal profile of the previous distribution with a straight line fit; bunch emittance as measured by Synchrotron Light Detector over bunch emittance as measured by the Flying Wire Detector at E11 versus bunch intensity (ACNET variables T:FBI[A,P]NG) (in E9) together with an overlaid horizontal profile and a straight line fit; bunch emittance as measured by Synchrotron Light Detector over bunch emittance as measured by the Flying Wire Detector at E11 versus store number with overlaid averaged ratios for each store and a horizontal line fit.

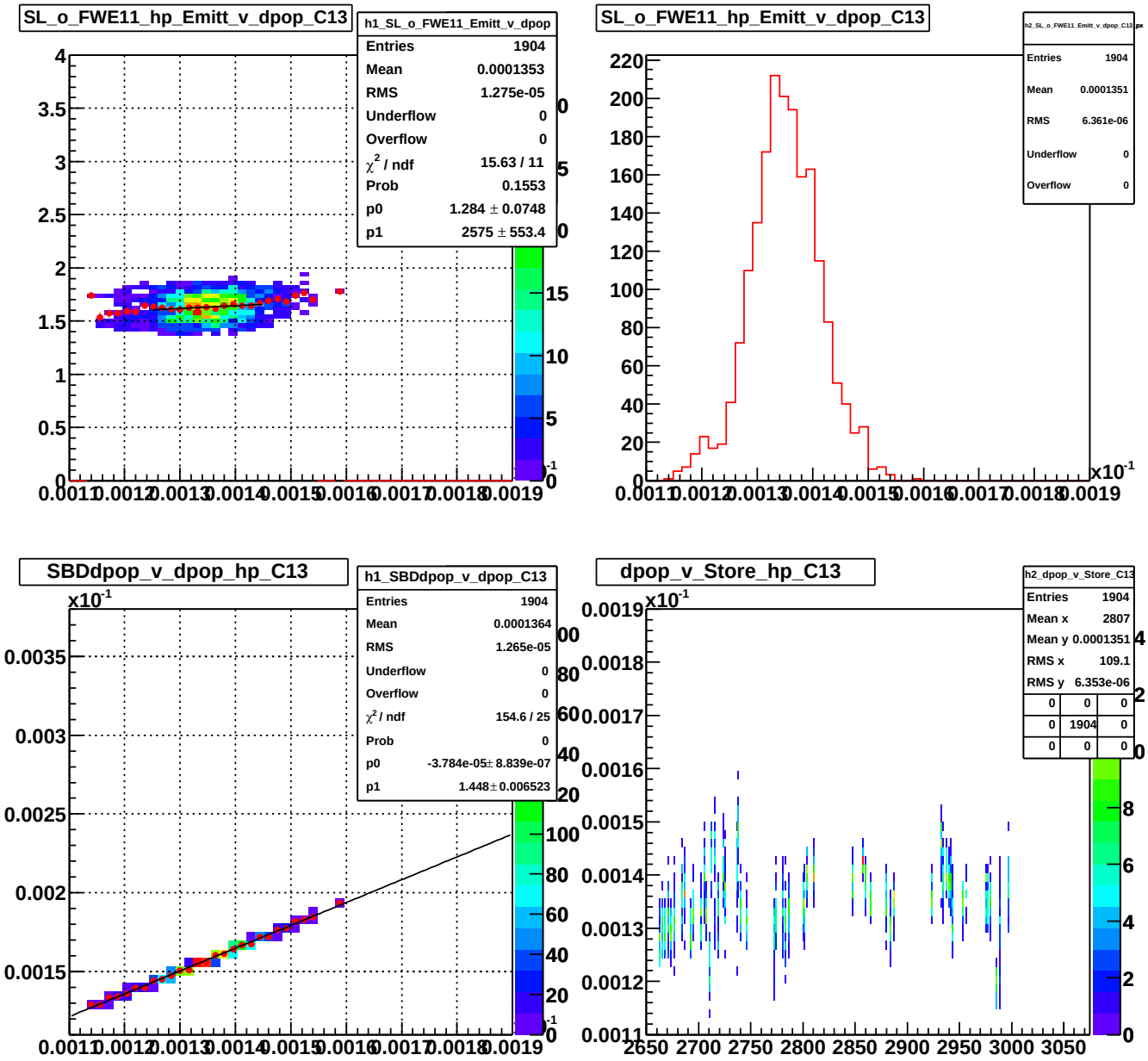

Figure 28: Proton beam, horizontal detectors: Comparisons of Emittance measurements as done by Synchrotron Light Detector at C11 and Flying Wire Detector at E11 during Tevatron Remove Halo case: Bunch emittance as measured by Synchrotron Light Detector over bunch emittance as measured by the Flying Wire Detector at E11 versus recalculated $\delta p/p$ (based on δt the T:SBD[A,P]SS ACNET variable) with an overlaid horizontal profile of the previous distribution with a straight line fit; $\delta p/p$ itself; frontend value of $\delta p/p$ versus recalculated $\delta p/p$; $\delta p/p$ versus store number.

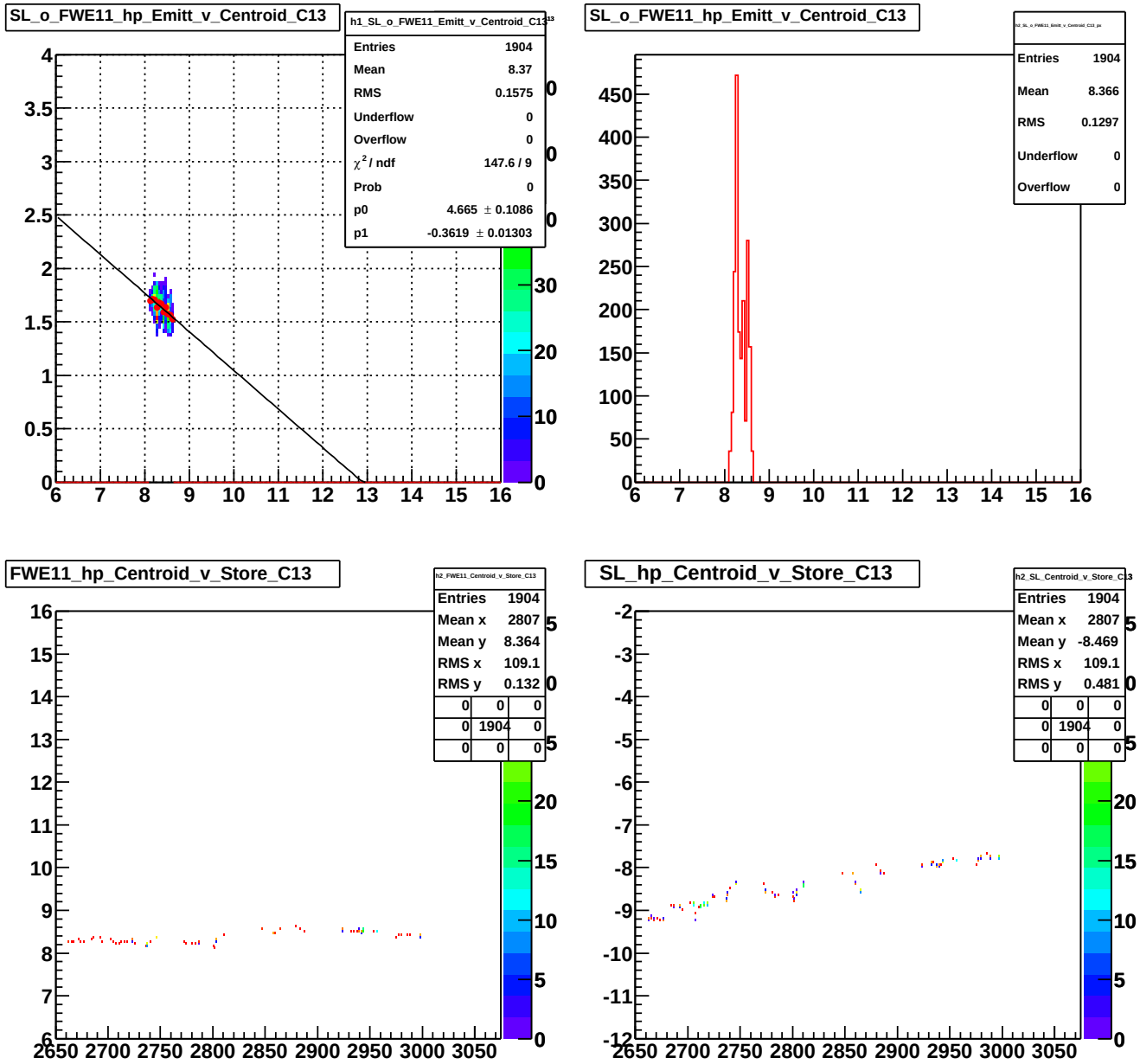

Figure 29: Proton beam, horizontal detectors: Comparisons of Emittance measurements as done by Synchrotron Light Detector at C11 and Flying Wire Detector at E11 during Tevatron Remove Halo case: Bunch emittance as measured by Synchrotron Light Detector over bunch emittance as measured by the Flying Wire Detector at E11 versus bunch E11 centroid (in *mm*) (based on the T:FW[E,H,V][A,P]CE ACNET variable) with an overlaid horizontal profile of the previous distribution with a straight line fit; bunch E11 centroid itself; bunch E11 centroid versus store number. bunch C11 centroid versus store number.

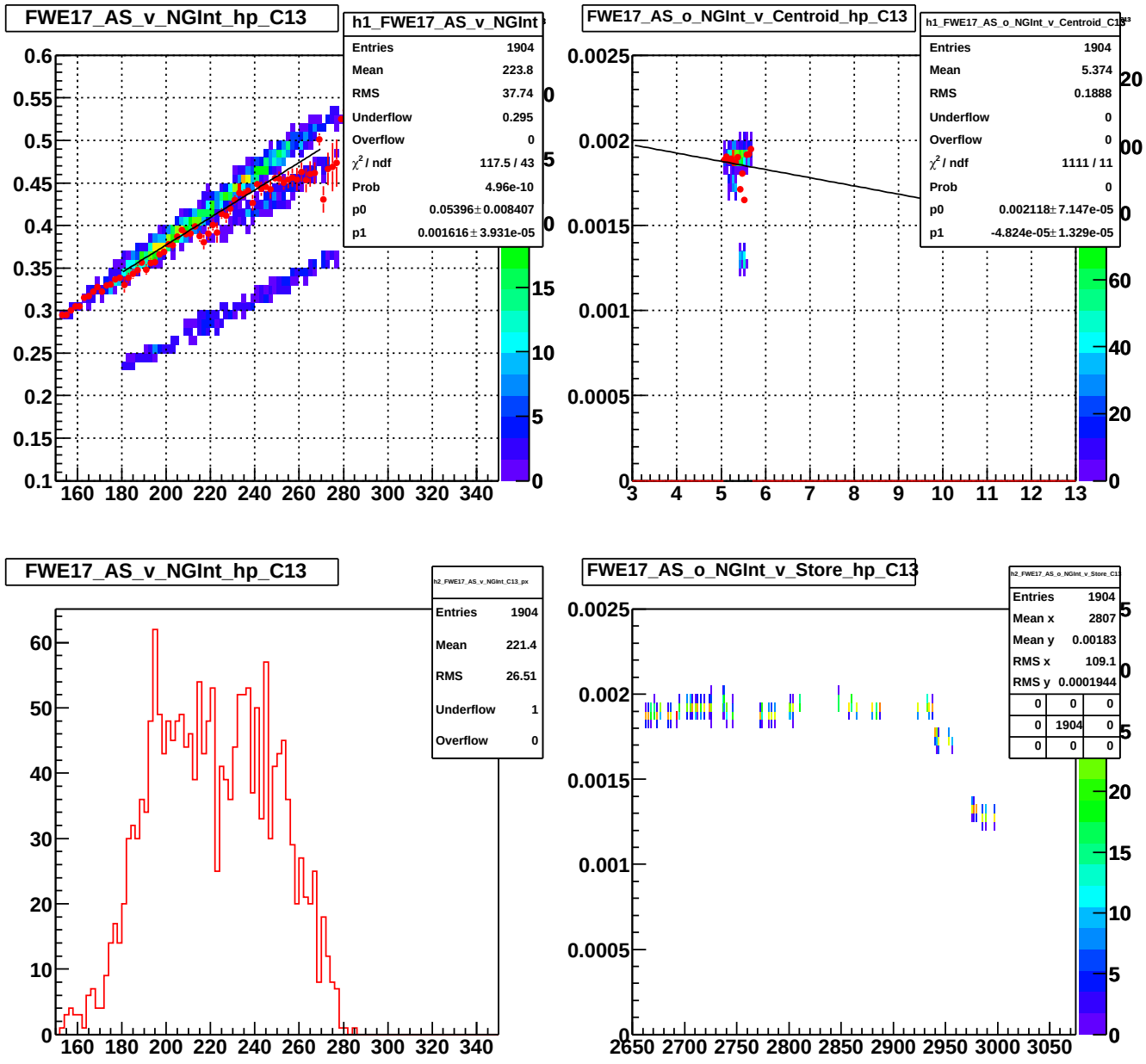

Figure 30: Proton beam, horizontal detectors: Performance of the Flying Wire Detector at the E17 location during Tevatron Remove Halo case: Amplitude (in arbitrary units) times sigma of the bunch width distribution (in *mm*) of the front end FW detector data versus bunch intensity (ACNET variables T:FBI[A,P]NG) (in E9) with an overlaid horizontal profile of that distribution with a straight line fit; Amplitude times sigma of the bunch width distribution of the front end FW detector data over bunch intensity versus bunch E17 centroid (in *mm*) (based on the T:FW[E,H,V][A,P]CE ACNET variable) with an overlaid horizontal profile of that distribution with a straight line fit; bunch intensity; amplitude times sigma of the bunch width distribution (in *mm*) of the raw FW detector distribution over bunch intensity versus store number.

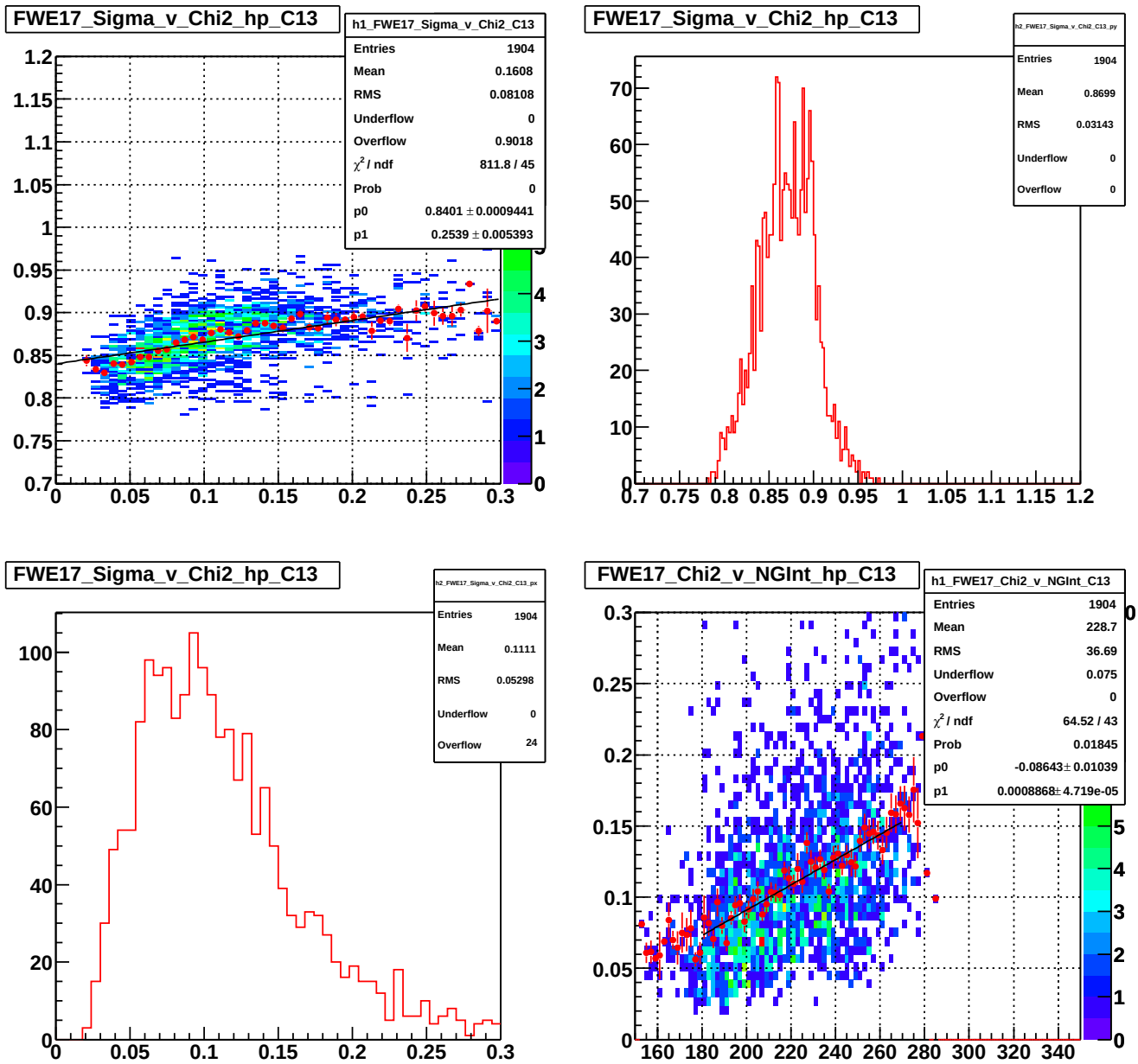

Figure 31: Proton beam, horizontal detectors: Performance of the Flying Wire Detector at the E17 location during Tevatron Remove Halo case: Sigma of the bunch width distribution (in *mm*) as measured by the FW detector versus front end measure of the goodness of fit together with an overlaid horizontal profile and a straight line fit; sigma itself, goodness of fit itself; goodness of fit versus bunch intensity together with an overlaid horizontal profile and a straight line fit.

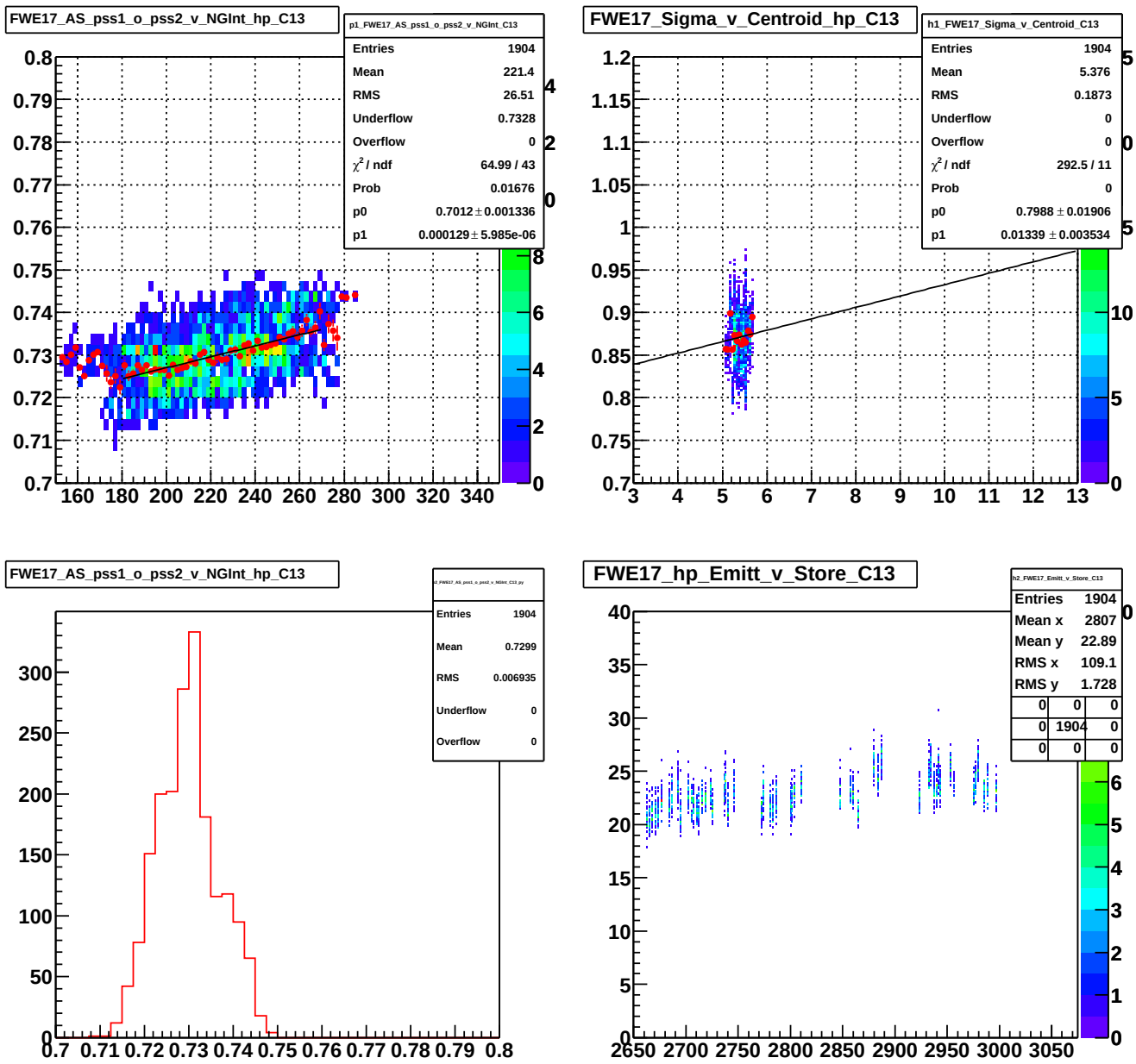

Figure 32: Proton beam, horizontal detectors: Performance of the Flying Wire Detector at the E17 location during Tevatron Remove Halo case: Amplitude (in arbitrary units) times sigma of the bunch width distribution (in *mm*) of the pass 1 over pass 2 of the front end FW detector data versus bunch intensity (ACNET variables T:FBI[A,P]NG) (in E9) together with an overlaid horizontal profile of that distribution with a straight line fit; sigma of the bunch width distribution versus bunch centroid (in *mm*) (based on the T:FW[E,H,V][A,P]CE ACNET variable) with an overlaid horizontal profile of that distribution with a straight line fit; amplitude (in arbitrary units) times sigma of the bunch width distribution (in *mm*) of the pass 1 over pass 2 of the front end FW detector data itself, bunch emittance (in $\pi \cdot mm \cdot mrad$) versus store number.

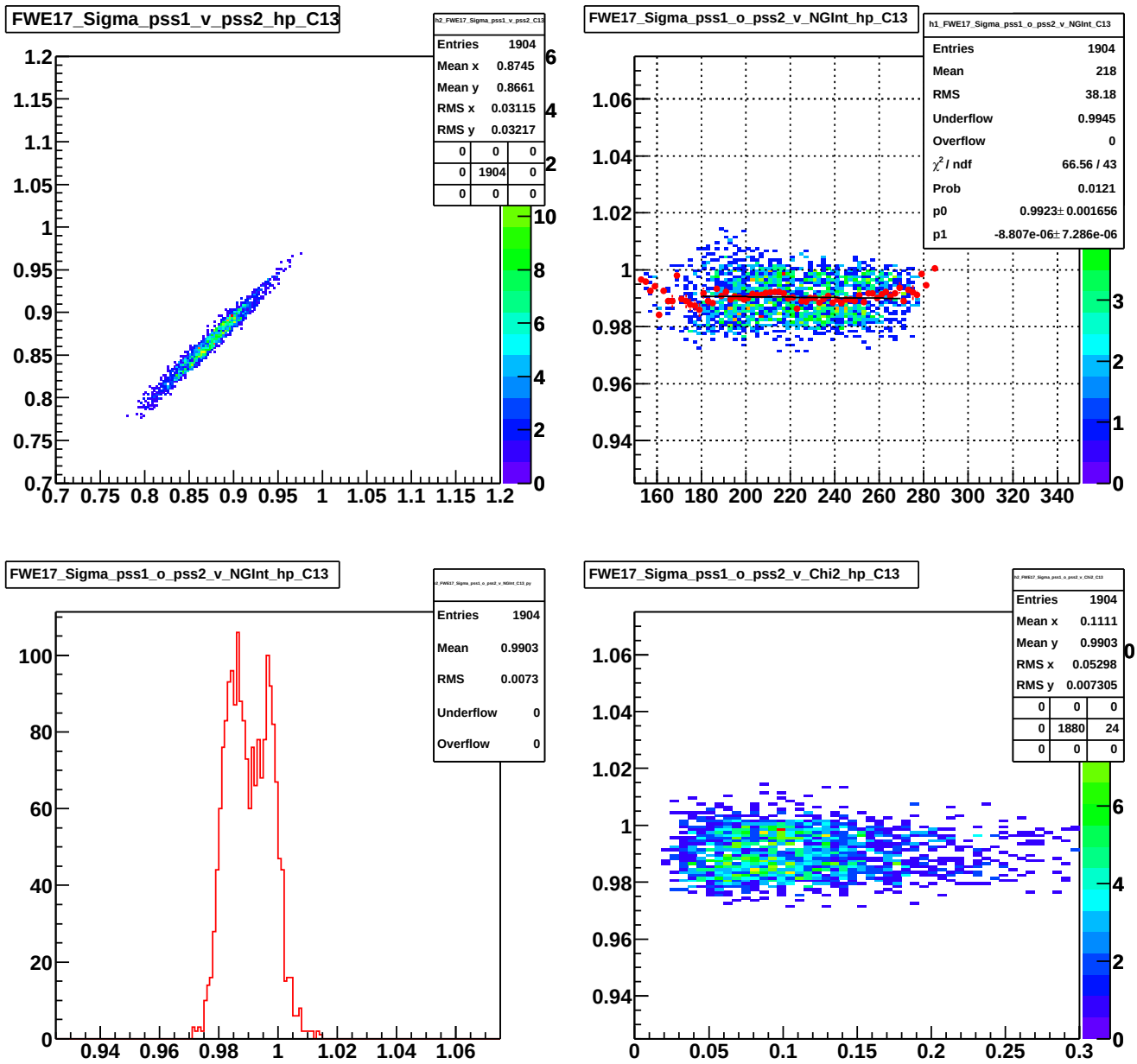

Figure 33: Proton beam, horizontal detectors: Performance of the Flying Wire Detector at the E17 location during Tevatron Remove Halo case: Sigma of the bunch width distribution (in *mm*) of the pass 1 versus pass 2 of the FW detector; sigma of the bunch width distribution (in *mm*) of the pass 1 over pass 2 of the FW detector versus bunch intensity (ACNET variables T:FBI[A,P]NG) (in E9) together with an overlaid horizontal profile and a straight line fit; sigma of the bunch width distribution (in *mm*) of the pass 1 over pass 2 of the FW detector itself, sigma of the bunch width distribution (in *mm*) of the pass 1 over pass 2 of the FW detector versus front end measure of the goodness of fit.

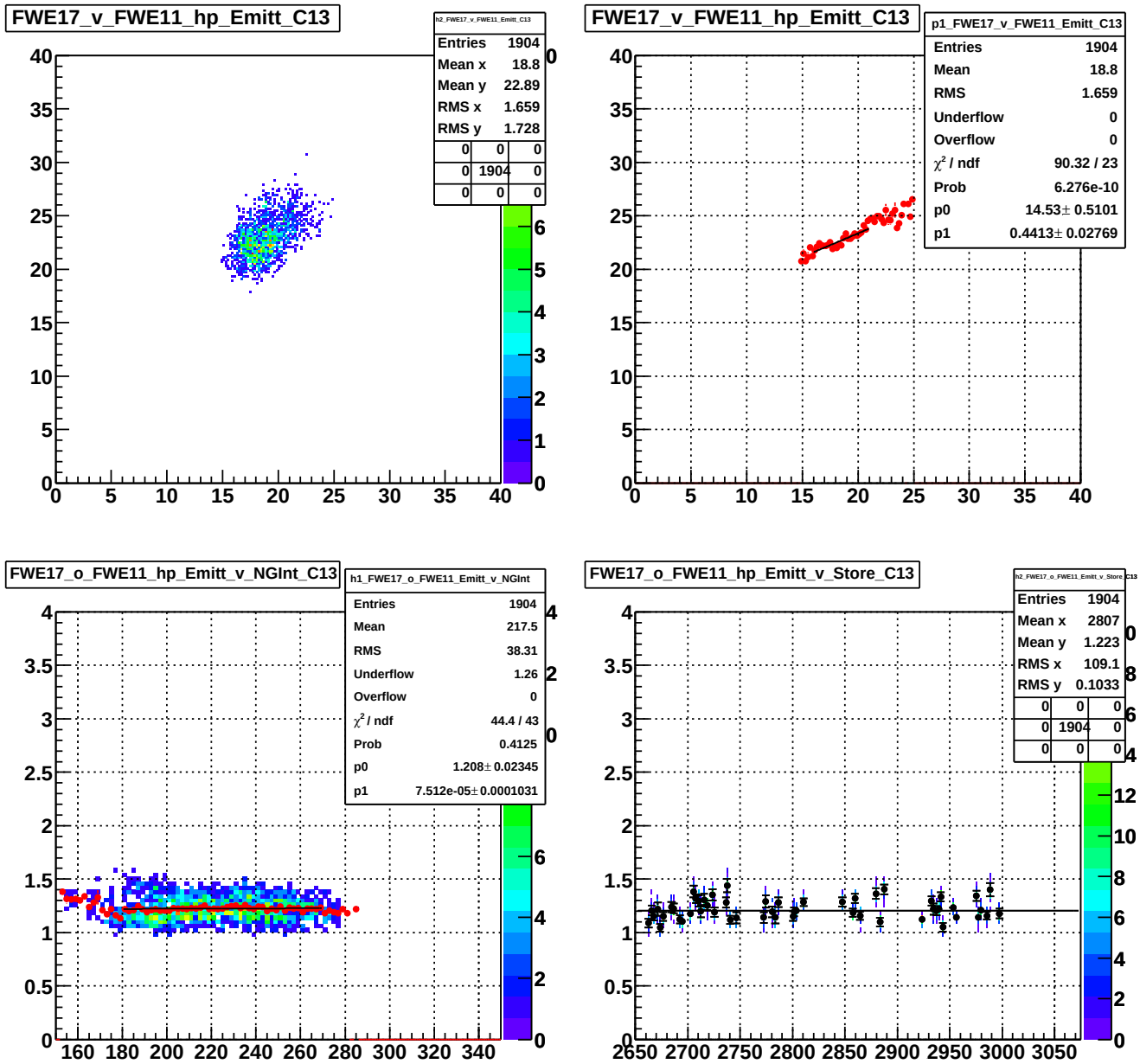

Figure 34: Proton beam, horizontal detectors: Comparisons of Emittance measurements as done by Flying Wire Detector at E17 and Flying Wire Detector at E11 during Tevatron Remove Halo case: Bunch emittance (in $\pi \cdot mm \cdot mrad$) as measured by Flying Wire Detector at E17 versus bunch emittance as measured by the Flying Wire Detector at E11; horizontal profile of the previous distribution with a straight line fit; bunch emittance as measured by Flying Wire Detector at E17over bunch emittance as measured by the Flying Wire Detector at E11 versus bunch intensity (ACNET variables T:FBI[A,P]NG) (in E9) together with an overlaid horizontal profile and a straight line fit; bunch emittance as measured by Flying Wire Detector at E17 over bunch emittance as measured by the Flying Wire Detector at E11 versus store number with overlaid averaged ratios for each store and a horizontal line fit.

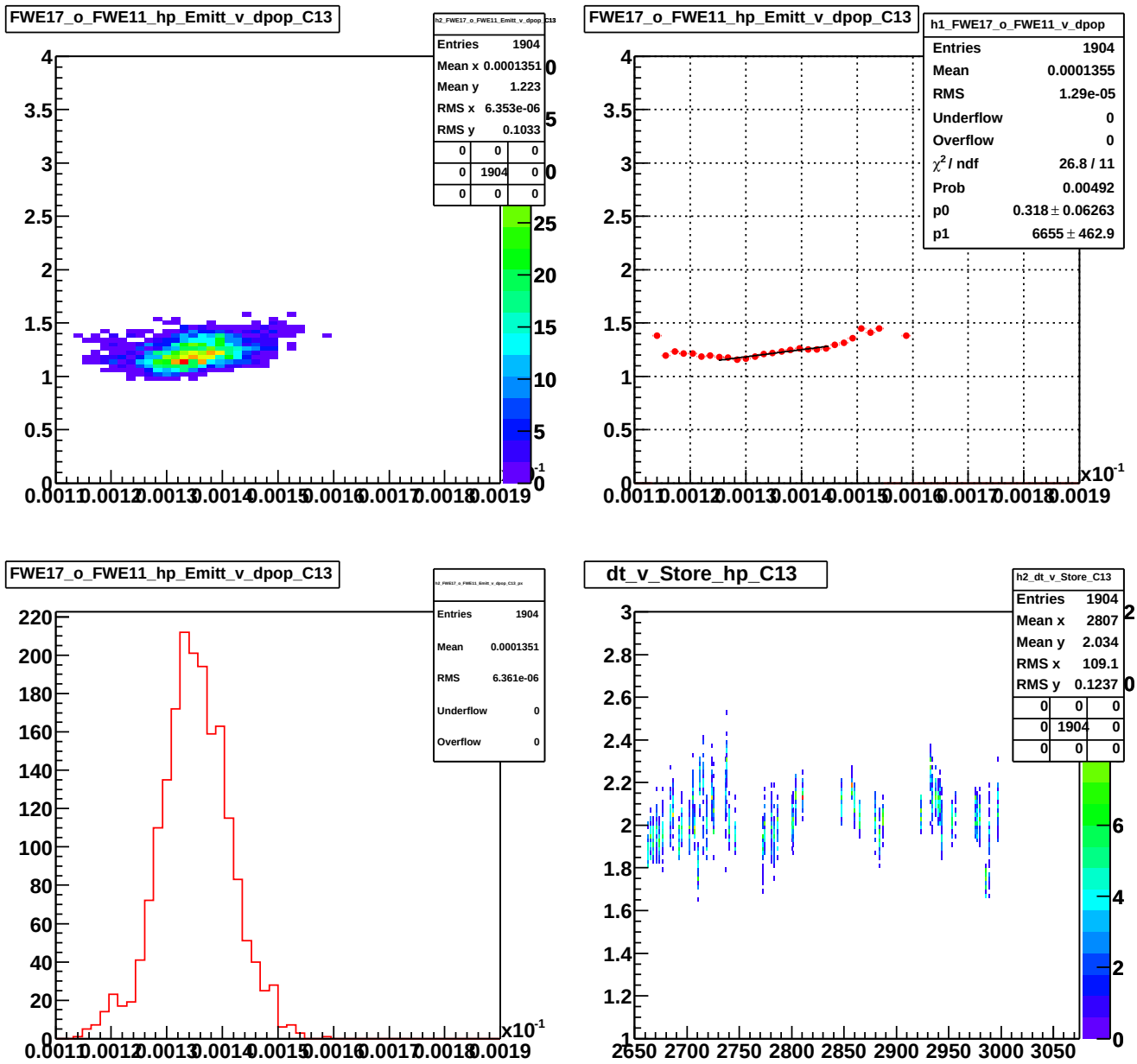

Figure 35: Proton beam, horizontal detectors: Comparisons of Emittance measurements as done by Flying Wire Detector at E17 and Flying Wire Detector at E11 during Tevatron Remove Halo case: Bunch emittance as measured by Flying Wire Detector at E17 over bunch emittance as measured by the Flying Wire Detector at E11 versus recalculated $\delta p/p$ (based on δt the T:SBD[A,P]SS ACNET variable); horizontal profile of the previous distribution with a straight line fit; $\delta p/p$ itself; δt versus store number.

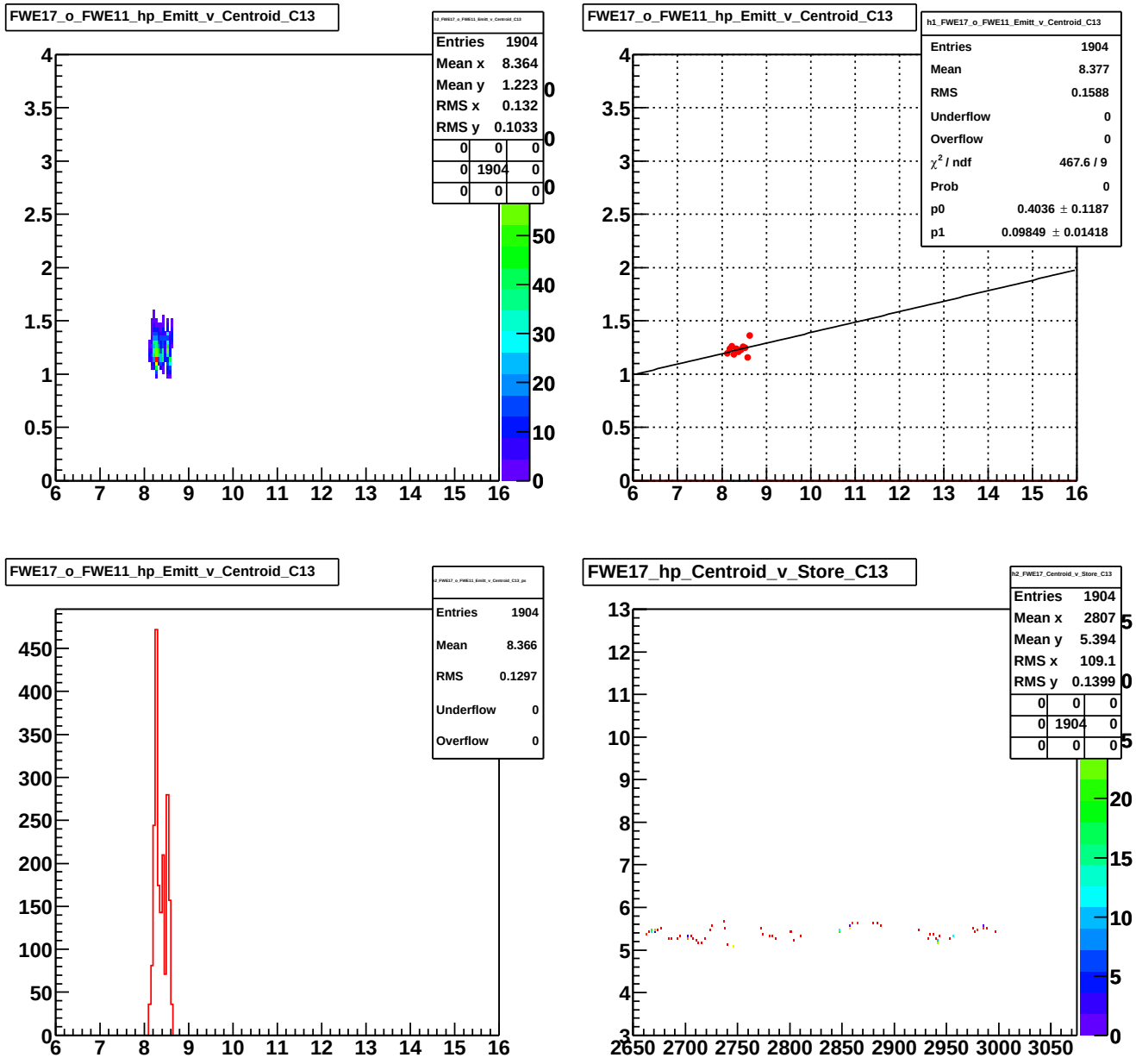

Figure 36: Proton beam, horizontal detectors: Comparisons of Emittance measurements as done by Flying Wire Detector at E17 and Flying Wire Detector at E11 during Tevatron Remove Halo case: Bunch emittance as measured by Flying Wire Detector at E17 over bunch emittance as measured by the Flying Wire Detector at E11 versus bunch E11 centroid (in *mm*) (based on the T:FW[E,H,V][A,P]CE ACNET variable); horizontal profile of the previous distribution with a straight line fit; bunch E17 centroid; bunch E17 centroid versus store number.

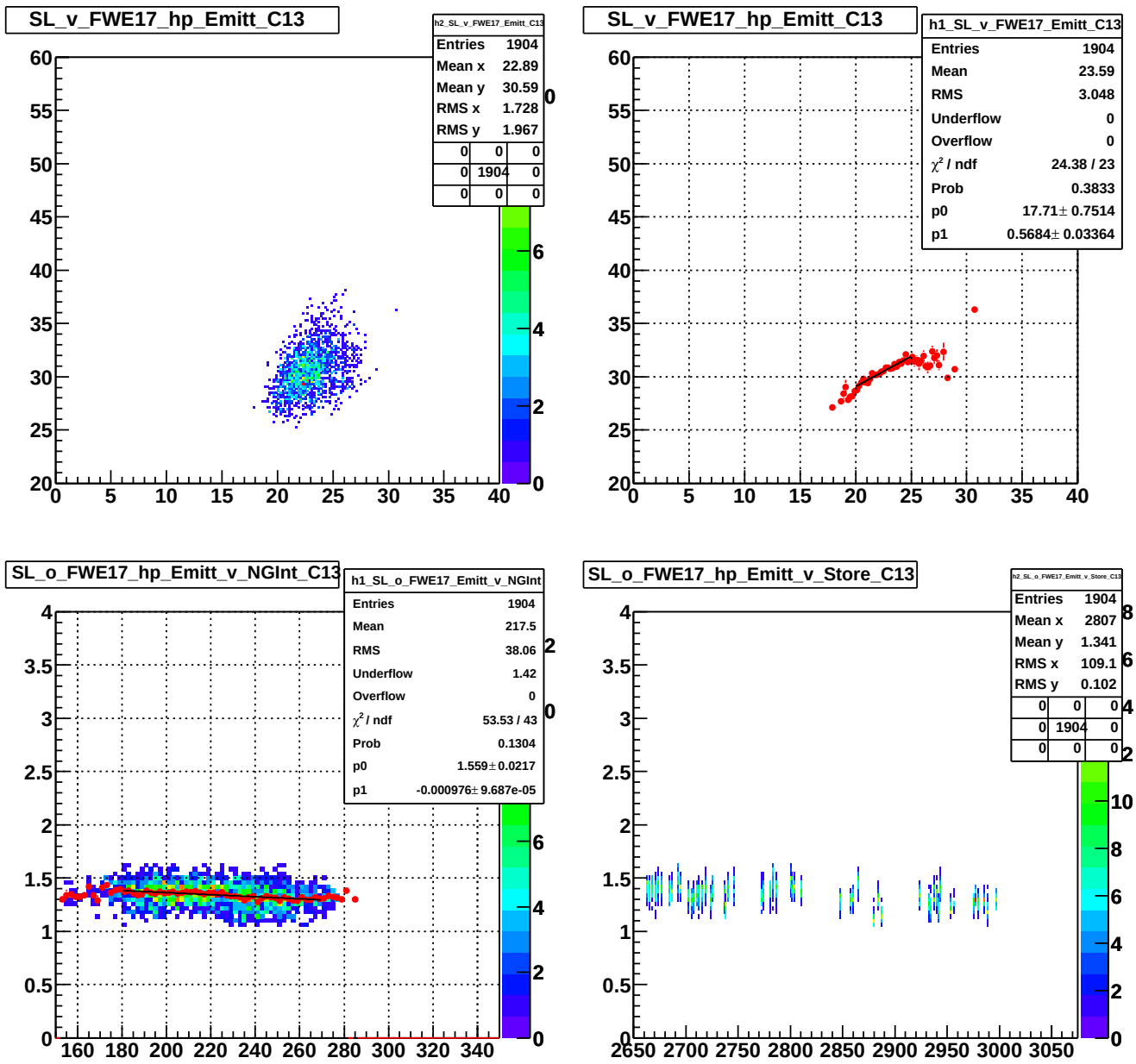

Figure 37: Proton beam, horizontal detectors: Comparisons of Emittance measurements as done by Synchrotron Light Detector at C11 and Flying Wire Detector at E17 during Tevatron Remove Halo case: Bunch emittance (in $\pi \cdot mm \cdot mrad$) as measured by Synchrotron Light Detector versus bunch emittance as measured by the Flying Wire Detector at E17; horizontal profile of the previous distribution with a straight line fit; bunch emittance as measured by Synchrotron Light Detector over bunch emittance as measured by the Flying Wire Detector at E17 versus bunch intensity (ACNET variables T:FBI[A,P]NG) (in E9) together with an overlaid horizontal profile and a straight line fit; bunch emittance as measured by Synchrotron Light Detector over bunch emittance as measured by the Flying Wire Detector at E17 versus store number.

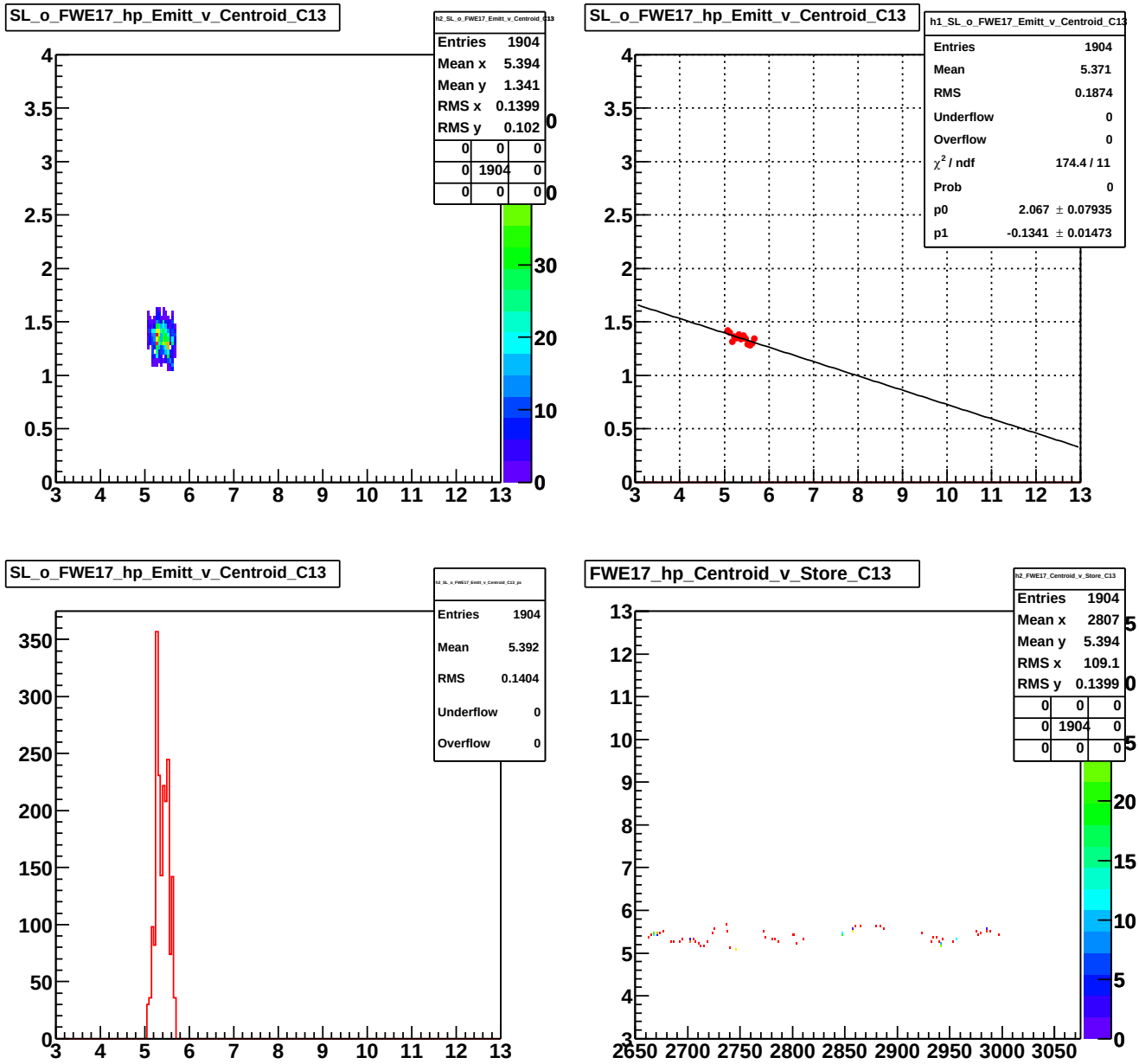

Figure 38: Proton beam, horizontal detectors: Comparisons of Emittance measurements as done by Synchrotron Light Detector at C11 and Flying Wire Detector at E17 during Tevatron Remove Halo case: Bunch emittance as measured by Synchrotron Light Detector over bunch emittance as measured by the Flying Wire Detector at E17 versus bunch E17 centroid (in *mm*) (based on the T:FW[E,H,V][A,P]CE ACNET variable); horizontal profile of the previous distribution with a straight line fit; bunch E17 centroid itself; bunch E17 centroid versus store number.

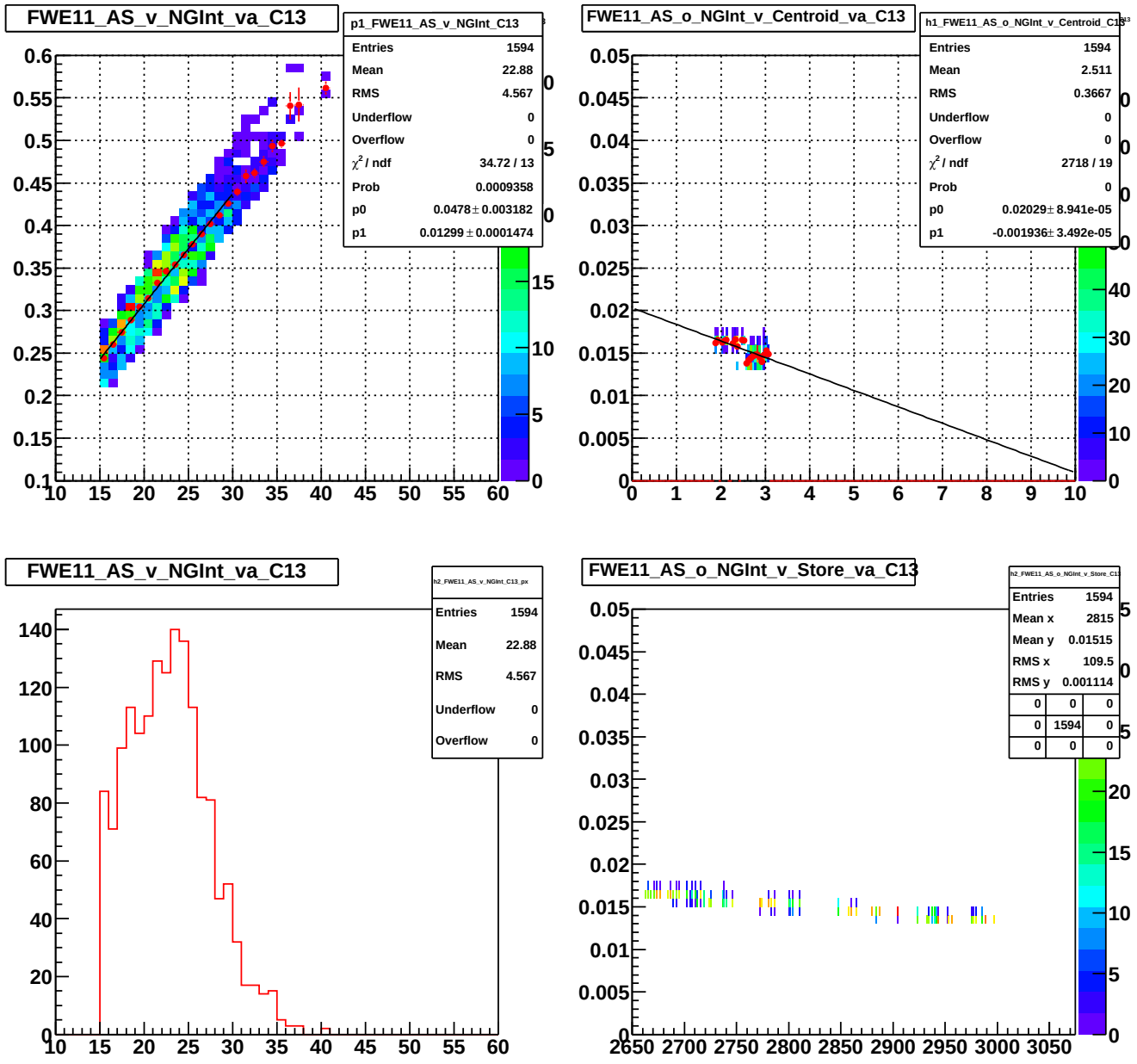

Figure 39: Antiproton beam, vertical detectors: Performance of the Flying Wire Detector at the E11 location during Tevatron Remove Halo case: Amplitude (in arbitrary units) times sigma of the bunch width distribution (in *mm*) of the front end FW detector data versus bunch intensity (ACNET variables T:FBI[A,P]NG) (in E9) with an overlaid horizontal profile of that distribution with a straight line fit; Amplitude times sigma of the bunch width distribution of the front end FW detector data over bunch intensity versus bunch E11 centroid (in *mm*) (based on the T:FW[E,H,V][A,P]CE ACNET variable) with an overlaid horizontal profile of that distribution with a straight line fit; bunch intensity; amplitude times sigma of the bunch width distribution (in *mm*) of the raw FW detector distribution over bunch intensity versus store number.

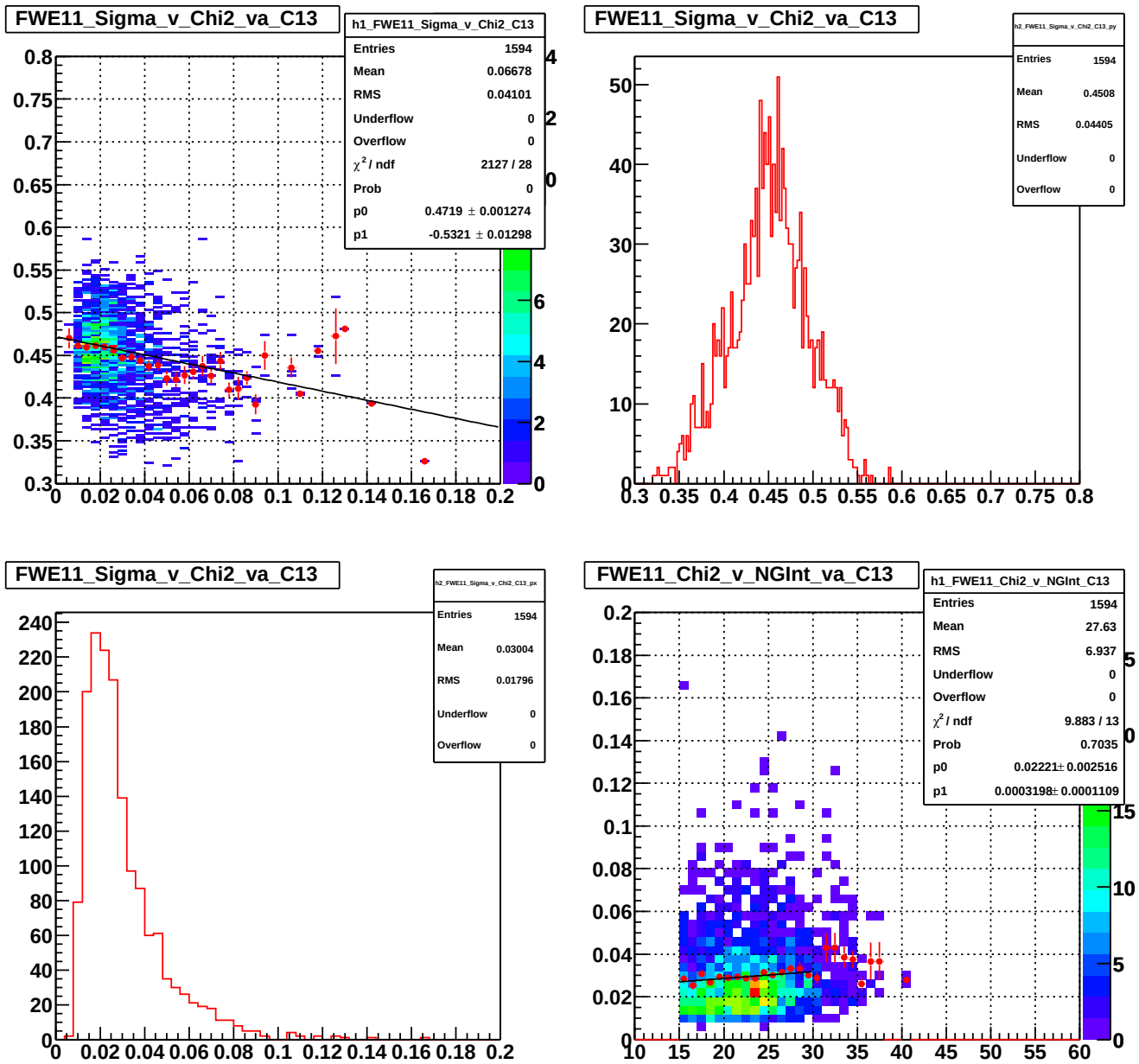

Figure 40: Antiproton beam, vertical detectors: Performance of the Flying Wire Detector at the E11 location during Tevatron Remove Halo case: Sigma of the bunch width distribution (in *mm*) as measured by the FW detector versus front end measure of the goodness of fit together with an overlaid horizontal profile and a straight line fit; sigma itself, goodness of fit itself; goodness of fit versus bunch intensity together with an overlaid horizontal profile and a straight line fit;

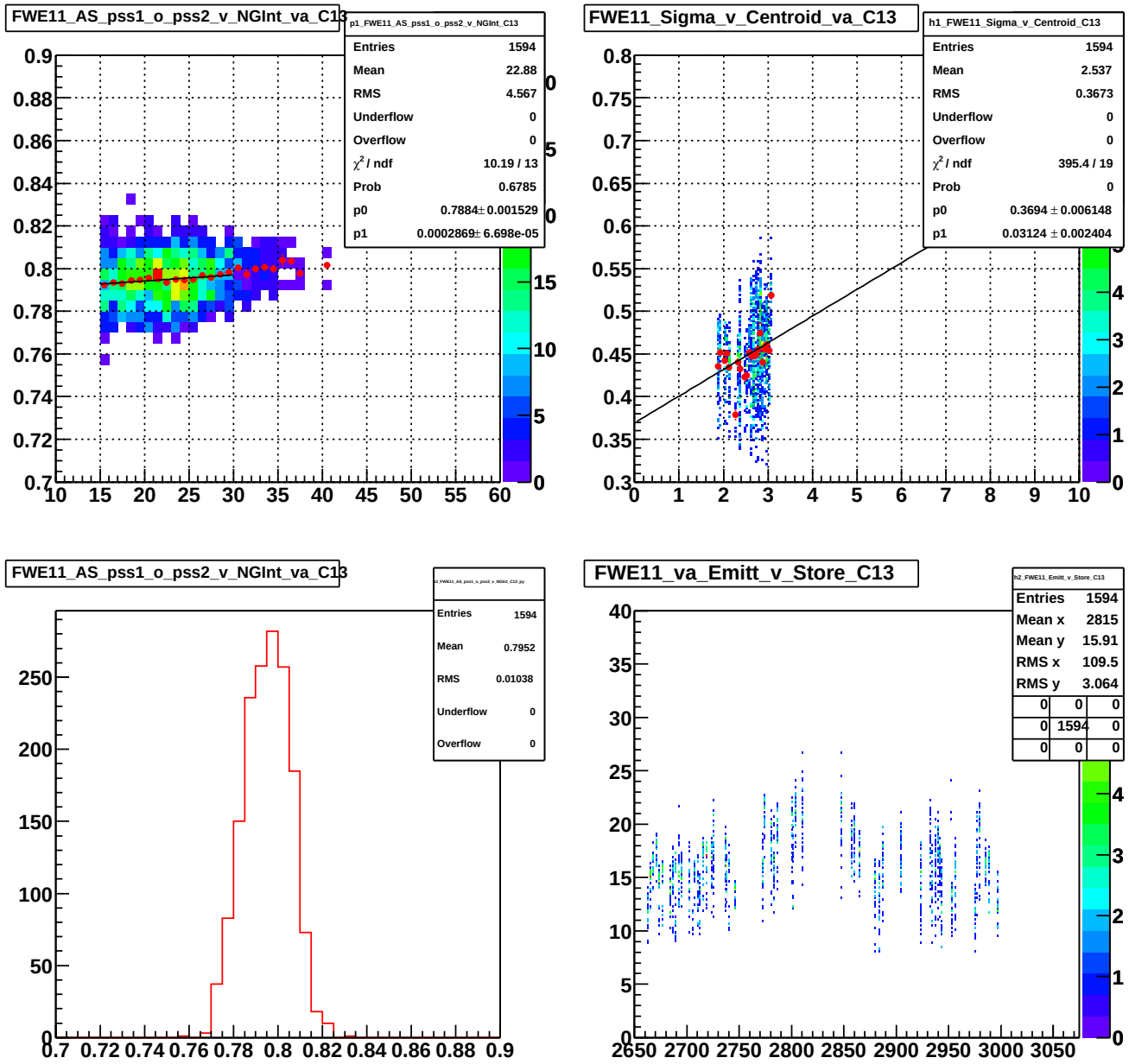

Figure 41: Antiproton beam, vertical detectors: Performance of the Flying Wire Detector at the E11 location during Tevatron Remove Halo case: Amplitude (in arbitrary units) times sigma of the bunch width distribution (in *mm*) of the pass 1 over pass 2 of the front end FW detector data versus bunch intensity (ACNET variables T:FBI[A,P]NG) (in E9) together with an overlaid horizontal profile of that distribution with a straight line fit; sigma of the bunch width distribution versus bunch centroid (in *mm*) (based on the T:FW[E,H,V][A,P]CE ACNET variable) with an overlaid horizontal profile of that distribution with a straight line fit; amplitude (in arbitrary units) times sigma of the bunch width distribution (in *mm*) of the pass 1 over pass 2 of the front end FW detector data itself, bunch emittance (in $\pi \cdot mm \cdot mrad$) versus store number.

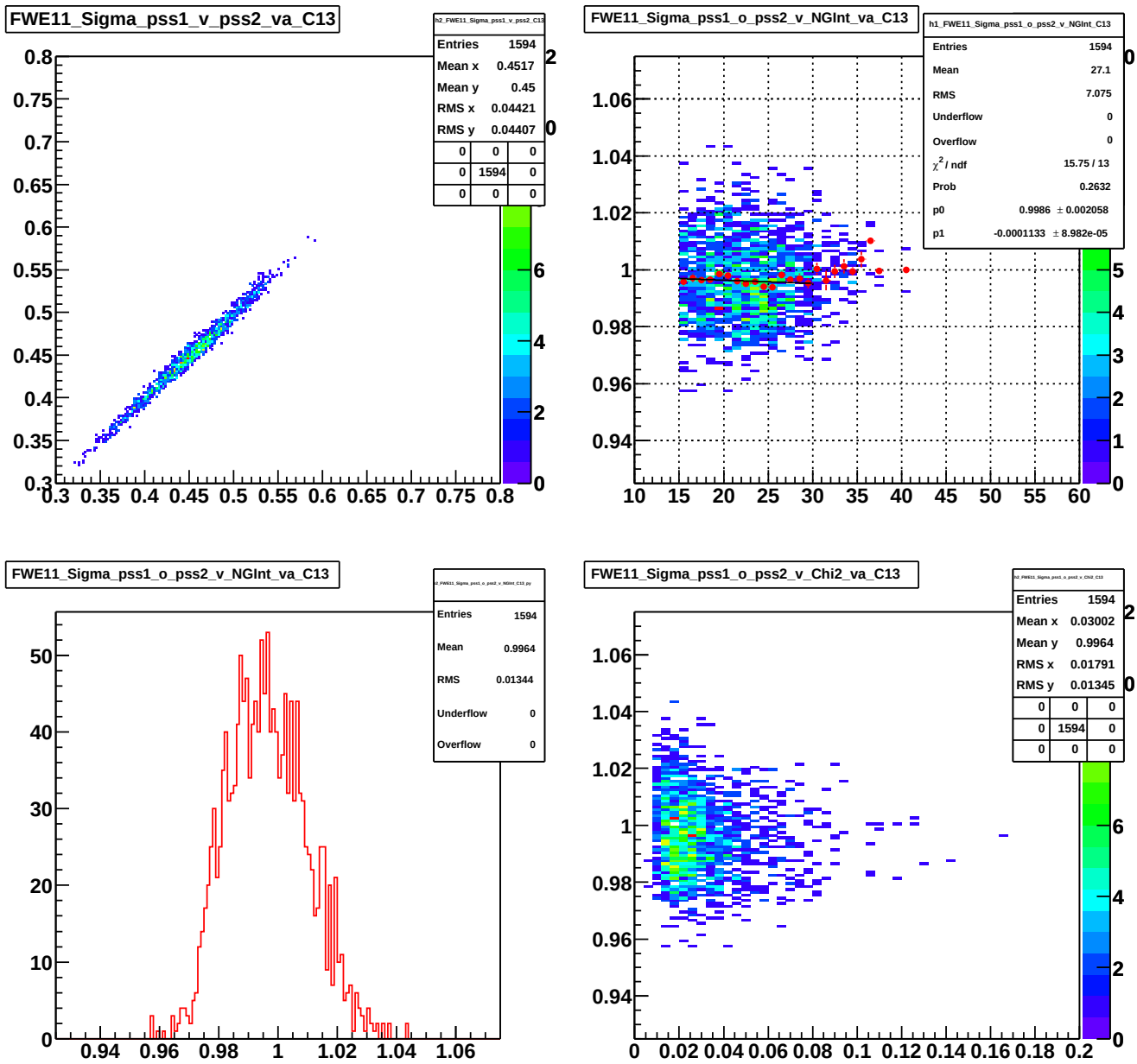

Figure 42: Antiproton beam, vertical detectors: Performance of the Flying Wire Detector at the E11 location during Tevatron Remove Halo case: Sigma of the bunch width distribution (in *mm*) of the pass 1 versus pass 2 of the FW detector; sigma of the bunch width distribution (in *mm*) of the pass 1 over pass 2 of the FW detector versus bunch intensity (ACNET variables T:FBI[A,P]NG) (in E9) together with an overlaid horizontal profile and a straight line fit; sigma of the bunch width distribution (in *mm*) of the pass 1 over pass 2 of the FW detector itself, sigma of the bunch width distribution (in *mm*) of the pass 1 over pass 2 of the FW detector versus front end measure of the goodness of fit.

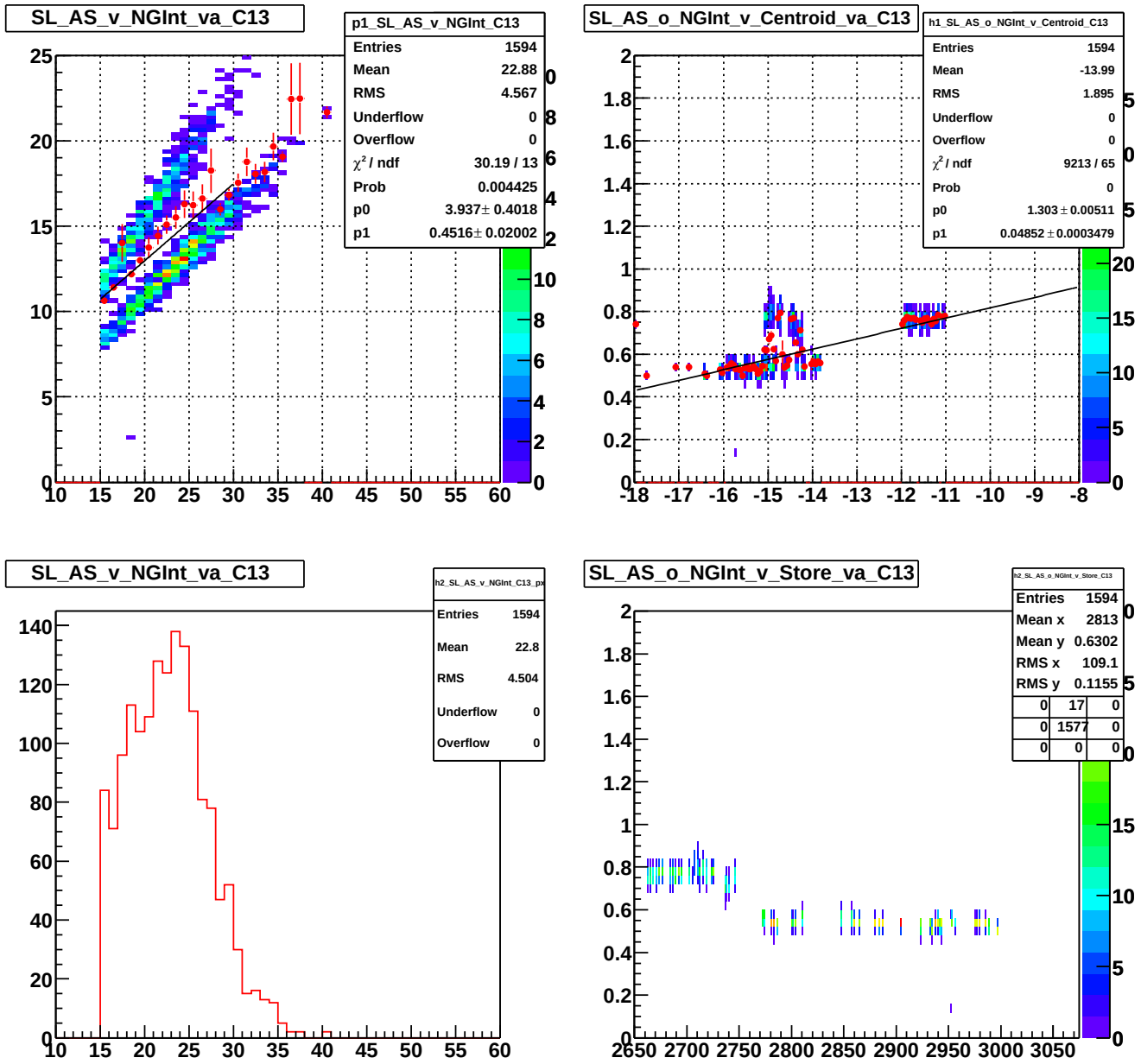

Figure 43: Antiproton beam, vertical detectors: Performance of the Synchrotron Light Detector at the C11 location during Tevatron Remove Halo case: Amplitude (in arbitrary units) times sigma of the bunch width distribution (in *mm*) of the raw SL detector distribution versus bunch intensity (ACNET variables T:FBI[A,P]NG) (in E9) with an overlaid horizontal profile of that distribution with a straight line fit; amplitude times sigma of the bunch width distribution (in *mm*) of the raw SL detector distribution over bunch intensity versus bunch E11 centroid (in *mm*) (based on the T:FW[E,H,V][A,P]CE ACNET variable) with an overlaid horizontal profile of that distribution with a straight line fit; bunch intensity; amplitude times sigma of the bunch width distribution (in *mm*) of the raw SL detector distribution over bunch intensity versus store number.

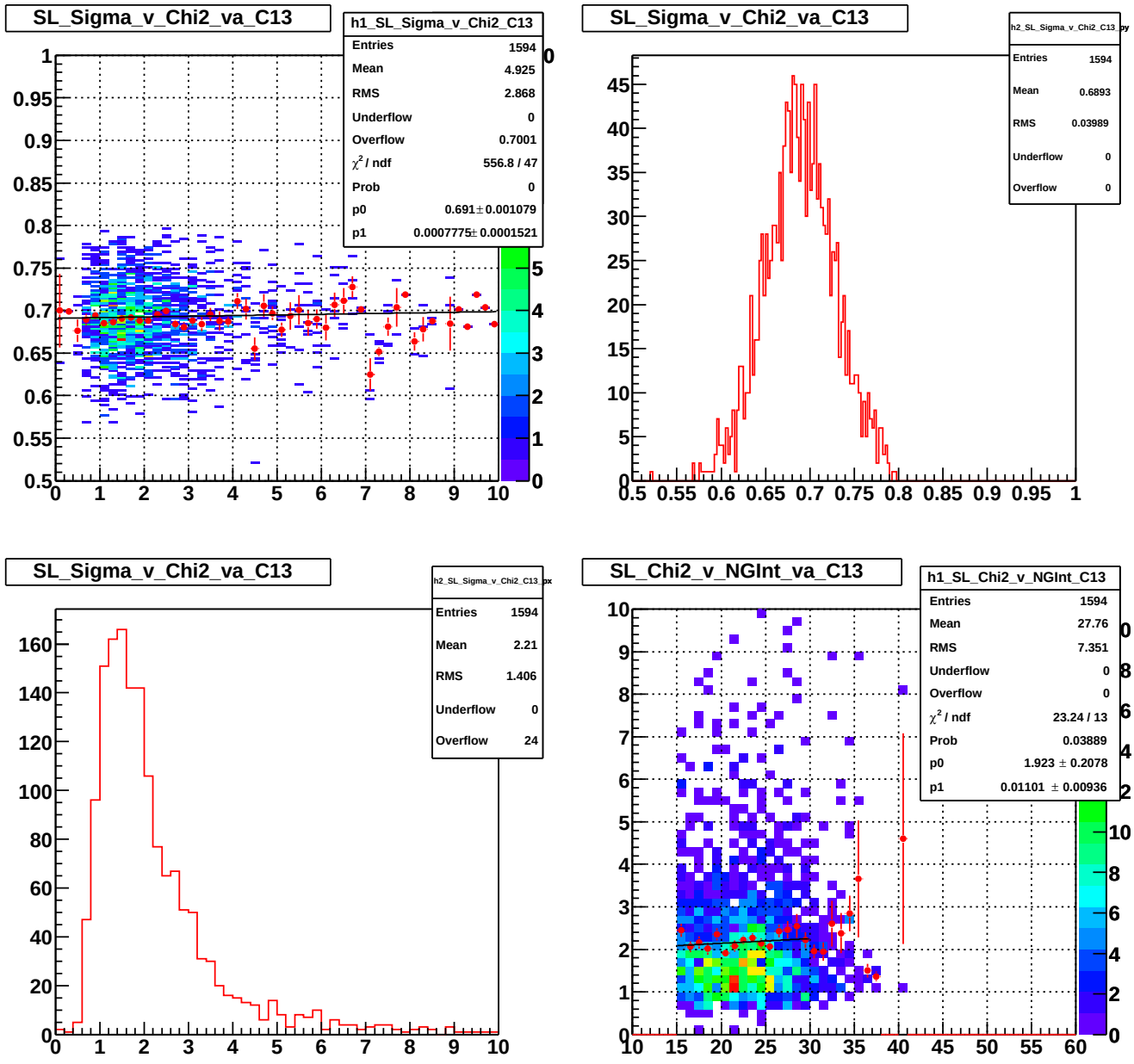

Figure 44: Antiproton beam, vertical detectors: Performance of the Synchrotron Light Detector at the C11 location during Tevatron Remove Halo case: Sigma of the bunch width distribution (in *mm*) as measured by the SL detector versus front end measure of the goodness of fit together with an overlaid horizontal profile and a straight line fit; sigma of the bunch width distribution (in *mm*) itself; goodness of fit itself; goodness of fit versus bunch intensity together with an overlaid horizontal profile and a straight line fit.

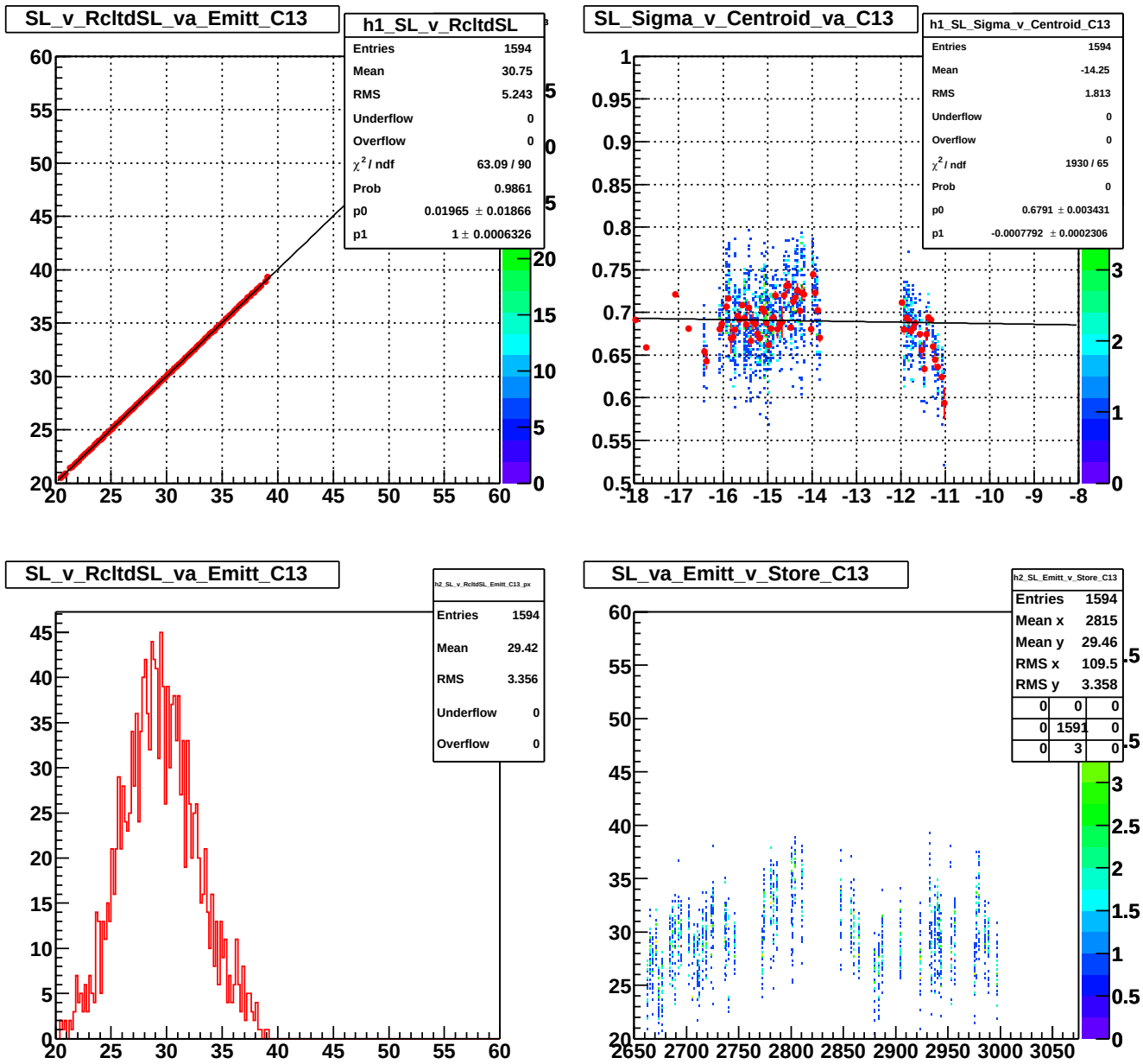

Figure 45: Antiproton beam, vertical detectors: Performance of the Synchrotron Light Detector at the C11 location during Tevatron Remove Halo case: Bunch emittance (in $\pi \cdot mm \cdot mrad$) as measured by the front end SL detector versus bunch emittance as recalculated using front end sigma of the bunch width distribution (in *mm*) (combined with SBD timing information in the horizontal cases) together with an overlaid horizontal profile of that distribution with a straight line fit; sigma of the bunch width distribution versus bunch E11 centroid (in *mm*) (based on the T:FW[E,H,V][A,P]CE ACNET variable) with an overlaid horizontal profile of that distribution with a straight line fit; bunch emittance; bunch emittance versus store number.

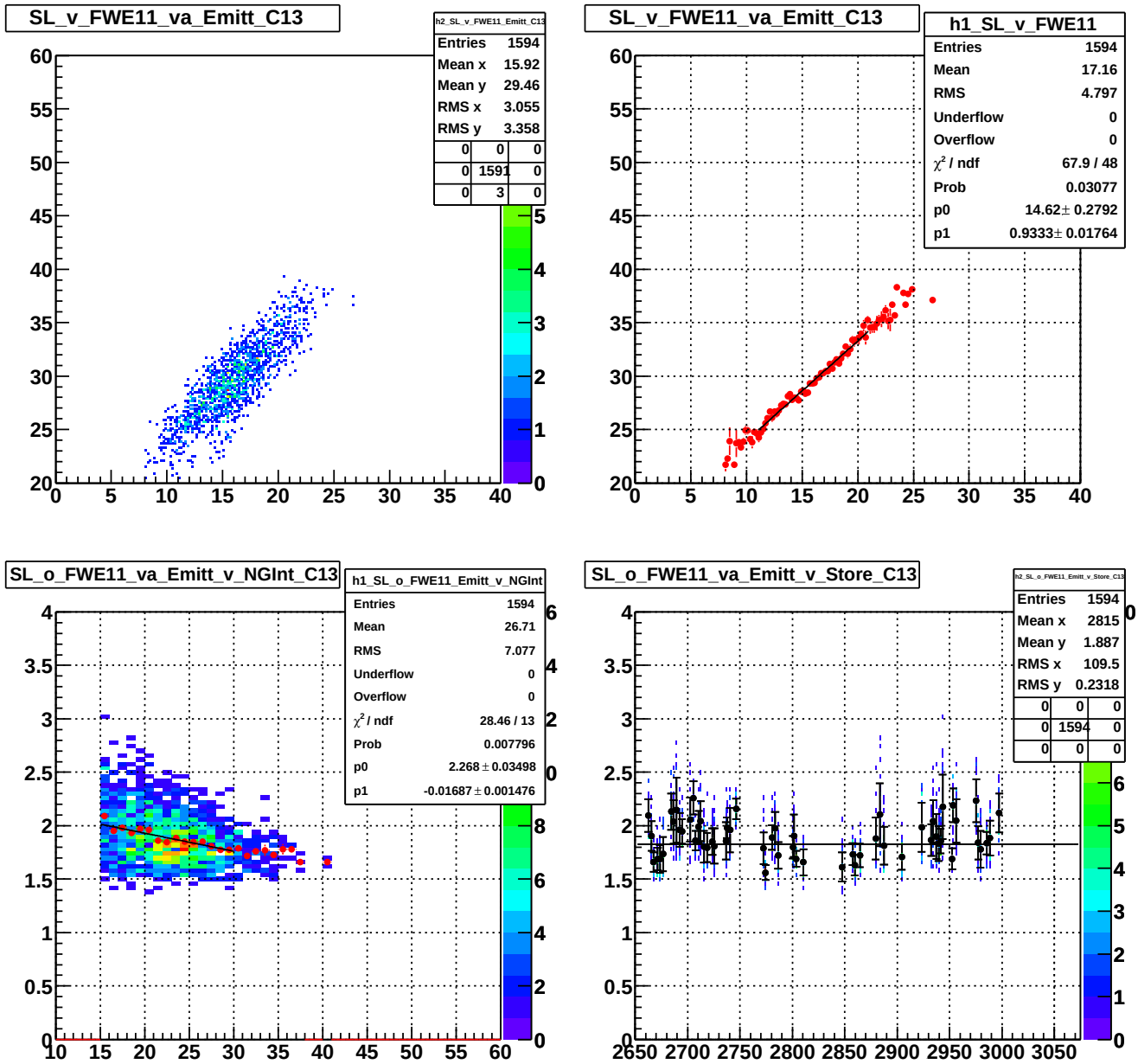

Figure 46: Antiproton beam, vertical detectors: Comparisons of Emittance measurements as done by Synchrotron Light Detector at C11 and Flying Wire Detector at E11 during Tevatron Remove Halo case: Bunch emittance (in $\pi \cdot mm \cdot mrad$) as measured by Synchrotron Light Detector versus bunch emittance as measured by the Flying Wire Detector at E11; horizontal profile of the previous distribution with a straight line fit; bunch emittance as measured by Synchrotron Light Detector over bunch emittance as measured by the Flying Wire Detector at E11 versus bunch intensity (ACNET variables T:FBI[A,P]NG) (in E9) together with an overlaid horizontal profile and a straight line fit; bunch emittance as measured by Synchrotron Light Detector over bunch emittance as measured by the Flying Wire Detector at E11 versus store number with overlaid averaged ratios for each store and a horizontal line fit.

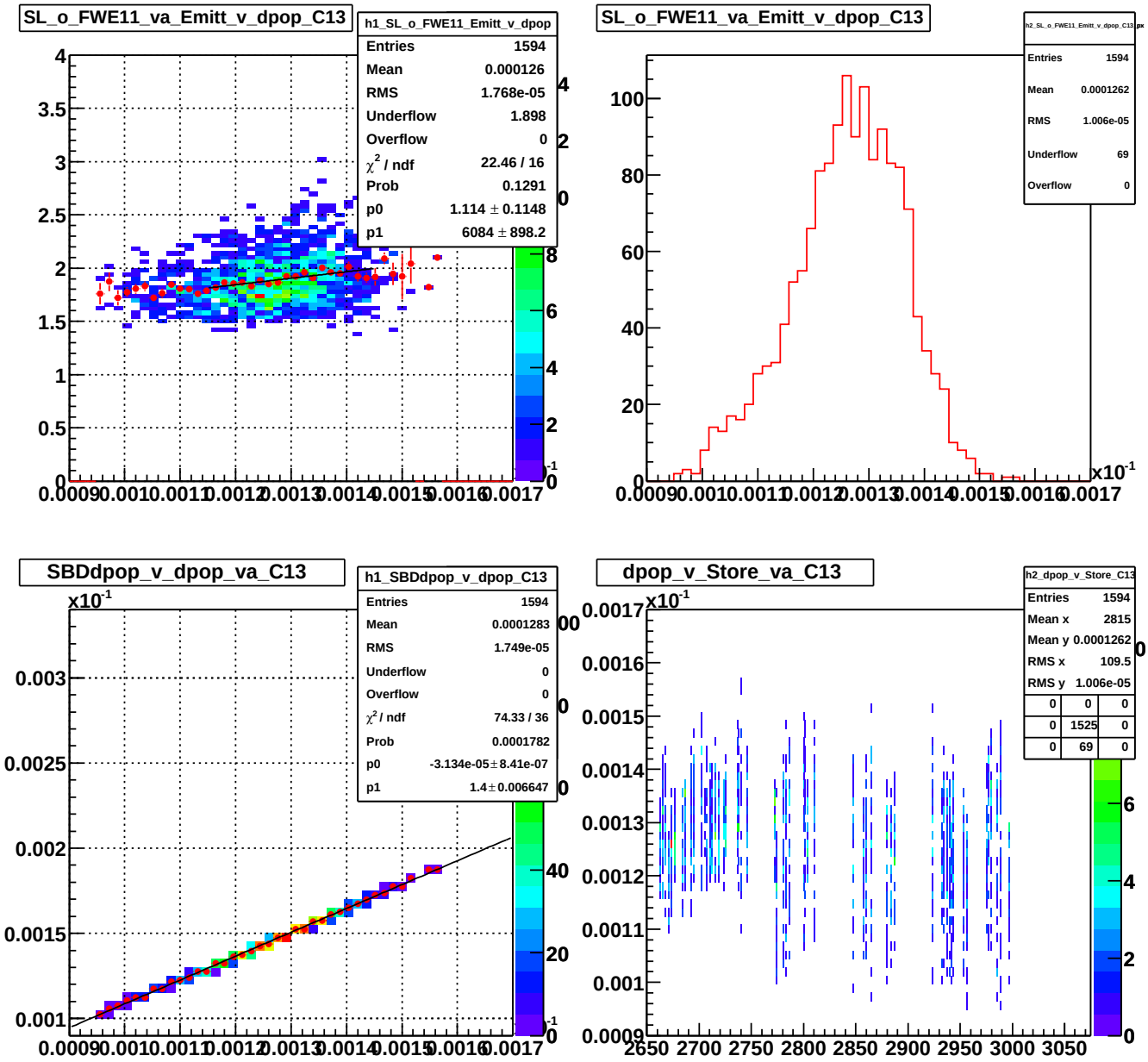

Figure 47: Antiproton beam, vertical detectors: Comparisons of Emittance measurements as done by Synchrotron Light Detector at C11 and Flying Wire Detector at E11 during Tevatron Remove Halo case: Bunch emittance as measured by Synchrotron Light Detector over bunch emittance as measured by the Flying Wire Detector at E11 versus recalculated $\delta p/p$ (based on δt the T:SBD[A,P]SS ACNET variable) with an overlaid horizontal profile of the previous distribution with a straight line fit; $\delta p/p$ itself; frontend value of $\delta p/p$ versus recalculated $\delta p/p$; $\delta p/p$ versus store number.

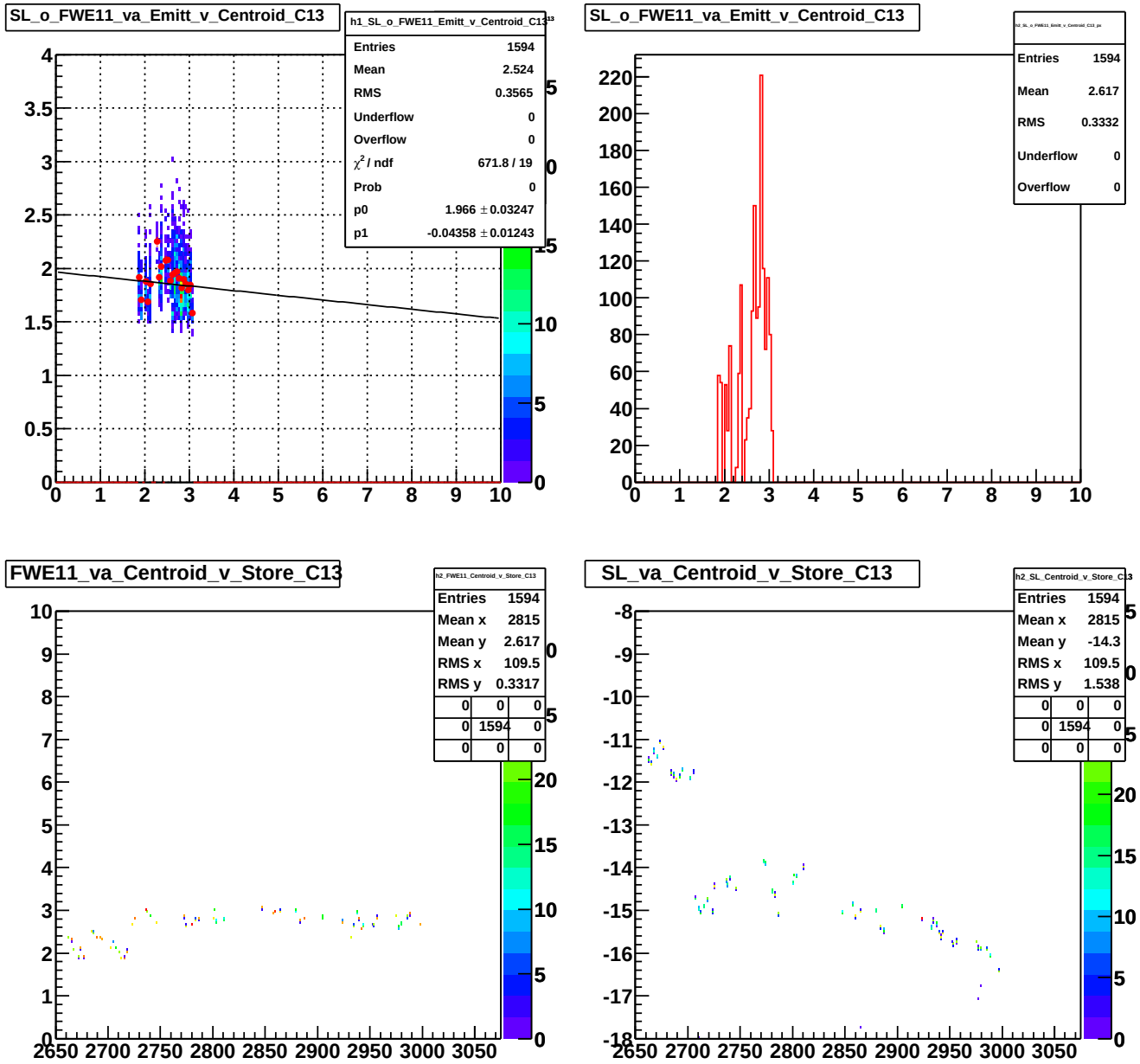

Figure 48: Antiproton beam, vertical detectors: Comparisons of Emittance measurements as done by Synchrotron Light Detector at C11 and Flying Wire Detector at E11 during Tevatron Remove Halo case: Bunch emittance as measured by Synchrotron Light Detector over bunch emittance as measured by the Flying Wire Detector at E11 versus bunch E11 centroid (in *mm*) (based on the T:FW[E,H,V][A,P]CE ACNET variable) with an overlaid horizontal profile of the previous distribution with a straight line fit; bunch E11 centroid itself; bunch E11 centroid versus store number. bunch C11 centroid versus store number.

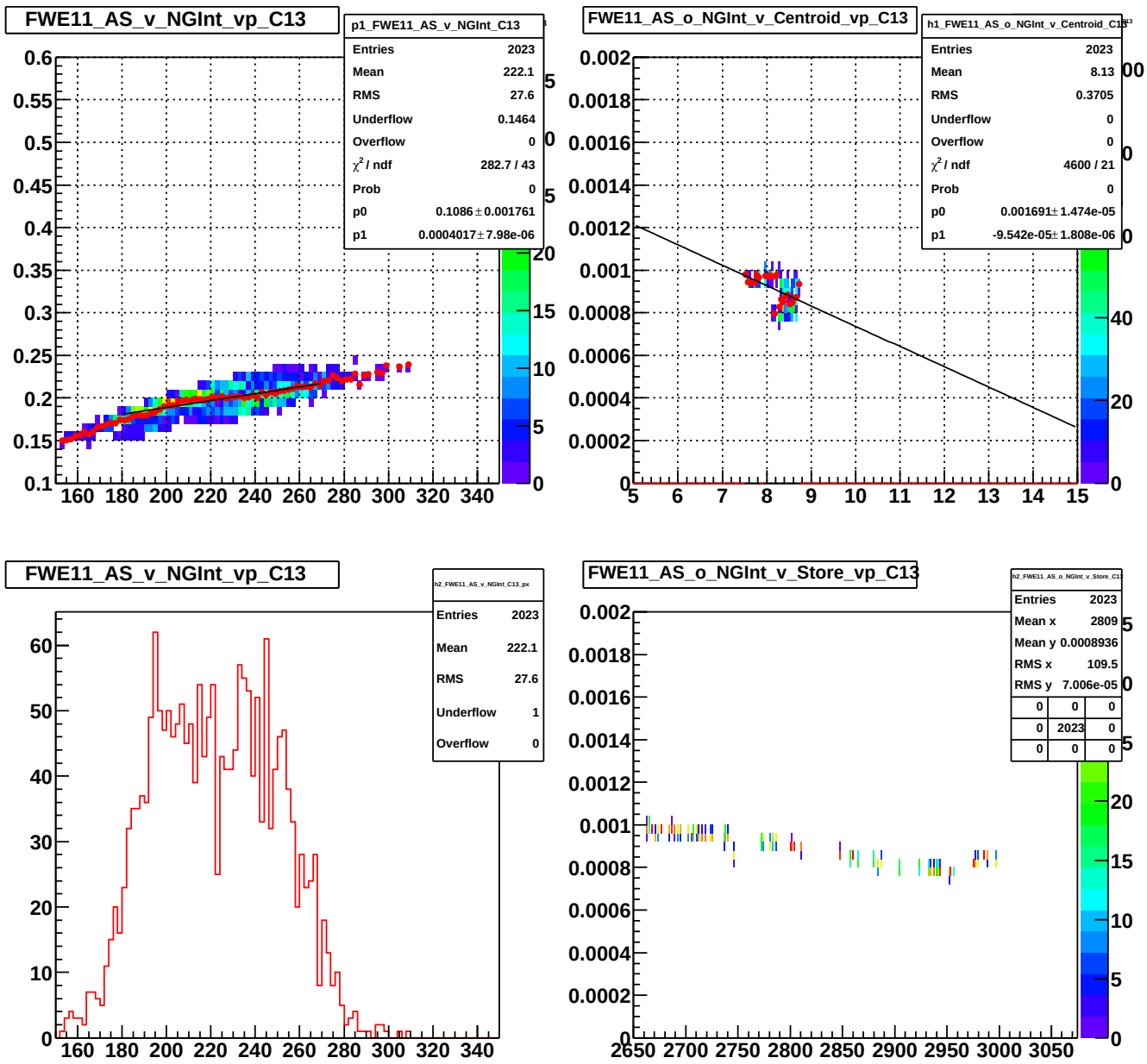

Figure 49: Proton beam, vertical detectors: Performance of the Flying Wire Detector at the E11 location during Tevatron Remove Halo case: Amplitude (in arbitrary units) times sigma of the bunch width distribution (in *mm*) of the front end FW detector data versus bunch intensity (ACNET variables T:FBI[A,P]NG) (in E9) with an overlaid horizontal profile of that distribution with a straight line fit; Amplitude times sigma of the bunch width distribution of the front end FW detector data over bunch intensity versus bunch E11 centroid (in *mm*) (based on the T:FW[E,H,V][A,P]CE ACNET variable) with an overlaid horizontal profile of that distribution with a straight line fit; bunch intensity; amplitude times sigma of the bunch width distribution (in *mm*) of the raw FW detector distribution over bunch intensity versus store number.

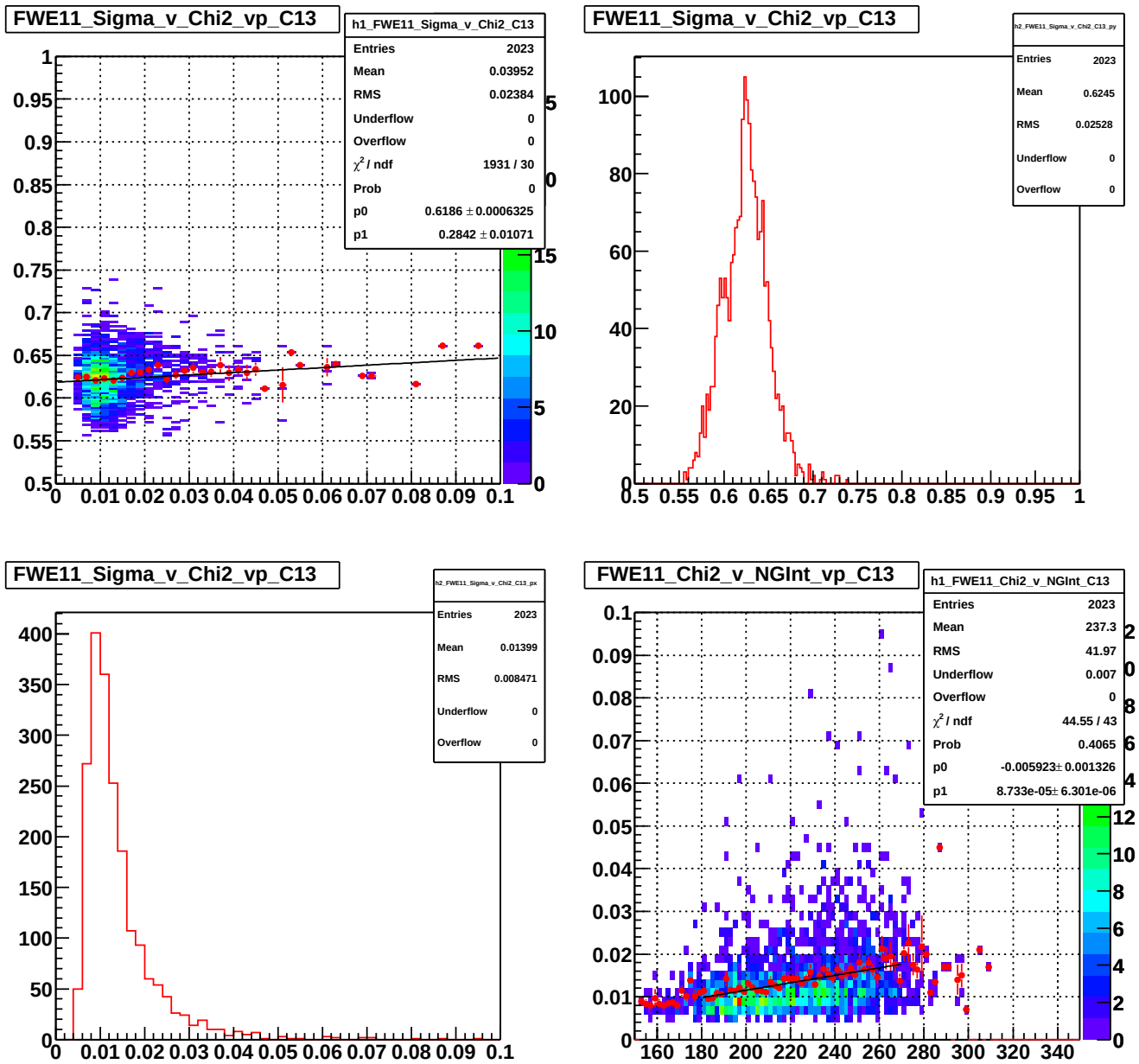

Figure 50: Proton beam, vertical detectors: Performance of the Flying Wire Detector at the E11 location during Tevatron Remove Halo case: Sigma of the bunch width distribution (in *mm*) as measured by the FW detector versus front end measure of the goodness of fit together with an overlaid horizontal profile and a straight line fit; sigma itself, goodness of fit itself; goodness of fit versus bunch intensity together with an overlaid horizontal profile and a straight line fit;

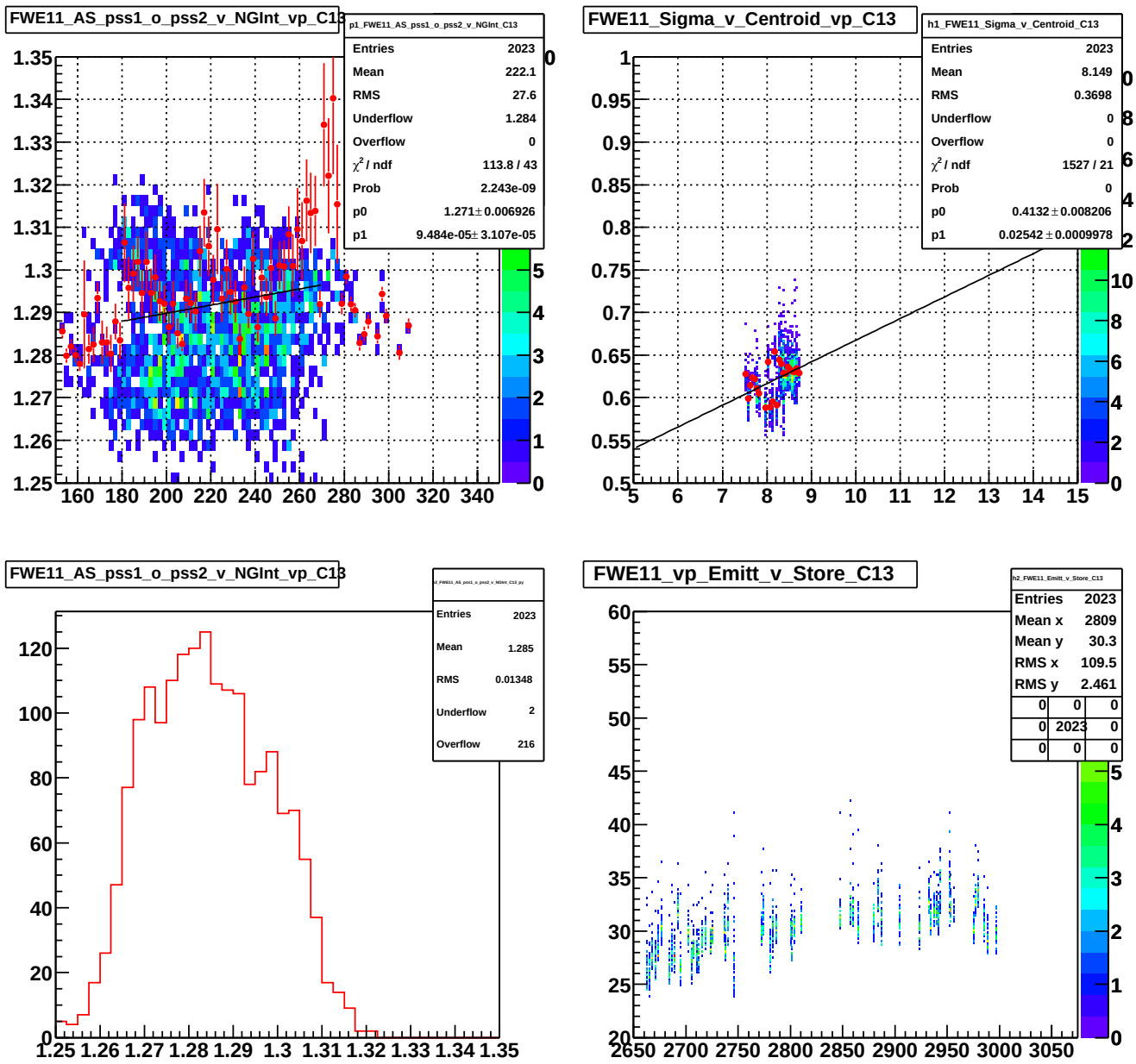

Figure 51: Proton beam, vertical detectors: Performance of the Flying Wire Detector at the E11 location during Tevatron Remove Halo case: Amplitude (in arbitrary units) times sigma of the bunch width distribution (in *mm*) of the pass 1 over pass 2 of the front end FW detector data versus bunch intensity (ACNET variables T:FBI[A,P]NG) (in E9) together with an overlaid horizontal profile of that distribution with a straight line fit; sigma of the bunch width distribution versus bunch centroid (in *mm*) (based on the T:FW[E,H,V][A,P]CE ACNET variable) with an overlaid horizontal profile of that distribution with a straight line fit; amplitude (in arbitrary units) times sigma of the bunch width distribution (in *mm*) of the pass 1 over pass 2 of the front end FW detector data itself, bunch emittance (in $\pi \cdot mm \cdot mrad$) versus store number.

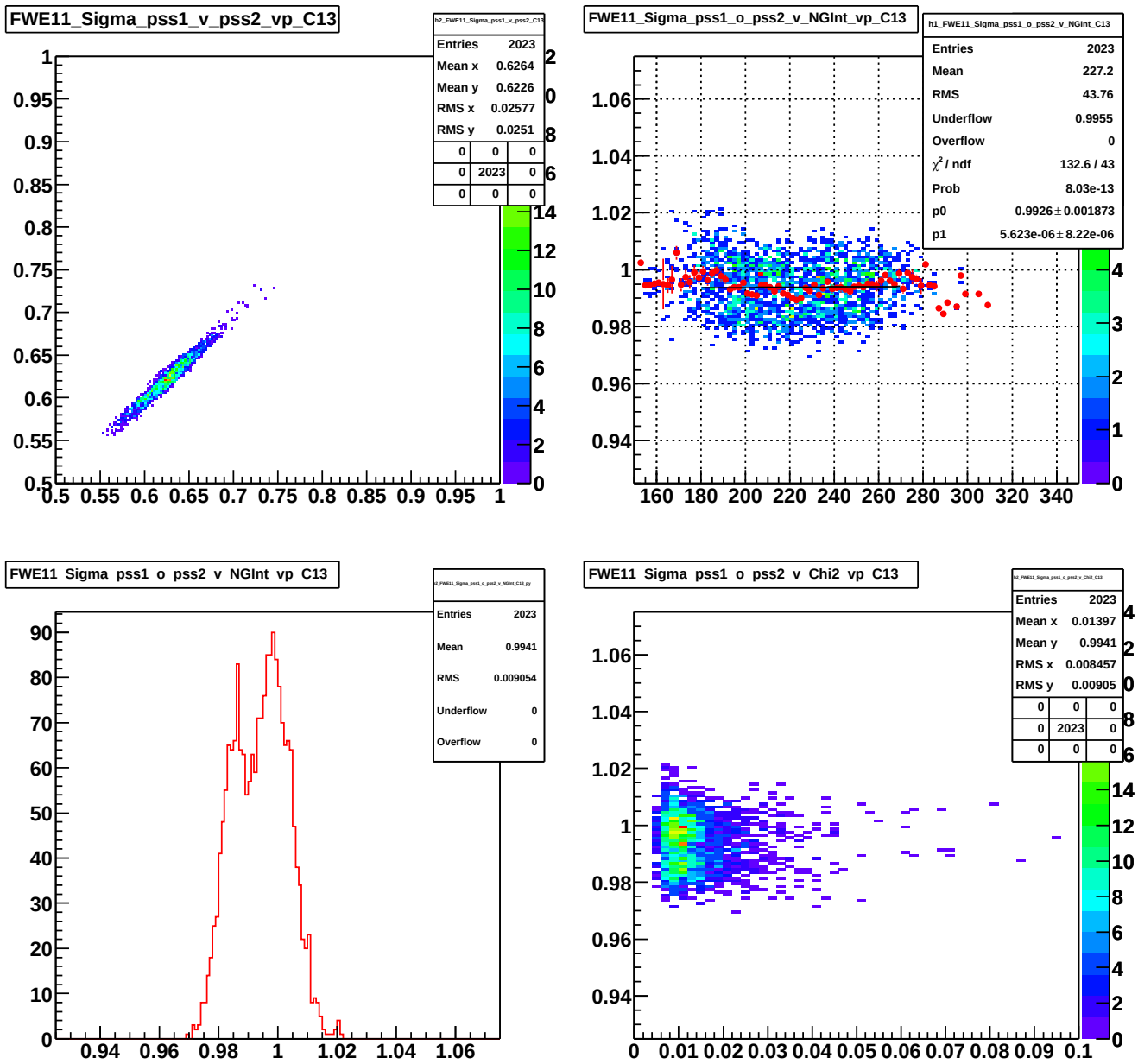

Figure 52: Proton beam, vertical detectors: Performance of the Flying Wire Detector at the E11 location during Tevatron Remove Halo case: Sigma of the bunch width distribution (in *mm*) of the pass 1 versus pass 2 of the FW detector; sigma of the bunch width distribution (in *mm*) of the pass 1 over pass 2 of the FW detector versus bunch intensity (ACNET variables T:FBI[A,P]NG) (in E9) together with an overlaid horizontal profile and a straight line fit; sigma of the bunch width distribution (in *mm*) of the pass 1 over pass 2 of the FW detector itself, sigma of the bunch width distribution (in *mm*) of the pass 1 over pass 2 of the FW detector versus front end measure of the goodness of fit.

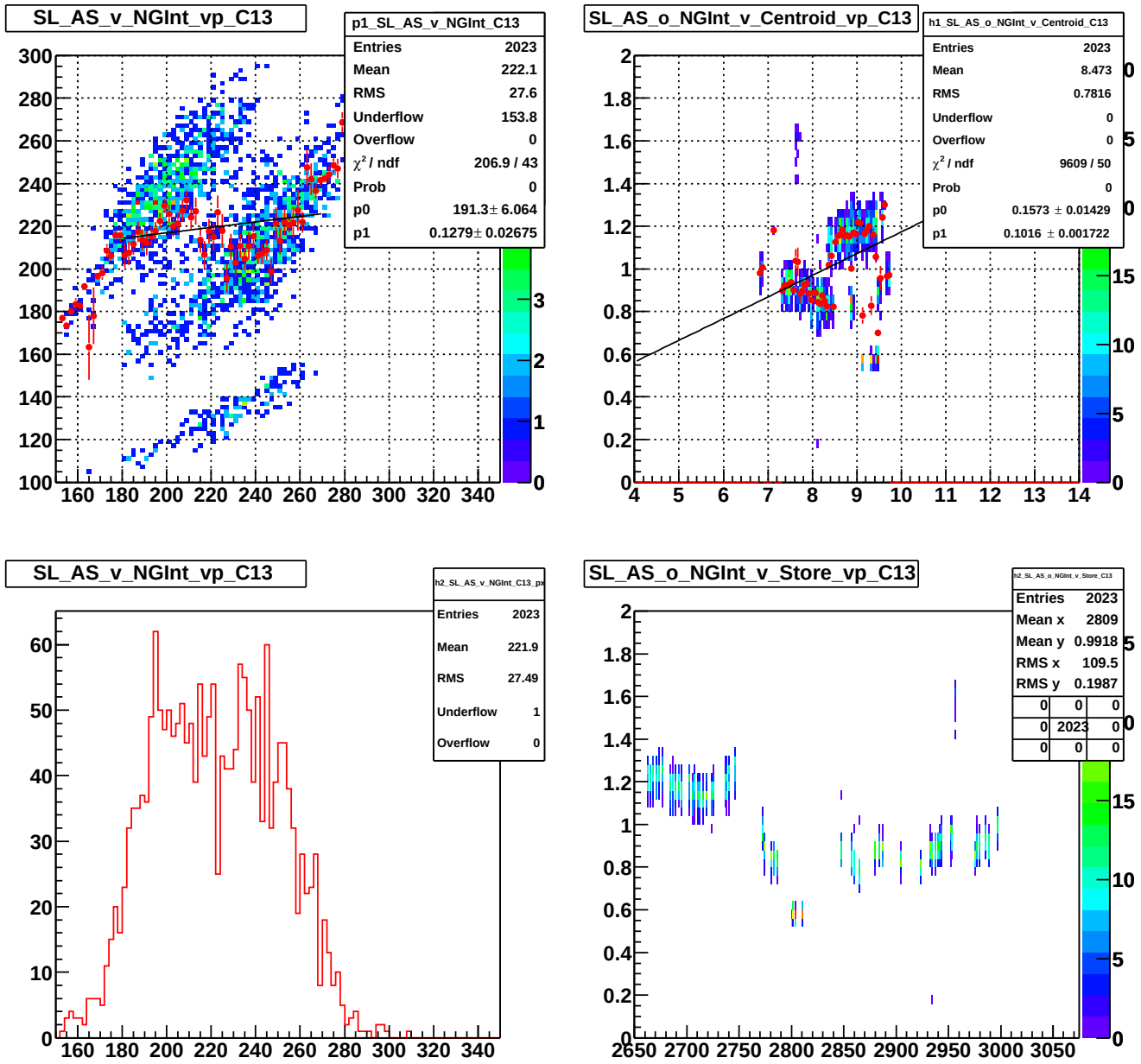

Figure 53: Proton beam, vertical detectors: Performance of the Synchrotron Light Detector at the C11 location during Tevatron Remove Halo case: Amplitude (in arbitrary units) times sigma of the bunch width distribution (in *mm*) of the raw SL detector distribution versus bunch intensity (ACNET variables T:FBI[A,P]NG) (in E9) with an overlaid horizontal profile of that distribution with a straight line fit; amplitude times sigma of the bunch width distribution (in *mm*) of the raw SL detector distribution over bunch intensity versus bunch E11 centroid (in *mm*) (based on the T:FW[E,H,V][A,P]CE ACNET variable) with an overlaid horizontal profile of that distribution with a straight line fit; bunch intensity; amplitude times sigma of the bunch width distribution (in *mm*) of the raw SL detector distribution over bunch intensity versus store number.

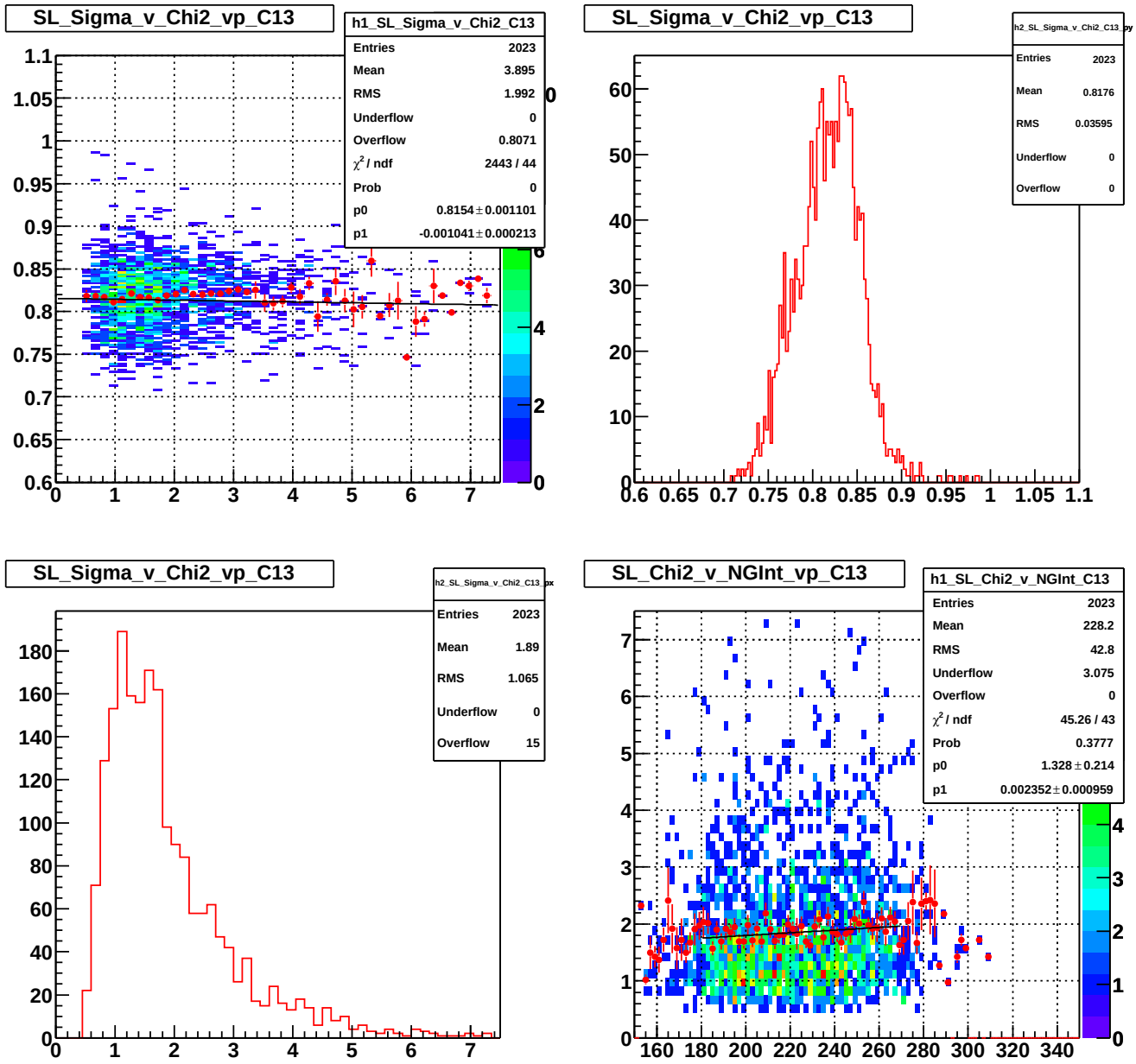

Figure 54: Proton beam, vertical detectors: Performance of the Synchrotron Light Detector at the C11 location during Tevatron Remove Halo case: Sigma of the bunch width distribution (in *mm*) as measured by the SL detector versus front end measure of the goodness of fit together with an overlaid horizontal profile and a straight line fit; sigma of the bunch width distribution (in *mm*) itself; goodness of fit itself; goodness of fit versus bunch intensity together with an overlaid horizontal profile and a straight line fit.

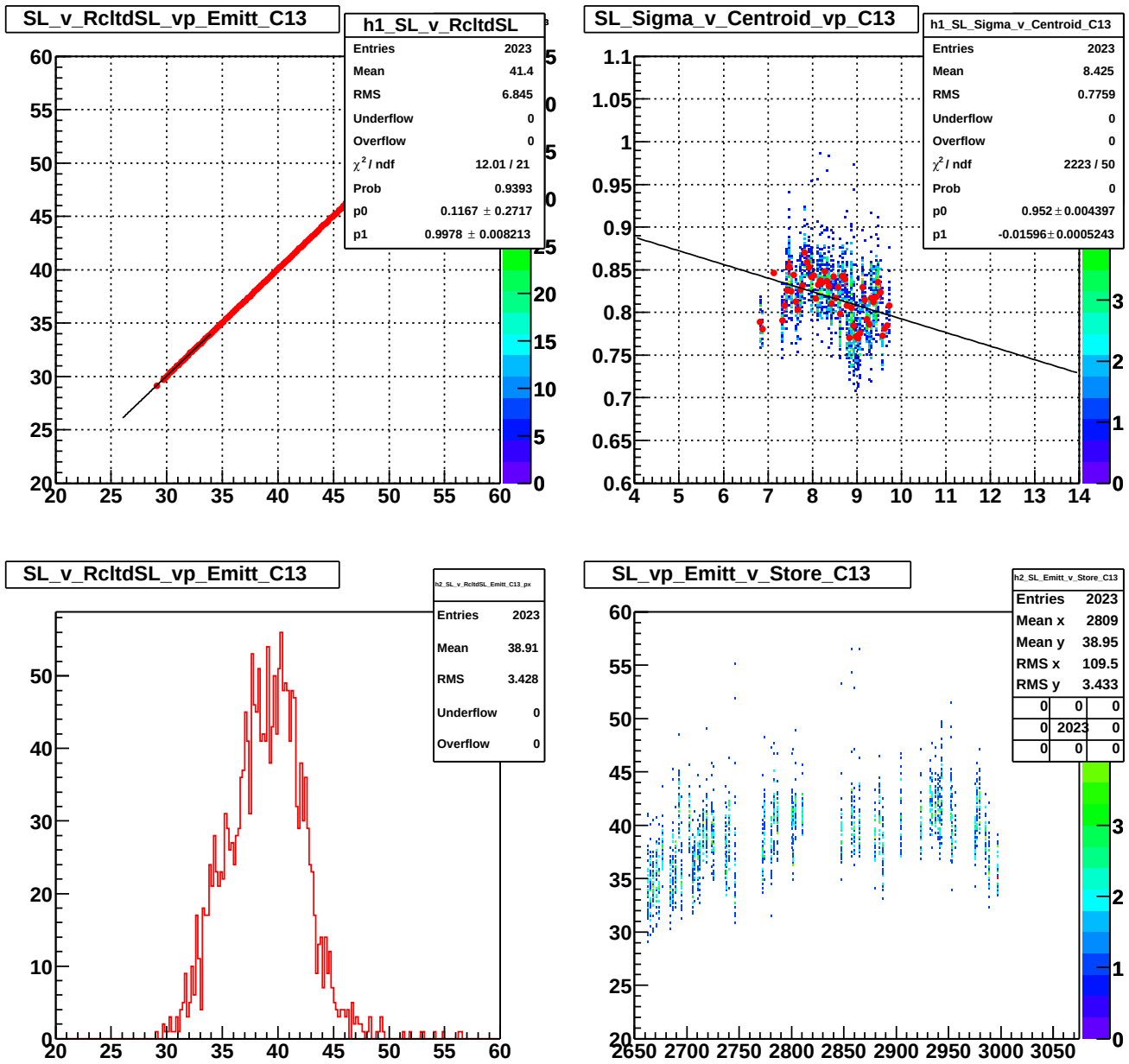

Figure 55: Proton beam, vertical detectors: Performance of the Synchrotron Light Detector at the C11 location during Tevatron Remove Halo case: Bunch emittance (in $\pi \cdot mm \cdot mrad$) as measured by the front end SL detector versus bunch emittance as recalculated using front end sigma of the bunch width distribution (in *mm*) (combined with SBD timing information in the horizontal cases) together with an overlaid horizontal profile of that distribution with a straight line fit; sigma of the bunch width distribution versus bunch E11 centroid (in *mm*) (based on the T:FW[E,H,V][A,P]CE ACNET variable) with an overlaid horizontal profile of that distribution with a straight line fit; bunch emittance; bunch emittance versus store number.

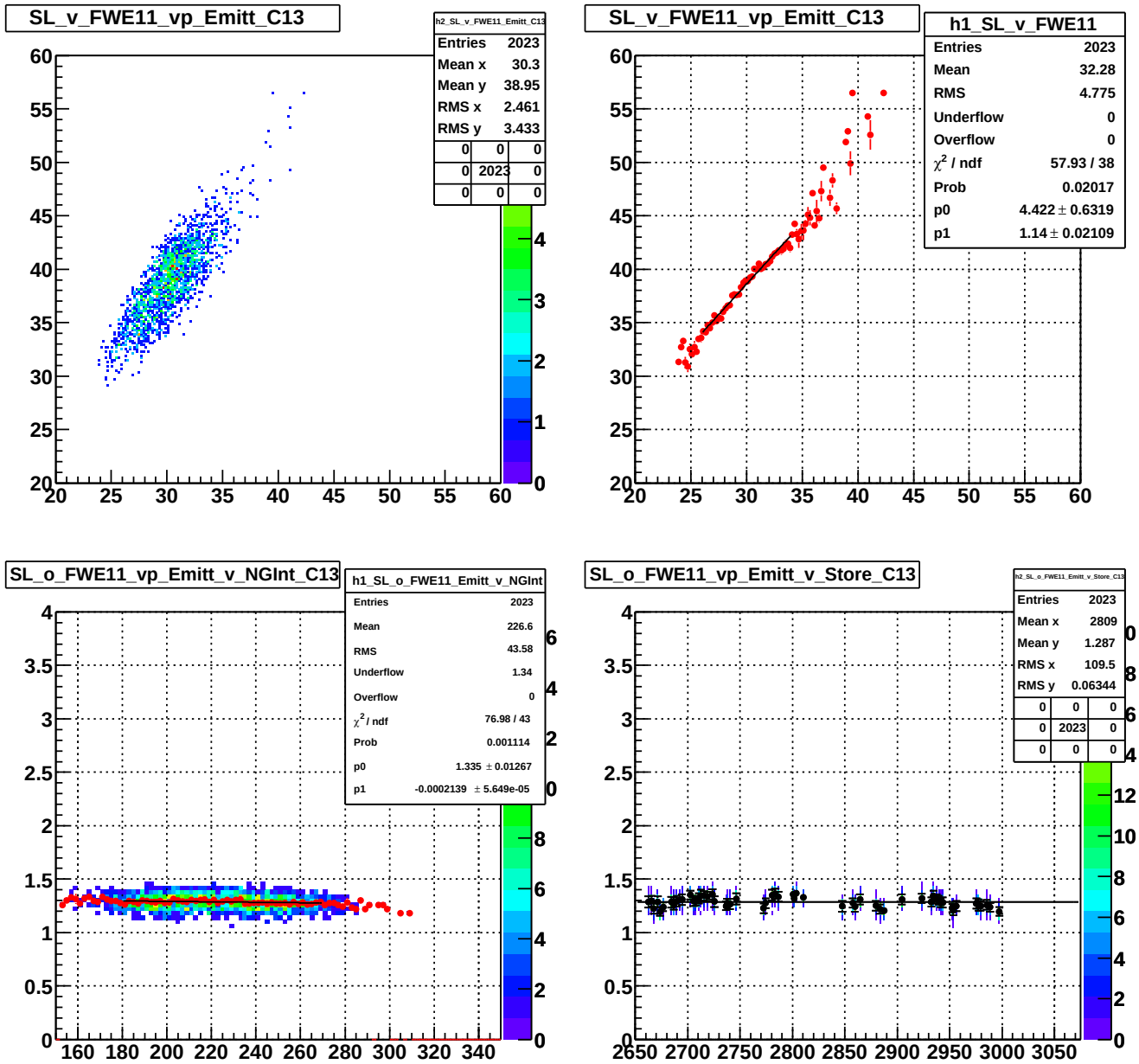

Figure 56: Proton beam, vertical detectors: Comparisons of Emittance measurements as done by Synchrotron Light Detector at C11 and Flying Wire Detector at E11 during Tevatron Remove Halo case: Bunch emittance (in $\pi \cdot mm \cdot mrad$) as measured by Synchrotron Light Detector versus bunch emittance as measured by the Flying Wire Detector at E11; horizontal profile of the previous distribution with a straight line fit; bunch emittance as measured by Synchrotron Light Detector over bunch emittance as measured by the Flying Wire Detector at E11 versus bunch intensity (ACNET variables T:FBI[A,P]NG) (in E9) together with an overlaid horizontal profile and a straight line fit; bunch emittance as measured by Synchrotron Light Detector over bunch emittance as measured by the Flying Wire Detector at E11 versus store number with overlaid averaged ratios for each store and a horizontal line fit.

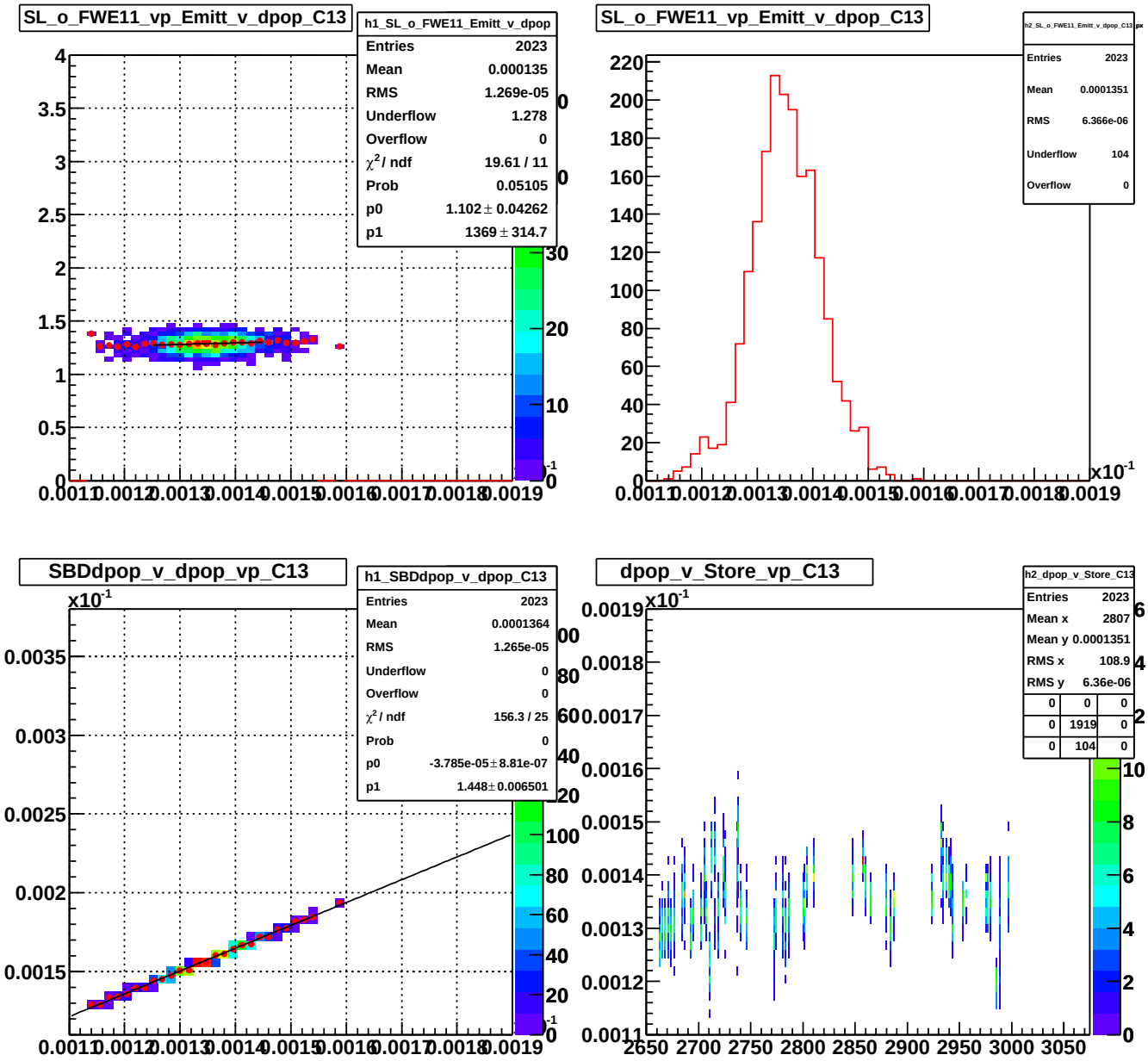

Figure 57: Proton beam, vertical detectors: Comparisons of Emittance measurements as done by Synchrotron Light Detector at C11 and Flying Wire Detector at E11 during Tevatron Remove Halo case: Bunch emittance as measured by Synchrotron Light Detector over bunch emittance as measured by the Flying Wire Detector at E11 versus recalculated $\delta p/p$ (based on δt the T:SBD[A,P]SS ACNET variable) with an overlaid horizontal profile of the previous distribution with a straight line fit; $\delta p/p$ itself; frontend value of $\delta p/p$ versus recalculated $\delta p/p$; $\delta p/p$ versus store number.

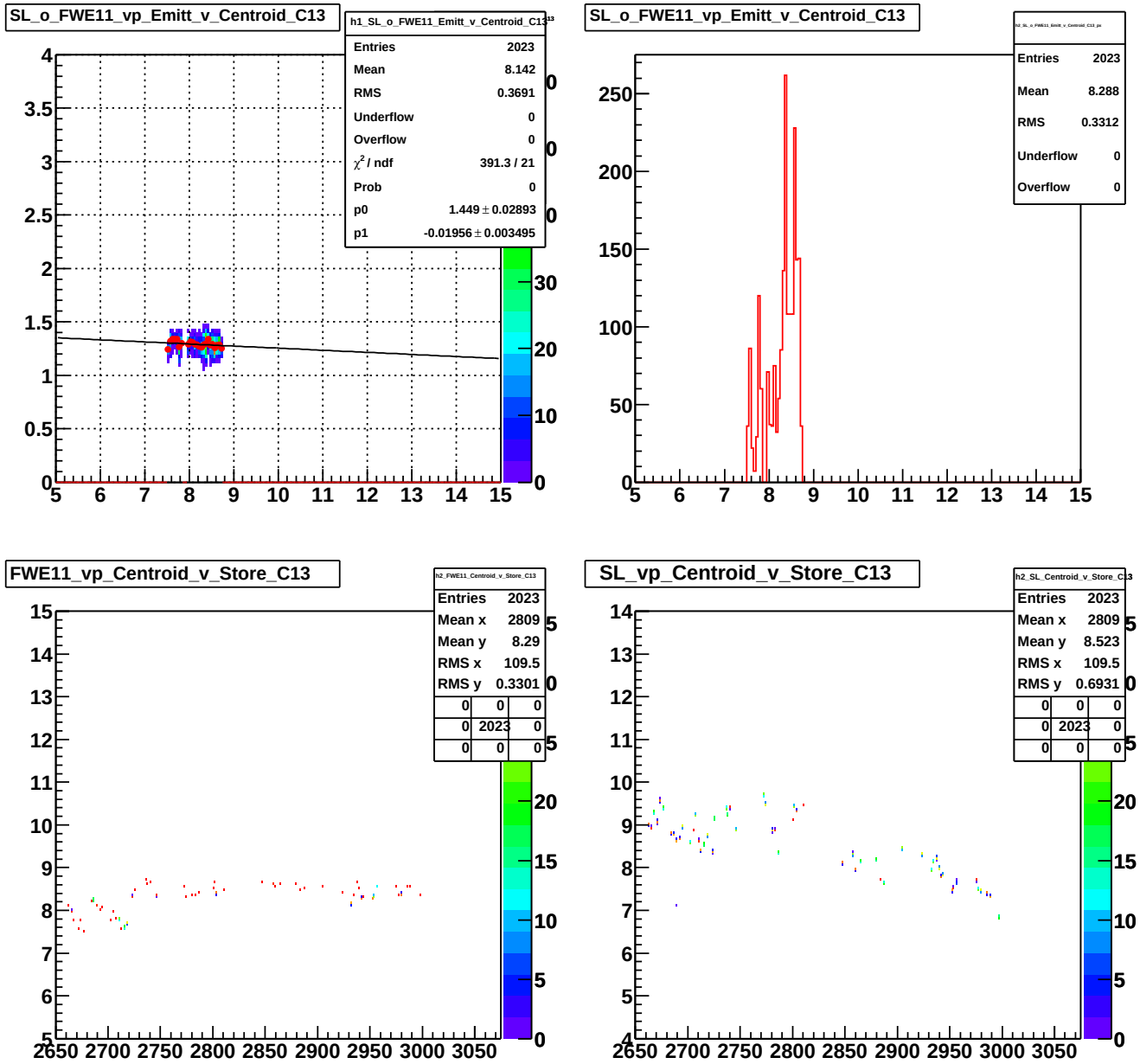

Figure 58: Proton beam, vertical detectors: Comparisons of Emittance measurements as done by Synchrotron Light Detector at C11 and Flying Wire Detector at E11 during Tevatron Remove Halo case: Bunch emittance as measured by Synchrotron Light Detector over bunch emittance as measured by the Flying Wire Detector at E11 versus bunch E11 centroid (in *mm*) (based on the T:FW[E,H,V][A,P]CE ACNET variable) with an overlaid horizontal profile of the previous distribution with a straight line fit; bunch E11 centroid itself; bunch E11 centroid versus store number. bunch C11 centroid versus store number.